UNIVERSITY OF OKLAHOMA

GRADUATE COLLEGE

NARROW OPEN TUBULAR LIQUID CHROMATOGRAPHY: SEPARATION OPTIMIZATION AND COLUMN IMPROVEMENT

A DISSERTATION
SUBMITTED TO THE GRADUATE FACULTY
in partial fulfillment of the requirements for the
Degree of

DOCTOR OF PHILOSOPHY

By

YU YANG
Norman, Oklahoma
2020

NARROW OPEN TUBULAR LIQUID CHROMATOGRAPHY: SEPARATION OPTIMIZATION AND COLUMN IMPROVEMENT

A DISSERTATION APPROVED FOR THE

DEPARTMENT OF CHEMISTRY AND BIOCHEMISTRY

By THE COMMITTEE CONSISTING OF

Dr. Shaorong Liu, Chair

Dr. Michael T. Ashby

Dr. Rakhi Rajan

Dr. Xiaolei Liu

Dr. Si Wu

This doctoral dissertation is dedicated to my family.

Acknowledgments

"No great mind has ever existed without a touch of madness." – Aristotle.

First and foremost, I would like to express my thanks to Dr. Shaorong Liu, who is an outstanding educator, mentor, and scientist. He dedicates his time and effort to teaching his students and developing new research ideas. I am so honored and grateful to have him as my advisor and supervisor. Without his encouraging words, generous support and considerable guidance, none of my research projects can be achieved. His thoughtful comments also shine upon this dissertation. Language is truly not powerful enough to express my sincere gratitude to Dr. Shaorong Liu. Even though the six-year lab life with Dr. Liu has reached to an end, I will continue applying the knowledge, skills as well as the never-give-up researcher spirit I learned from Dr. Liu in my future career. I cherish the six years spent in this lab very much. I believe no matter when to look back, this would be a productive and pleasant page in my whole life. This page will equip me with perseverance and passion to conquer every difficulty and climb on each new peak.

I would also like to give many thanks to my committee members. They are Dr. Michael T. Ashby, Dr. Si Wu, Dr. Rakhi Rajan, Dr. Xiaolei Liu and former committee member Dr. Laura E. Bartley. They have spent time attending my evaluation meeting every year and providing me with valuable feedback and advice. Their help has been upholding me throughout the six years.

I also wish to thank all my lab members for their collaboration and support. They are Dr. Zaifang Zhu, Dr. Huang Chen, Dr. Apeng Chen, Dr. Kyle Lynch, Dr. Min Zhang, Mitchell Weaver, Piliang Xiang, Matthew Beckner, Zhitao Zhao, and Joann Lu. Special thanks are given to Dr. Preston Larson who has been assisting us on SEM support and Barry Bergeron for machining the equipment we have been using.

Last but not least, I would like to say, “Thank you!” to my family for constantly supporting me in this doctoral degree chasing journey and during the completion of this dissertation. Thanks Hongxiao Guo for becoming my closest family member and life partner in the 5th year of my Ph.D. journey. Your optimism and positivity have filled me with energy and enthusiasm to become a better man.

Table of Contents

Acknowledgments v
Table of Contents vii
List of Figures x
List of Abbreviations xi
Abstract xii
Chapter1. Introduction 1
1.1. Background 1
1.2. Open tublar (OT) capillary column preparation 6
1.2.1. Stationary phase by chemical bonding 6
1.2.2. Stationary phase by physical absorption 10
1.3. Detection 12
1.3.1. UV-vis Detection 13
1.3.2. Evaporative light scattering detection (ELSD) 15
1.3.3. Fluorescence detection (FLD) 16
1.3.4. Electrochemical detection (ECD) 18
1.3.5. Capacitively coupled contactless conductivity detector (C^4D) 18
1.3.6. Mass spectrometer (MS) 19
1.4. Dissertation Synopsis 19
Chapter2. On-column and gradient focusing-induced high-resolution separation in narrow open tubular liquid chromatography and a simple and economic approach for pico-gradient separation 16
2.1. Abstract 16
2.2. Introduction 17
2.3. Materials and methods 19
2.3.1. Reagents and materials 19
2.3.2. Narrow open tubular column preparation 20
2.3.3. Amino acid labelling 22
2.3.4. NOTLC apparatus 24
2.3.5. NOTLC separation 24
2.4. Results and Discussion 25
2.4.1. High efficiency NOTLC separation 25
2.4.2. Hypothesis of reduced-diffusion 28
2.4.3. Confirmation of on-column focusing 28

2.4.4. Observation of a re-focusing effect 30
2.4.5. Gradient focusing 32
2.4.6. Developemnt of a simple and economic approach to run gradient NOTLC 33
2.5. Conclusion and perspectives 36
Chapter3. Experimentally Validating the Open Tubular Liquid Chromatography for a Peak Capacity of 2000 in 3 h 39
3.1. Abstract 39
3.2. Introduction 40
3.3. Experimental section 43
3.3.1. Materials and Reagents 43
3.3.2. Preparation of NOTLC Column 44
3.3.3. Peptide Sample Preparation 44
3.3.4. Fluorescent Dye Labeling 45
3.3.5. Apparatus 47
3.4. Results and discussion 47
3.4.1. Ultrahigh-Resolution NOTLC Spearation 47
3.4.2. Ultrafast NOTLC Separation 54
3.4.3. NOTLC Limit of Detection 55
Chapter4. Coating 2-μm-Bore Capillaries for Ultrahigh-Resolution Open Tubular Liquid Chromatograhy 39
4.1. Abstract 39
4.2. Introduction 40
4.3. Experimental section 42
4.3.1. Chemicals and materials 42
4.3.2. NOTLC column preparation 42
4.3.3. Apparatus for running NOTLC separations 44
4.4. Results and discussion 45
4.4.1. Effect of OTMS concentration on amino acid retention and resolution 45
4.4.2. Optimization of temperature, pressure and duration for flushing OTMS through NOTLC column 46
4.4.3. Column coating reproducibility 47
4.4.4. Performance of NOTLC column. 48
4.5. Conclusion 49
Chapter5. Overall Summary and Future Perspective 65
Appendix 2: Chapter 2 Supplemental 65

Appendix 3: Chapter 3 Supplemental 65
Appendix 4: Chapter 4 Supplemental 65
Appendix 5: Copyright Clarification 74

List of Figures

Figure 1-1. Effect of inner diameter on resolution from OT column. 5
Figure 1-2. Schematic of typical PLOT column and separation chromatogram with MS 7
Figure 1-3. SEM images of capillary samples with different i.d. 10
Figure 1-4. The schematic images of structure for MA-BDDE copolymer. The monomers are methylamine (MA) and 1,4-butanedioldiglycidylether (BDDE). 12
Figure 1-5. UV-vis for off-column cap-LC detection 14
Figure 1-6. Agilent UV-vis PDA for on-column nano-LC detection 15
Figure 1-7. ELSD for cap-LC 16
Figure 1-8. Bare narrow capillary hydrodynamic chromatography (BaNC-HDC) system with Laser induced fluorescence (LIF) detector[48] 18
Figure 2-1. Graphic abstract 17
Figure 2-2. Apparatus for NOTLC column preparation. 21
Figure 2-3. Apparatus for performing NOTLC separation. 23
Figure 2-4. Chromatogram of a typical high-efficiency NOTLC separation. 26
Figure 2-5. “Isocratic” separation of amino acid mixture. 27
Figure 2-6. Peak profiles with or without on-column focusing. 29
Figure 2-7. Observation of re-focusing. 31
Figure 2-8. Schematic of gradient focusing mechanism. 33
Figure 2-9. Simple and economic approach to run gradient NOTLC. 35
Figure 2-10. Comparison between method #1 and method #2. 36
Figure 3-1. Graphic abstract 40
Figure 3-2. Schematic diagrams of experimental apparatus. 46
Figure 3-3. Ultrahigh-resolution NOTLC separation. 49
Figure 3-4. SEM images of 2-μm-i.d. capillary before treatment, after NaOH activation and after C18 coating 50
Figure 3-5. Typical ultra-high-resolution chromatograms 52
Figure 3-6. Relationship between peak capacity and gradient time 52
Figure 3-7. Chromatograms for repeated peptide separations. 53
Figure 3-8. Typical chromatograms for fast NOTLC separations 55
Figure 3-9. LOD determination of NOTLC column 56
Figure 4-1. Graphic abstract. 40
Figure 4-2. Apparatus for coating NOTLC column. 44
Figure 4-3. Influence of reagent concentration on NOTLC column. 46
Figure 4-4. Effects of temperature, pressure and duration for flushing OTMS on resolution. 47
Figure 4-5. Ultrahigh performance of NOTLC column. 50

List of Abbreviations

liquid chromatography (LC)

open tubular (OT)

open tubular liquid chromatography (OTLC)

narrow open tubular liquid chromatography (NOTLC)

inner diameter (i.d.)

high-pressure liquid chromatography (HPLC)

ultrahigh-pressure liquid chromatography (UPLC)

capillary LC (cap-LC)

gas chromatography (GC)

porous layer open tubular (PLOT)

bovine serum albumin (BSA)

solid phase extraction (SPE)

mass spectrometry (MS)

sodium dodecyl sulfate polyacrylamide gel electrophoresis (SDS-PAGE)

electrospray ionization mass spectrometry (ESI-MS)

scanning electron microscope (SEM)

methylamine (MA)

1,4-butanedioldiglycidylether (BDDE)

evaporative light scattering detection (ELSD)

microfluidic evaporative light scattering detection (μELSD)

fluorescence detection (FLD)

electrochemical detection (ECD).

photodiode array detection (PDA)

capillary electrophoresis (CE)

laser induced fluorescent (LIF)

potassium cyanide (KCN)

bare narrow capillary hydrodynamic chromatography (BaNC-HDC)

capacitively coupled contactless conductivity detector (C^4D)

Escherichia coli (E. coli)

octadecyltrimethoxysilane (C18 or OTMS)

Abstract

The continuous progress of life sciences such as genome sequencing, proteomics and metabolomics has facilitated the development of effective tools to better analyze the large numbers of bio-samples with low quantities and high complexities. Liquid chromatography (LC), as an essential analytical tool for analyzing many bio-samples, has encountered an unprecedented demand for enhanced resolving power and lower detection level. Open tubular (OT) column had been theoretically predicted to offer the greatest potential for extremely high separation efficiency in LC and produce superior resolving power in the bioanalytical studies during the past four decades. Recently, works from Dr. Shaorong Liu's group practically validated the predicted potential of ultrahigh-resolution and ultrahigh-speed open tubular liquid chromatography separations.

This dissertation focuses on the studies investigating the on-column and gradient focusing mechanism for the narrow open tubular liquid chromatography (NOTLC) to induce high-resolution separation, and the experimental explorations for the ultrahigh efficiencies and ultrafast separations. In addition, the key parameters for optimizing the NOTLC column were systematically tested and improved according to the separation efficiency and reliability.

The integration of the high-resolution NOTLC separation techniques and advanced detection method can potentially benefit fundamental research and broad types of applications such as single cell analysis and studies of proteomics.

Chapter1. Introduction

1.1. Background

One core concept in analytical chemistry is separation. With better separation, analytical chemists can solve more complex bio-samples with even lower trace of the sample amount. Liquid chromatography is one of the most powerful separation tools scientists invented. The history of liquid chromatography includes but is not limited to the evolution of the liquid chromatography column, which shows the trend of using a smaller column inner diameter (i.d.) , particle packing materials and flowrate.[1,2] One powerful separation tool is high-pressure liquid chromatography (HPLC). Generally speaking, commercial HPLC systems use columns 25 cm in length and 4.6 mm in diameter packed with particles 5 μm in diameter and the operation pressure is maximized to 400 bar (6000 psi). With the great development of the liquid delivering system and the column making techniques, 1.5 μm nanoporous silica particles were packed into a capillary column[3] for fast and high-efficiency separations applied with ultrahigh pressure (~1400 bar). Today's ultrahigh-pressure liquid chromatography (UPLC) was achieved.

Fundamentally, the objective of reducing the monodisperse-particle size (or channel size inside column) is to decrease the pore sizes among the particles and shorten the mass-transfer time in the stationary phase. An effective way to achieve this goal is to use bare open tubular columns with narrow inner diameter. In fact, under optimized conditions, OT columns have been theoretically [4-7] and practically[8,9] shown to provide improved chromatographic performance compared to other nano-LC columns. There are theory predicting that the optimal inner diameter (i.d.) for separation lay in the range of 1- 2 μm.

In terms of nomenclature, according to the column inner diameter (i.d.) and mobile phase flowrate, nano-liquid chromatography (nano-LC) is commonly used for describing systems with capillary columns up to 100-μm i.d. with a flowrate range of nL/min ; Capillary LC (cap-LC) includes the columns with the i.d. range of 100-500 μm and a flowrate range of μL/min. Generally, packed columns, monolithic columns and open tubular (OT) columns are the three main formats of nano-LC columns. Among them, the open tubular column, as the name suggests, retains the bare capillary structure and most of them possess a thin layer of stationary phase on the inner surface of the capillary.

After the mid of 20th century , open tubular columns were used massively in gas chromatography (GC) since Golay[10] initially applied OT columns in gas chromatography (GC) at the end of the 1950s. Soon people found the OT columns can obtain higher efficiency compared to packed columns. The OT columns maintain higher permeability compared to the packed column under similar conditions, which is good for gaseous analytes to be separated. The OT columns were taking place the roles of packed columns in the field of GC.

At that moment, it was predicted that open tubular liquid chromatography (OTLC) [5,7,11-13] has high efficiencies because there is no instinct difference between gaseous mobile phase and liquid mobile phase. The main difference is that analyte diffusivities in liquid phases are 100 - 1000 times smaller than those in gas phases. The inner diameters for GC column are usually around several hundred micrometers. That means the i.d. of OTLC column must be also reduced by around 100 - 1000 times if the predicted high efficiency wants to be achieved.[14]

Even though there were constantly interests in developing coating for OTLC column during 1970s - 1980s [15], the practical studies on developing the coated columns were slowed down mainly because the reduced column i.d. in the range of sub-micrometer to several micrometers has caused challenges for preparing columns. The practical problems include low sample loadability, nano-column preparation, picoliter volume detecion and so on.

In the trial to increase the column loadability, Jorgenson *et al.*[7] increased the internal surface area of a borosilicate-glass capillary for around 30 times by leaching non-silica compounds in the capillary with hydrochloric acid at high temperature. Pesek and Matyska[16,17] used ammonium hydrogen difluoride to etch a 400-μm i.d. capillary column and 1000-fold increased internal surface area was obtained. The freshly etched internal wall of capillary become porous and suitable for chemical bonding of stationary phase. Those efforts of changing the smooth geometry of the internal surface of the OT columns into porous structure do help to increase the retention of analyte in the separation. Another option is to form a porous polymer layer on the interior wall of a fused silica capillary, which increases the loadbiliy.[4,6,18,19] Those types of columns are now named as porous layer open tubular (PLOT) columns. Yue *et al.* [20] carefully prepared one kind of PLOT columns by loading a layer of poly(styrene-divinylbenzene) on the wall of the capillary. The 4.2 m × 10-μm-i.d. PLOT column with a loading capacity of ~ 50 - 100 fmol of peptides yielded a peak capacity of ~ 400 for separating a mixture of bovine serum albumin (BSA) tryptic digest and β-casein Lys-C digest. Other researchers[20,21] also showed high-peak-capacity separations by utilizing the PLOT columns.

The recent advancements in microfluidics fabrication facilitated the development of complex separation devices such as two-dimensional structures for LC separations.[22,23] Desmet *et al.*[24]

microfabricated a packed bed column with 4 cm in length and uniformly loaded with elongated pillars. Each channel was identically machined and worked as one 2.5-μm-i.d. channel of OTLC column except with turns. The device merged both the high-efficiency feature from OT format and the loadability advantages from packed-bed LC. They demonstrated efficiencies of 160 000 theoretical plates for unretained analytes and 70 000 theoretical plates for a retained Coumarin derivative.

Regarding to the channel size of the OTLC column, the closer the column i.d.. is to the range of 1 ~ 2 μm, the efficiency is predicted to be better as previously mentioned above if all the other coating conditions are the same. Forster *et al.*[2] compared OT columns of different i.d. (10 μm, 15 μm and 20 μm) with a 100-μm-i.d. silica monolith capillary column. According to the dimensionless column efficiency and retention time, the 10-μm-i.d. OTLC column presented better kinetic performance when compared to the other columns with larger i.d. Reducing the column diameter is important for increasing the separation efficiencies. With careful column treatment, the smaller i.d. of the column was successfully made in our lab. Huang *et al.* [25]shows similar trend from the inner diameter change. (Fig. 1-1) Using a 2-μm-i.d. column, a mixture of 11 labeled amino acids were all baseline resolved. While using a 5-μm-i.d. column, most peaks were unresolved. When a 10-μm-i.d. column was tested, poorer separation efficiency as expected was observed. This might lead one way for the future development of OTLC.

Recently, our group developed a series of techniques to reliably coat the 2-μm-i.d. reverse phased capillary column. Since the i.d. is much smaller than conventional nano-LC column, we termed it narrow open tubular liquid chromatography (NOTLC) column. To detect the molecules in such a tiny channel, we utilized the home-made laser induced fluorescent (LIF) detector to

analyze the fluorophore-labeled biomolecules. Ultra-high efficiency separation was obtained via the NOTLC column under optimal conditions. Also, ultra-fast separation based on the same technique was achieved. However, the major issue related to the extremely narrow capillary (< 2 μm) is that the required pressure (either for coating or running the separation) is much higher (up to 4000 psi) to run at a greatly lower flow rate (up to hundreds of pL/min). Another challenge caused from the reduced column i.d. is that the required sample volume decreases to even picoliter levels. Thus, to precisely control the injected sample volume and dead volume in the system become one of the tasks need to be solved in NOTLC studies. In this dissertation, solutions for the mentioned challenges are addressed. The goal is to develop a NOTLC column combined with powerful detectors (e.g. LIF, MS, etc.) for resolving many complex bio-samples.

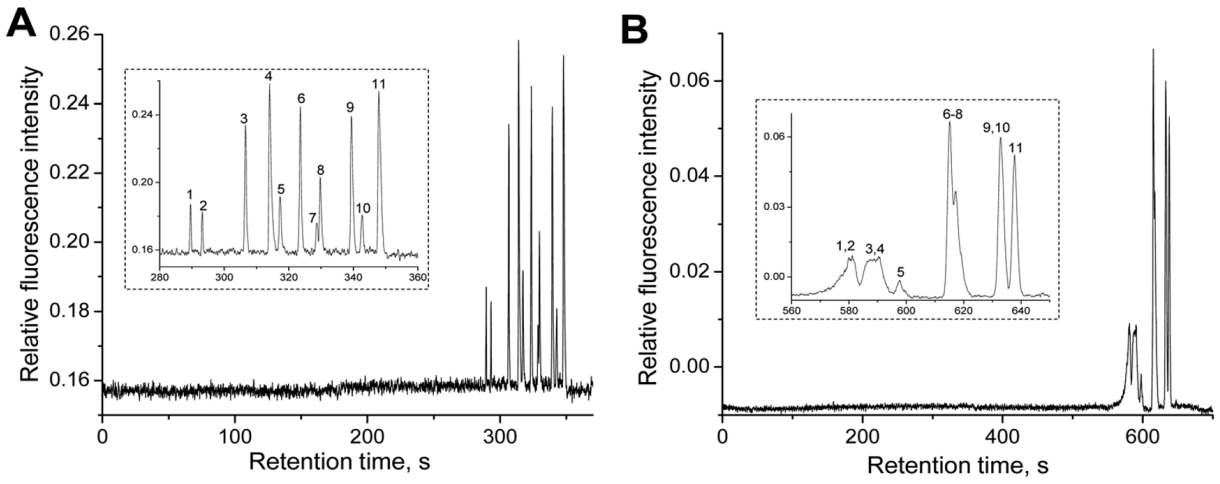

Figure 1-1. Effect of inner diameter on resolution from OT column.

The chromatograms from NOTLC columns with different inner diameters. The 48 x 2-μm-i.d. NOTLC column (left) and 48 x 5-μm-i.d. column (right) were both 44 cm effective length and 150 μm o.d. The gradient profile for both was the same: mobile phase B 0% to 50% from 0 to 1.5

min, stayed at 50% B from 1.5 min to 2 min, then decreased from 50% to 0% from 2 min to 2.5 min. For separation using the 5-μm-i.d. column, the elution pressure was 100 psi and concentration of each amino acid was 0.3 μM. For separation using the 2-μm-i.d. column, the elution pressure was 600 psi and sample concentration was 6.5 μM. Figure with permission from Elsevier (Ref. 25).

1.2. Open tubular (OT) capillary column preparation

1.2.1. Stationary phase by chemical bonding

The stationary phases are the layer(s) loaded in the internal wall of capillary columns. Typical chemical bonding interaction for fixing the stationary phase is through the covalent bond. The most popular capillaries available today are made from fused silica with polyimide coating outside. The chemistry reactions for chemical bonding generally involve the activation of the silanol groups on the inner wall of capillaries, silanization reactions for covalently bonding and subsequential attachment of other stationary phase moieties.

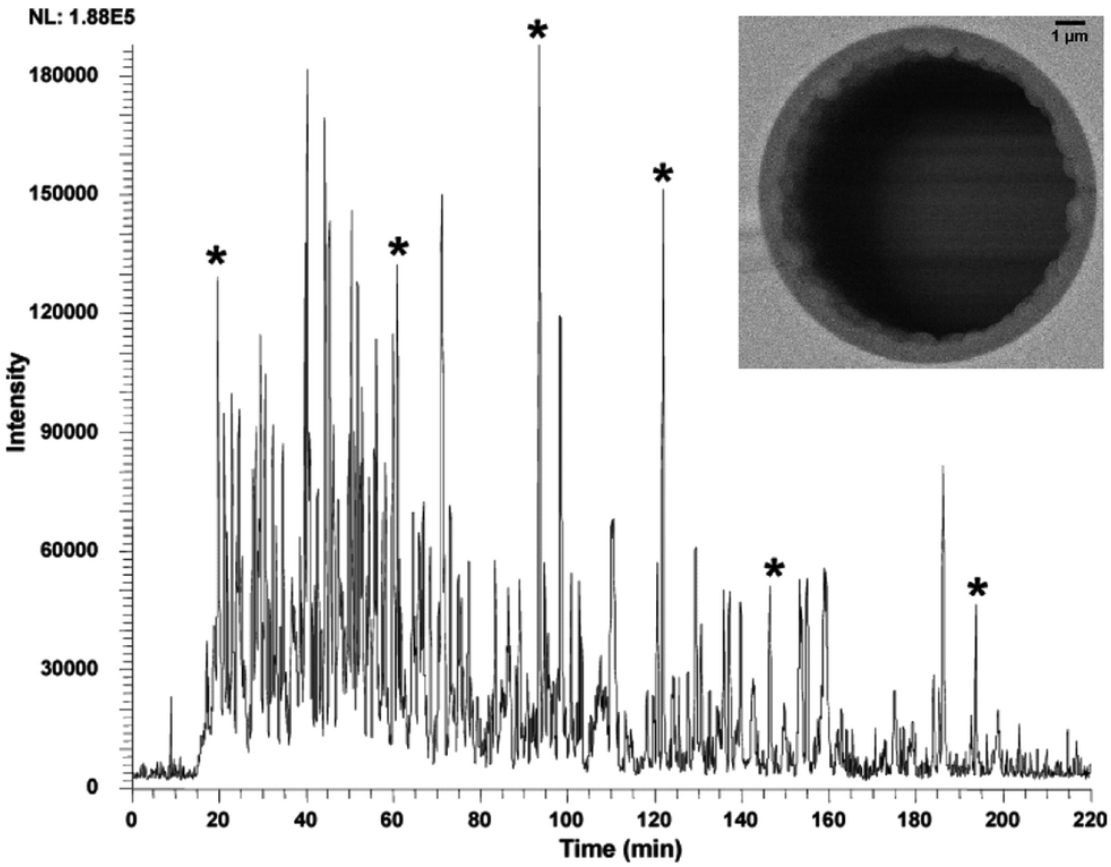

Figure 1-2. Schematic of typical PLOT column and separation chromatogram with MS

The chromatogram from the microSPE-nano-LC/ESI-MS analysis of a 4-ng tryptic digest of a single SDS-PAGE cut of *M. acetivorans*. The PLOT column dimension: 4.2 m × 10 µm ID PLOT column. The insect at the right corner shows the SEM image for the middle section of the PLOT column. Figure with permission from Ref. 20 from Elsevier.

1.2.1.1. Polymer open tubular and Polymer-based porous layer open tubular (PLOT) columns.

Due to the relatively simplified synthesis procedure, polymer PLOT columns are one of the most popular bonded porous layer OT column formats. Compared to other coating materials like inorganic compounds and physical structures such as pore, meso pore and globule size, polymer PLOT columns are easier for developing specific coatings and more capable of separating wide range of analytes. Even though the polymer layer coated in the PLOT column is typically thin

layer, the coating is fairly stable under some extreme conditions, such as high or low pH of mobile phase, wide range of temperature changes or corrosive analytes.[14] Generally, based on the chemical properties of the polymerization reagents, there are two kinds of solutions that involved in the polymerization procedure, monomer mixtures (polymerized inside of the capillary), and preformed polymers (polymerized outside of the column).[26] After the polymerization reagents (premixed or individual) are loaded into the activated capillary, polymerization reaction can be initiated by thermal change or photo irradiation.[14] The typical reagents include monomers, porogenic agents and free radical initiators for the polymerization in columns. Compared to full polymer monolith columns, the monomer-mixed PLOT columns have higher chance of clogging because the polymerization rates are easily affected by many factors (e.g. temperatures, concentrations of the reagents, etc.) resulting in varying thicknesses of the layer or pore distributions.

A significant amount of works on polymerization of PLOT columns were carried out by the group from Karger *et al*.[20]. The group also contributed on coupling the PLOT columns with one of the most powerful detectors, electrospray ionization mass spectrometry (ESI-MS).[21] 10-μm-i.d. columns were utilized for multi-dimensional LC separations and tandem LC-MS. The PLOT columns were made through the polymerization of a styrene-divinylbenzene mixture in fused silica capillaries at 74 °C for 16 hours. The Fig. 1-2 shows a scanning electron microscope (SEM) image of the polymer layer in their PLOT columns.

1.2.1.2. Silica-based open tubular (OT) columns

Another material that is widely used in open tubular, monolithic and packed columns is silica. For those OT columns utilizing silica as the stationary phase, better solvent compatibility and higher structural stability are shown when compared to those columns with polymer stationary phase. [27] Also, when the i.d. of the capillary column goes down to the range of sub to 10 μm, the thickness of the thin layer of the silica OT is easier to control compared to PLOT.

However, silica-based substrates are sensitive to extreme change of pH value (lower than pH=2 or higher than pH=8), which can cause bond-breaking for the surface groups and the silica surface may dissolve. Also, the procedures (sol-gel methods) for fabricating the silica-based OT columns are more tedious compared to that of polymer-based OT columns.[15] Complicated steps in the coating process often mean poorer reproducibility for making columns in a mass production.

Forster *et al*.[28] contributed a typical sol-gel procedure to make monolith silica-based PLOT column. The group improved the solution composition of tetramethoxysilane and polyethyleneglycol for coating. Porous layer of silica was loaded on the inner wall of capillary columns. Fig. 1-3 presents the SEM images of the middle sections of the silica-based OT columns with different i.d. (100 μm, 50 μm and 15 μm). When the other reaction condition is the same, porous aggregates are more easily accumulated in channels with larger i.d. A thin and uniform layer of porous silica was observed in 15-μm-i.d. column, which implies that using column with narrow i.d. is helpful for controlling coating quality.

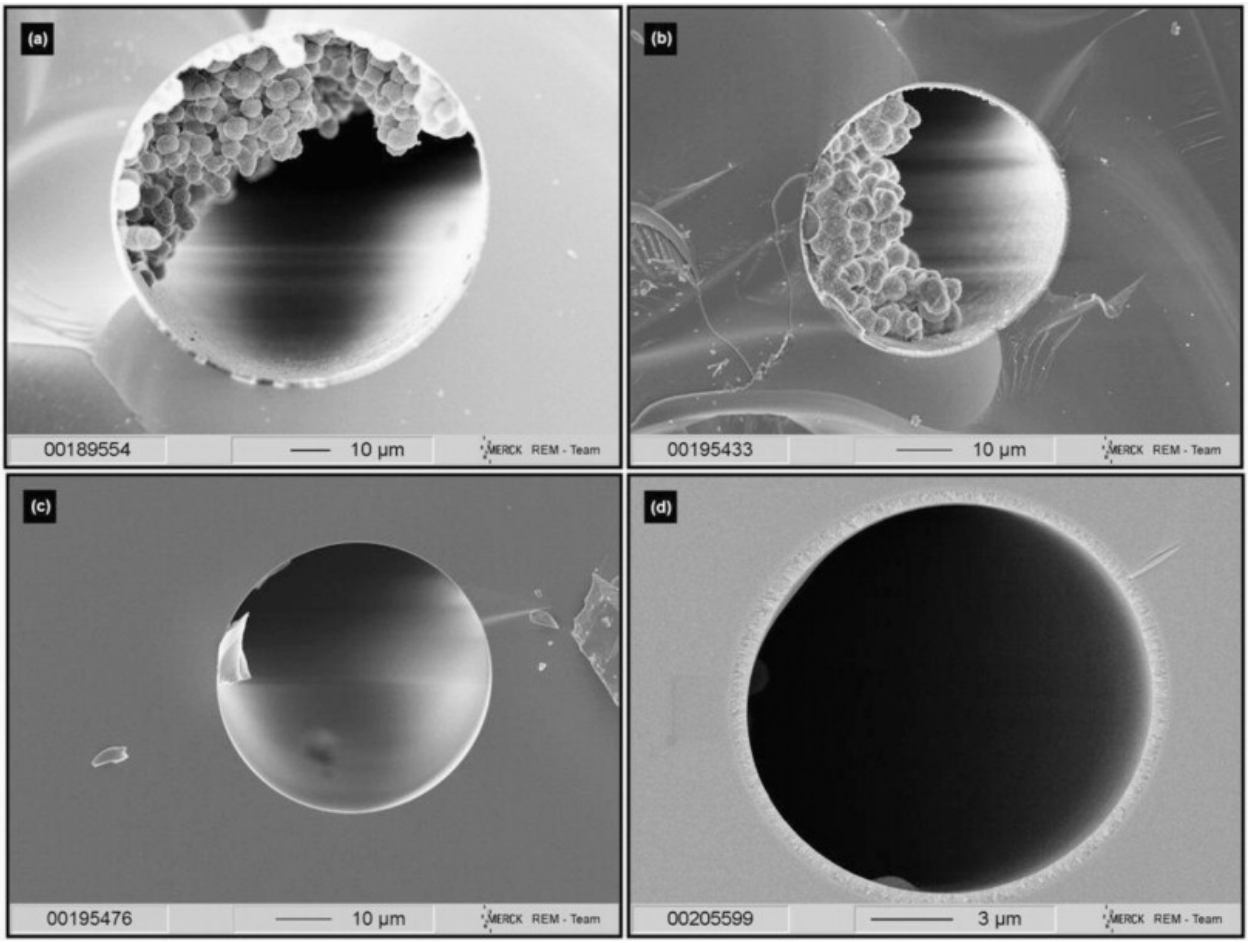

Figure 1-3. SEM images of capillary samples with different i.d.

Schematic illustration shows silica-based OT column with different i.d. (a) 100 µm i.d., (b) 50 µm i.d., (c) 50 µm i.d. after nitrogen treatment and (d) 15 µm i.d. Figure with permission from Ref. 28 from Elsevier (license # 4821480950343).

1.2.2. Stationary phase by physical absorption

Noncovalent coating means there is only physical absorption for immobilizing the coating layer(s) on the wall of OT columns. A typical method named layer-by-layer assembly is used for loading the functional groups with specific properties onto a surface via electrostatic or non-electrostatic interactions. Even though the defective part is that the durability and reproducibility

is not as good as the those chemically bonded OT columns, physical absorption methods exhibited the potential for diverse material choices, fabricating methods, resulting in more applications in the separations fields.[29,30]

Dasgupta *et al.*[31-35] led series of works in the area of ion chromatography by using OT capillary columns. The stationary phase in their works consists of charged polymer layers and was fixed via physical absorption. Kubáň *et al.*[21] prepared a multi-layer structure as the coating for an anion-exchange capillary column (5 m x 75 μm). Fig. 1 - 4 shows represents the structure of the coating components. A bare capillary was initially etched and activated via several strong acids. Then a water solution dissolved with methylamine (MA) and 1,4-butanedioldiglycidylether (BDDE) was rinsed through the capillary for loading a base layer. Several sequential runs with individual MA and BDDE solutions were applied and 25 layers of MA-BDDE copolymer was formed through diepoxide-amine interactions.

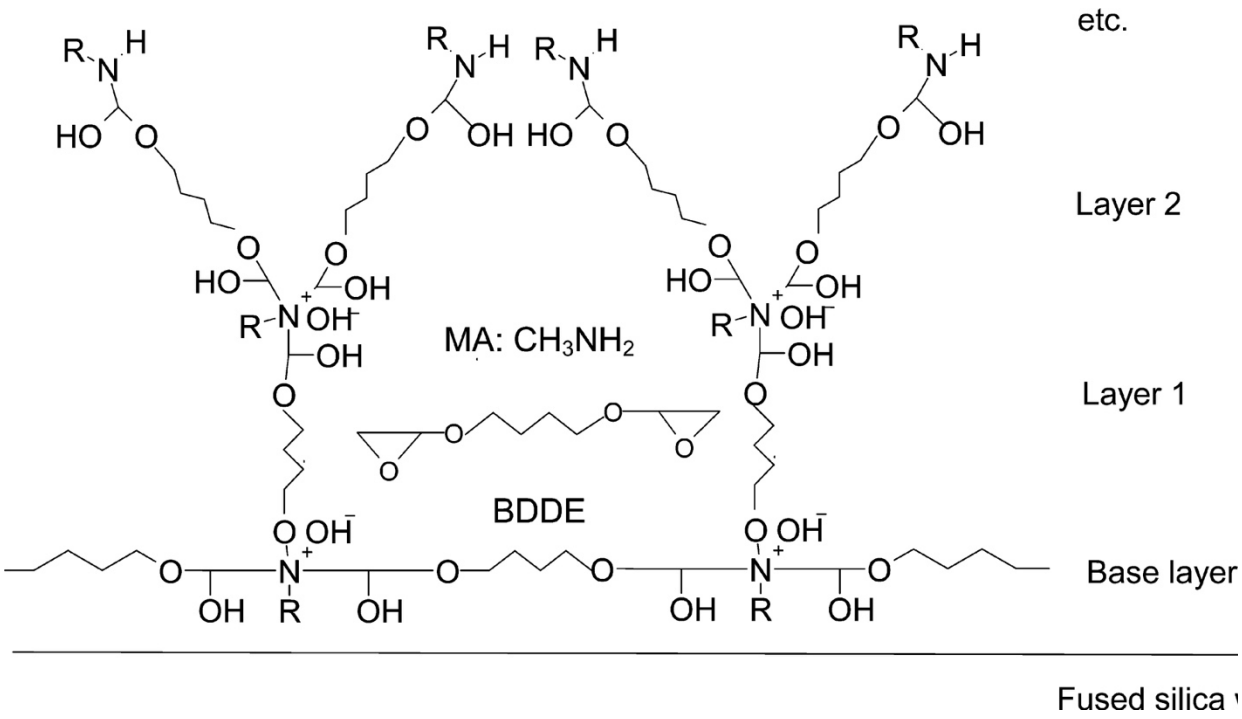

Figure 1-4. The schematic images of structure for MA-BDDE copolymer. The monomers are methylamine (MA) and 1,4-butanedioldiglycidylether (BDDE).

Figure with permission from Ref. 32 from the ACS.

1.3. Detection

Conventional detection methods, such as UV-vis absorbance, evaporative light scattering detection (ELSD) and conductivity, are widely used in LC separation. When the conventional detection methods are applied in cap-LC or nano-LC, smaller injection volumes are required and thus, as a result, miniaturized detection flow cells are needed. Therefore, flow-cells for off-column detection in nano-LC are miniaturized to the nanoliter scale to prevent the extra dead volume. Another alternative for detection in nano-LC, specifically NOTLC, is to apply the on-

column detection, which directly uses part of the capillary (often the end part) as the detection window. On-column detection is significantly decreasing the extra-column dispersion.[36]

However, no matter off-column or on-column detection is employed, with such small sample volumes, better sensitivity of the detector is required. If there is a need, there is a solution. More sensitive detection methods have been used in the nano-scale detection, especially fluorescence detection (FLD) and electrochemical detection (ECD).

1.3.1. UV-vis Detection

The UV-vis spectrometer is the most commonly utilized detector in cap-LC because most solutes can be detected with a UV-vis wavelength change. There are many OTLC applications involving UV-vis as the detection approach, such as proteins and their digested fractions,[14,37] organic small molecules,[38-41] and chiral compounds.[42,43]

However, when the sample volume goes down to a few nano liters, the UV-vis detector is not a good choice due to limitations of the sensitivity. S. E. Moring *et al.* [44] introduced a "Z-shaped" cell for the capillary electrophoresis detection to improve the poor concentration sensitivity. The optical enhancement of the cell improves the signal-to-noise ratio (MDC 10^{-8} M) for more than 10 times over that of a conventional cell with sapphire ball optics. (Fig. 1-5)

To further diminish the broadening of chromatographic peaks, on-column UV-vis detection was applied to OTLC, usually by removing a small portion of the polyimide coating of the capillary column as a detection window. This time, the sensitivity is increased and only limited to the internal diameter of the capillary column.

Nowadays, photodiode array detections (PDA) have become more and more popular for UV-vis detectors due to several advantages, such as simultaneous multi-wavelength measurement, wavelength precision, high sensitivity and minimal stray light. (Fig. 1-6) A good example is that Ali *et al.* [45] utilized the on-column PDA in capillary electrophoresis (CE) analysis for 5 peptides.

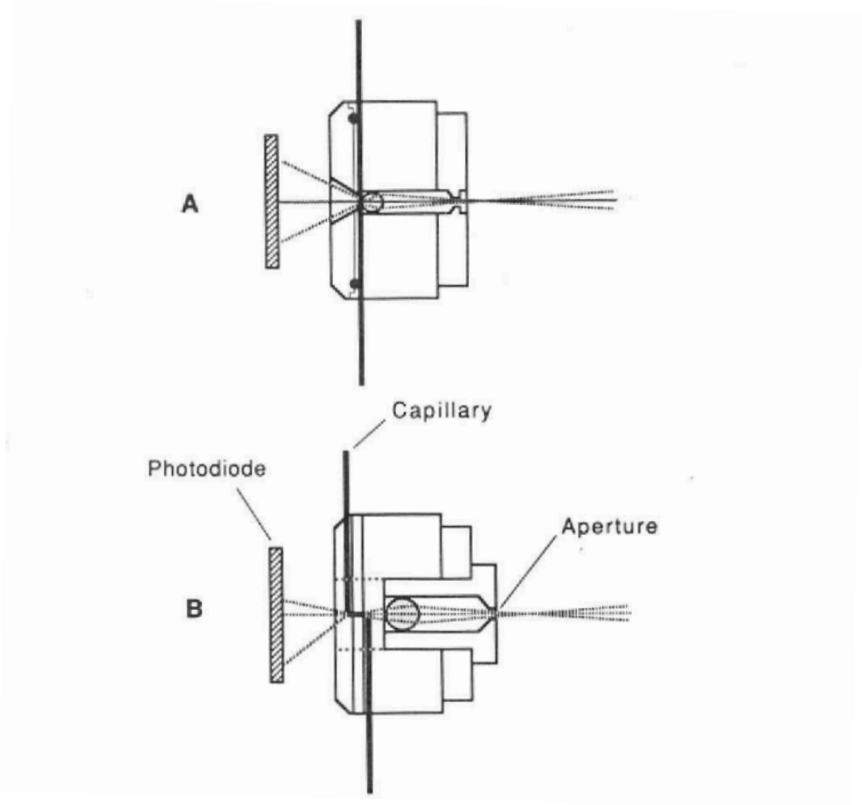

Figure 1-5. UV-vis for off-column cap-LC detection

The schematic figure illustrates optical designs for UV-vis flow cells: (A) optical cell with a 2-mm sapphire ball lens and a 0.5-mm aperture in front of a capillary window; (B) Z-cell with a 4-mm quartz ball lens and 1.5-mm aperture. Figure is from Ref. 44 with permission from the ACS.

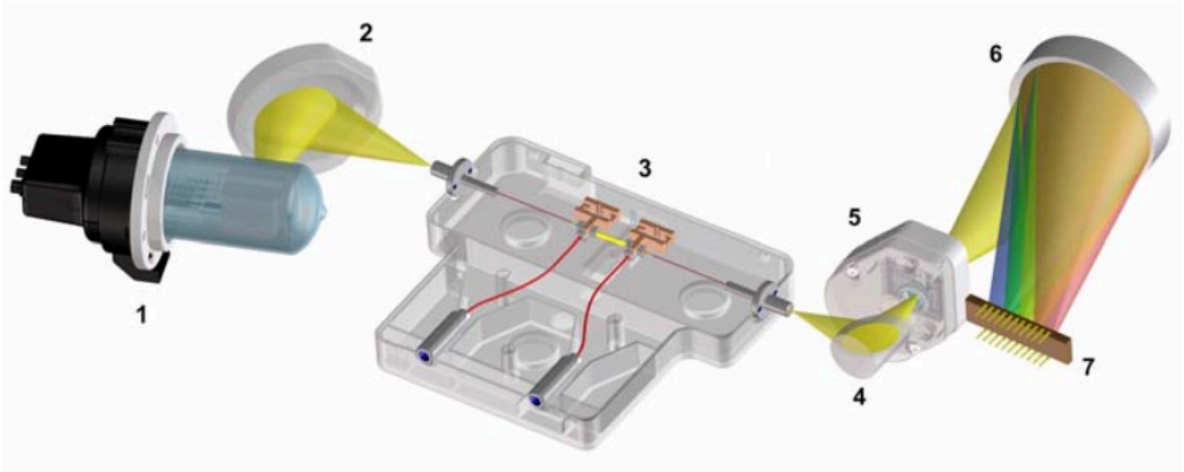

Figure 1-6. Agilent UV-vis PDA for on-column nano-LC detection

Figure is from Agilent InfinityLab LC Series Diode Array Detectors User Manual from Agilent Technologies.

1.3.2. Evaporative light scattering detection (ELSD)

Evaporative light scattering detection (ELSD) has been utilized widely for liquid chromatography and supercritical chromatography.[46] The working principle for ELSD is to nebulize the solvent from the LC flow and entrain the formed droplets into a gas stream to the detecting area where photomultiplier picks up the signals from the scattered light beam. Zhou *et al.*[47] introduced an evaporative light scattering detector coupled with CE or cap-LC (Fig. 1-7). An optimal microfluidic evaporative light scattering detection (μELSD) linearity as 3 orders of magnitude (0.2-40 ng; R^2 = 0.9998) was obtained and the limit of detection for glucose with a capillary column goes down to 100 pg.

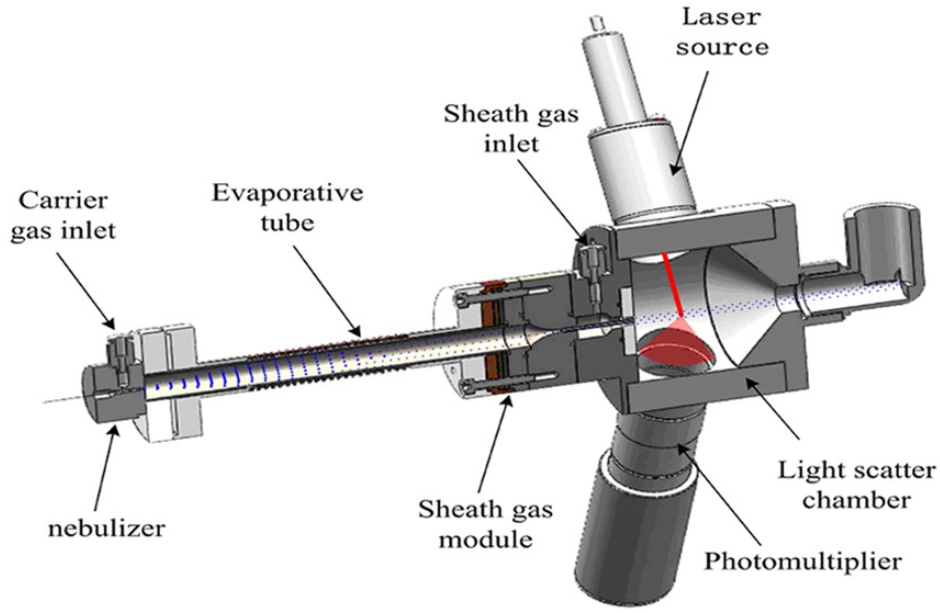

Figure 1-7. ELSD for cap-LC

Schematic illustration of the inner view of a microfluidic evaporative light scattering detector (μELSD). Figure with permission from Ref. 47 from the ACS.

1.3.3. Fluorescence detection (FLD)

One powerful detection approach that has been used in OTLC system, especially for narrow capillary columns (i.d. < 5 μm) is fluorescence detection. Even though one downside is the analytes are required to either have a native fluorophore or to be derivatized to introduce a fluorophore, FLD is still a very useful detection method for small volume of sample within narrow optical length due to its sensitivity and simplicity. Compared to the two major methods mentioned above, the minimal detection level of FLD can go much lower (~yoctomole), which helps to fully explore the potential capability of the NOTLC.

Weaver *et al.*[48] described a bare narrow capillary hydrodynamic chromatography (BaNC-HDC) system with a laser induced fluorescence (LIF) detector (Fig. 1-8). The LIF detector was optimized well and tested. It turned out that the system obtained very low limit of detection (~ 70 fluorescein molecules). Also, the more than 3 orders of magnitude linear dynamic range were validated.

For labelling of proteins, Wang *et al.*[35] used the commercialized ATTO-TAG™ kit and potassium cyanide (KCN) to label the protein samples, including transferrin, α-lactalbumin, insulin, and α-2-macroglobulin. The researchers achieved a baseline resolution for a protein sample from femtoliter to picoliter.

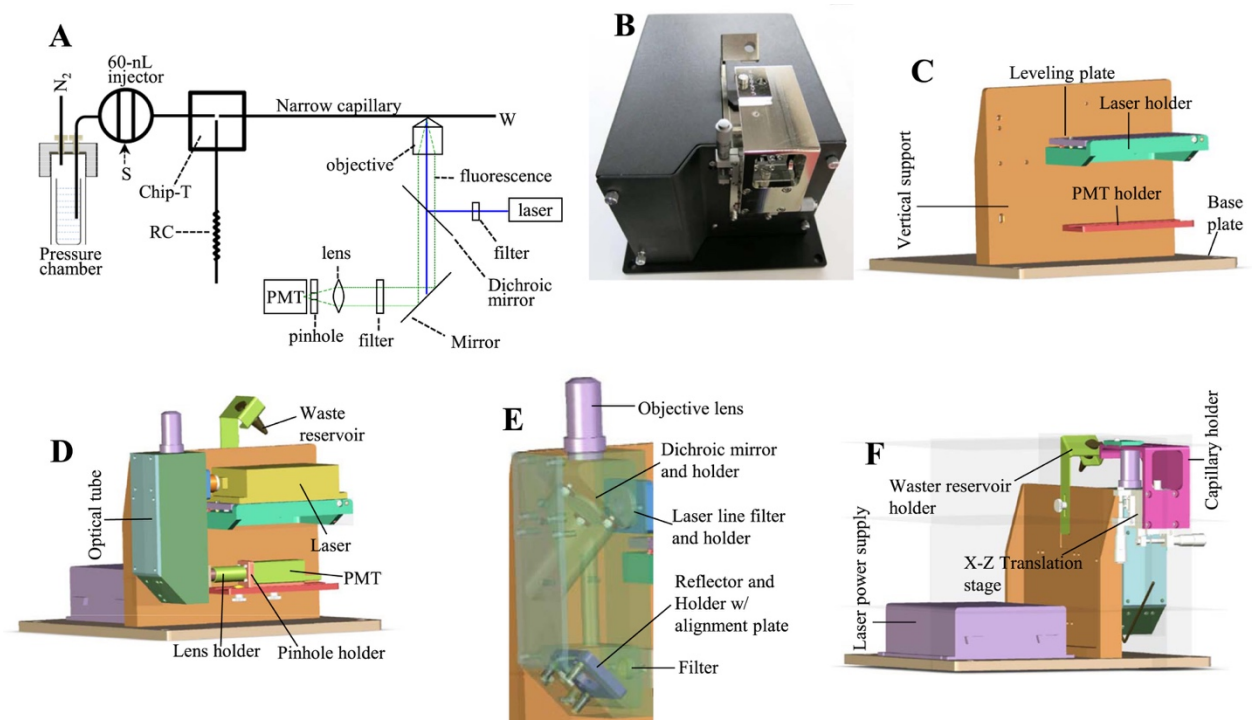

Figure 1-8. Bare narrow capillary hydrodynamic chromatography (BaNC-HDC) system with Laser induced fluorescence (LIF) detector[48]

Schematic illustration shows laser induced fluorescence detector. (A) apparatus for testing hydrodynamic chromatography (B) top-view of the real LIF detector. (C) structure of the backbone. (D) individual components in the detector. (E) the arrangement of the optical parts in the detector. (F) view from the back side of the system. Figure with permission from Ref. 48 from Elsevier (license # 4821481377865).

1.3.4. Electrochemical detection (ECD)

Electrochemical detection (ECD) can only be applied to oxidizable/reducible solutes and can be used to detect the sample of ppb-levels. However, ECD are easily affected by changes in temperature and pH of the sample matrix. Also, the contaminated electrodes may give poor reproducibility and loss of sensitivity.

1.3.5. Capacitively coupled contactless conductivity detector (C^4D)

The capacitively coupled contactless conductivity detector (C^4D) was initially introduced in 1998 to monitor concentration change of targeted samples for capillary electrophoresis.[33] C^4D detector allows the detection of small inorganic ions and organic and biochemical species without invasion to the liquid loop or sample. The C^4D device is more and more popular in the detection of ionic compounds,[49-51] because it is durable, cheap, robust and contactless to analytes. However, the sensitivity and limit of detection is not competitive as other detectors mentioned in this paper.

1.3.6. Mass spectrometer (MS)

When LC, a powerful separation tool is coupled to mass spectrometer (MS), a powerful analyzer, a field will be greatly improved. [52]

Commonly, if a HPLC column needs to couple to an electrospray ionization mass spectrometer (ESI-MS), the flow rate match between the LC and MS is a key part. Therefore a splitting tee is used to split the flow that directly goes into the MS sample injection cone because relative low flow rates help increase sensitivity and reduce ion suppression. While for OTLC, especially NOTLC, the flow-rate scale seems born to be compatible with ESI-MS. Different MS analyzers such as ion traps, orbitraps, quadrupoles and time-of-flight (TOF), have now been widely used based on the detection requirement. MS/MS or MS^n fragmentations can be effectively achieved by collision-induced dissociation (CID), electron-capture dissociation or electron-transfer dissociation (ETD). High-resolution separation based upon OTLC have been achieved through tandem mass analyzers in the area of proteomic analysis. [53,54] The main issue now for effectively coupling the NOTLC with ESI-MS is the precise control of picoliter flowrate and stability of the ionization efficiency.

1.4. Dissertation Synopsis

The objective of this dissertation is to investigate the separation mechanism of NOTLC column, optimze the separation of NOTLC and develop a series of reliable methods for coating the columns.

In Chapter 2, the focusing effects in NOTLC were identified and these effects were used to interpret the exceptionally sharp peaks obtained from “isocratic” NOTLC. Based on this focusing mechanism, a simple and economic approach to perform pico-gradient NOTLC was developed.

In Chapter 3, the predicted potential of NOTLC was experimentally demonstrated. High peak capacities (1900 - 2000 for digested Escherichia coli lysate in 3 h) were obtained by using a 2-μm-i.d. × 75 cm long capillary column coated with trimethoxy(octadecyl)silane. Also the ultrafast separation has been achieved by using a 2-μm-i.d. × 2.7 cm. A mixture of six amino acids was separated and resolved within ~400 ms under a pressure of ~230 bar.

In Chapter 4, the procedure of coating the NOTLC column was demonstrated in detail. Various coating parameters (reagent concentration, coating temperature, reagent flushing pressure and time) were optimized. For all optimizations, the mixtures of amino acids were used for targeted high resolutions. The coating reproducibility was tested by selecting 8 columns from 4 different batches and using them to separate an amino acid mixture. A relative standard deviation of <0.2% for retention times and a relative standard deviation of <11% for peak areas were obtained. Last, the columns prepared under the optimized conditions were utilized to separate a pepsin and trypsin digested Escherichia coli (E. coli) lysate. The results including a peak capacity of 770 within 47 min (using a 45-cm-long column) and a peak capacity of 1900 within 158 min (using a 155-cm-long column) were obtained.

In chapter 5, There is a concise conclusion for reviewing of all the projects mentioned above. In an optimistic view, the predicted and validated features of NOTLC will be utilized in more analytical applications soon once the combination of NOTLC with MS is tuned well.

References

(1) Jorgenson, J. W. *Annual review of analytical chemistry* **2010**, *3*, 129-150.
(2) Forster, S.; Kolmar, H.; Altmaier, S. *J. Chromatogr. A* **2013**, *1315*, 127-134.
(3) MacNair, J. E.; Lewis, K. C.; Jorgenson, J. W. *Anal. Chem.* **1997**, *69*, 983-989.
(4) Knox, J. H.; Gilbert, M. T. *J. Chromatogr. A* **1979**, *186*, 405-418.
(5) Knox, J. H. *J. Chromatogr. Sci.* **1980**, *18*, 453-461.
(6) Guiochon, G. *Anal. Chem.* **1981**, *53*, 1318-1325.
(7) Jorgenson, J. W.; Guthrie, E. J. *J. Chromatogr. A* **1983**, *255*, 335-348.
(8) Xiang, P.; Yang, Y.; Zhao, Z.; Chen, A.; Liu, S. *Anal. Chem.* **2019**, *91*, 10518-10523.
(9) Causon, T. J.; Shellie, R. A.; Hilder, E. F.; Desmet, G.; Eeltink, S. *J. Chromatogr. A* **2011**, *1218*, 8388-8393.
(10) Golay, M.; In, E.; NewYork: Academic Press, 1958.
(11) Tock, P.; Stegeman, G.; Peerboom, R.; Poppe, H.; Kraak, J.; Unger, K. *Chromatographia* **1987**, *24*, 617-624.
(12) Crego, A. L.; Diez-Masa, J. C.; Dabrio, M. V. *Anal. Chem.* **1993**, *65*, 1615-1621.
(13) Guo, Y.; Colon, L. A. *Anal. Chem.* **1995**, *67*, 2511-2516.
(14) Collins, D. A.; Nesterenko, E. P.; Paull, B. *Analyst* **2014**, *139*, 1292-1302.
(15) Knob, R.; Kulsing, C.; Boysen, R. I.; Macka, M.; Hearn, M. T. *TrAC Trends in Analytical Chemistry* **2015**, *67*, 16-25.
(16) Pesek, J. J.; Matyska, M. T. *J. Chromatogr. A* **1996**, *736*, 255-264.
(17) Onuska, F.; Comba, M.; Bistricki, T.; Wilkinson, R. *J. Chromatogr. A* **1977**, *142*, 117-125.
(18) Tijssen, R.; Bleumer, J.; Van Kreveld, M. *J. Chromatogr. A* **1983**, *260*, 297-304.
(19) Kennedy, R. T.; Oates, M. D.; Cooper, B. R.; Nickerson, B.; Jorgenson, J. W. *Science* **1989**, *246*, 57-63.
(20) Yue, G.; Luo, Q.; Zhang, J.; Wu, S.-L.; Karger, B. L. *Anal. Chem.* **2007**, *79*, 938-946.
(21) Rogeberg, M.; Wilson, S. R.; Greibrokk, T.; Lundanes, E. *J. Chromatogr. A* **2010**, *1217*, 2782-2786.
(22) He, B.; Tait, N.; Regnier, F. *Anal. Chem.* **1998**, *70*, 3790-3797.
(23) De Malsche, W.; Eghbali, H.; Clicq, D.; Vangelooven, J.; Gardeniers, H.; Desmet, G. *Anal. Chem.* **2007**, *79*, 5915-5926.
(24) Desmet, G.; Callewaert, M.; Ottevaere, H.; De Malsche, W. *Anal. Chem.* **2015**, *87*, 7382-7388.
(25) Chen, H.; Yang, Y.; Qiao, Z.; Xiang, P.; Ren, J.; Meng, Y.; Zhang, K.; Lu, J. J.; Liu, S. *Analyst* **2018**, *143*, 2008-2011.
(26) Tarongoy Jr, F. M.; Haddad, P. R.; Boysen, R. I.; Hearn, M. T.; Quirino, J. P. *Electrophoresis* **2016**, *37*, 66-85.
(27) Lam, S. C.; Rodriguez, E. S.; Haddad, P. R.; Paull, B. *Analyst* **2019**, *144*, 3464-3482.
(28) Forster, S.; Kolmar, H.; Altmaier, S. *J. Chromatogr. A* **2012**, *1265*, 88-94.
(29) Decher, G. *Science* **1997**, *277*, 1232-1237.
(30) Richardson, J.; Bjornmalm, M.; Caruso, F. *CAS PubMed Article*.
(31) Kuban, P.; Dasgupta, P. K. *J. Sep. Sci.* **2004**, *27*, 1441-1457.
(32) Kubáň, P.; Dasgupta, P. K.; Pohl, C. A. *Anal. Chem.* **2007**, *79*, 5462-5467.
(33) Kubáň, P.; Hauser, P. C. *Anal. Chim. Acta* **2008**, *607*, 15-29.

(34) Kubáň, P.; Pelcová, P.; Kubáň, V.; Klakurková, L.; Dasgupta, P. K. *J. Sep. Sci.* **2008**, *31*, 2745-2753.
(35) Wang, X.; Cheng, C.; Wang, S.; Zhao, M.; Dasgupta, P. K.; Liu, S. *Anal. Chem.* **2009**, *81*, 7428-7435.
(36) Zhang, Q.; Xu, L.; Zhou, Z.; Yang, L.; Wang, Q.; Zhang, B. *J. Chromatogr. A* **2014**, *1362*, 225-230.
(37) Nesterenko, E.; Yavorska, O.; Macka, M.; Yavorskyy, A.; Paull, B. *Anal. Methods* **2011**, *3*, 537-543.
(38) Peng, L.; Zhu, M.; Zhang, L.; Liu, H.; Zhang, W. *J. Sep. Sci.* **2016**, *39*, 3736-3744.
(39) Wang, H.; Yao, Y.; Li, Y.; Ma, S.; Peng, X.; Ou, J.; Ye, M. *Anal. Chim. Acta* **2017**, *979*, 58-65.
(40) Ying, L.-L.; Wang, D.-Y.; Yang, H.-P.; Deng, X.-Y.; Peng, C.; Zheng, C.; Xu, B.; Dong, L.-Y.; Wang, X.; Xu, L. *J. Chromatogr. A* **2018**, *1544*, 23-32.
(41) Qu, Q.; Gu, C.; Gu, Z.; Shen, Y.; Wang, C.; Hu, X. *J. Chromatogr. A* **2013**, *1282*, 95-101.
(42) Zaidi, S. A.; Cheong, W. J. *J. Sep. Sci.* **2008**, *31*, 2962-2970.
(43) Aydoğan, C. *Chirality* **2018**, *30*, 1144-1149.
(44) Moring, S. E.; Reel, R. T.; van Soest, R. E. *Anal. Chem.* **1993**, *65*, 3454-3459.
(45) Ali, A.; Cheong, W. J. *J. Sep. Sci.* **2017**, *40*, 2654-2661.
(46) Lucena, R.; Cardenas, S.; Valcarcel, M. *Anal. Bioanal. Chem.* **2007**, *388*, 1663-1672.
(47) Zhou, W.; Kan, W.; Wang, Y.; Liu, Y.; Wang, Y.; Yan, C. *Anal. Chem.* **2015**, *87*, 9329-9335.
(48) Weaver, M. T.; Lynch, K. B.; Zhu, Z.; Chen, H.; Lu, J. J.; Pu, Q.; Liu, S. *Talanta* **2017**, *165*, 240-244.
(49) Huang, X.; Foss Jr, F. W.; Dasgupta, P. K. *Anal. Chim. Acta* **2011**, *707*, 210-217.
(50) Zhang, M.; Yang, B.; Dasgupta, P. K. *Anal. Chem.* **2013**, *85*, 7994-8000.
(51) Huang, W.; Dasgupta, P. K. *Anal. Chem.* **2016**, *88*, 12021-12027.
(52) Desmet, G.; Eeltink, S. *Anal. Chem.* **2013**, *85*, 543-556.
(53) Hustoft, H. K.; Brandtzaeg, O. K.; Rogeberg, M.; Misaghian, D.; Torsetnes, S. B.; Greibrokk, T.; Reubsaet, L.; Wilson, S. R.; Lundanes, E. *Scientific reports* **2013**, *3*, 3511.
(54) Rogeberg, M.; Vehus, T.; Grutle, L.; Greibrokk, T.; Wilson, S. R.; Lundanes, E. *J. Sep. Sci.* **2013**, *36*, 2838-2847.

Chapter2. On-column and gradient focusing-induced high-resolution separation in narrow open tubular liquid chromatography and a simple and economic approach for pico-gradient separation

This project was a collaborative work that consists of the following authors: Yu Yang, Piliang Xiang, Huang Chen, Zhitao Zhao, Zaifang Zhu, Shaorong Liu

Piliang Xiang conducted the gradient flow injection valve installation and adjustment.

Zhitao Zhao assisted the parking experiment.

Huang Chen and Zaifang Zhu optimized the labeling procedure for amino acids.

All the rest of the work was done by Yu Yang.

2.1. Abstract

We have recently obtained extraordinarily high efficiencies and sharp peaks using narrow open tubular liquid chromatography (NOTLC) columns for liquid chromatographic separations. On-column focusing is commonly observed in liquid chromatography, but this effect alone could not satisfactorily explain the sharpness of these peaks. In this work we investigated the reasons that could have led to the peak sharpness. We hypothesized initially that analytes confined in a NOTLC column might have significantly reduced analyte diffusivities and the reduced diffusivities consequently resulted in the peak sharpness. This hypothesis was invalidated immediately after we measured the diffusion coefficients and did not notice any noticeable diffusivity increases of the analytes inside such columns. We then designed an experiment and revealed a “re-focusing effect”. Investigation of this re-focusing effect eventually led us to the observation of a gradient focusing caused by the composition difference between the eluent and the sample matrix. It was this gradient focusing that had contributed primarily to the peak

sharpness. Based on this insightful understanding, we further developed a simple and economic approach to perform picogradient narrow open tubular liquid chromatographic separations.

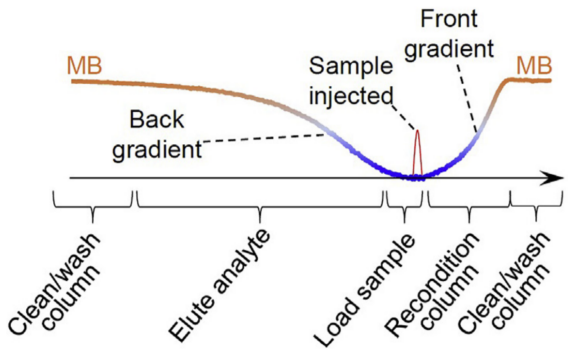

Figure 2-1. Graphic abstract

Figure with permission from Elsevier.

2.2. Introduction

We have recently obtained exceptionally sharp peaks when we used a NOTLC column for amino acid and peptide separations[1,2]. The column had an i.d. of 2 mm and often a length of 50-80 cm. Usually a few to a few hundred pL sample was injected into the column for separation, and the separation was completed in minutes under an elution pressure of a few hundred psi. The question is: what had caused these extremely sharp peaks? For an analyte in a confined space, its diffusion coefficients can be reduced significantly[3-6]. For example, the ionic diffusion of 0.05 M KCl in a 70-nm channel can be reduced to about 1% that in a bulk solution[3] , the diffusion coefficient of a protein confined in a 80-nm nanopore can be decreased by more than 99%[4,5] , and the diffusion coefficient of a lipid confined in a 9.0-nm nanopore can be reduced by a factor of 1.4[6] . The NOTLC column we used had an i.d. of 2 μm. Was the analyte diffusion slowed down inside the NOTLC column? Could the sharp peaks be resulted from reduced diffusions of

analytes confined in such a column? On-column focusing is commonly observed in liquid chromatography[7-12]. When a sample matrix has a weaker eluting power than that of a mobile phase, the width of an analyte zone will be compressed compared to that of the injected sample zone in the column. This phenomenon is called on-column focusing or preconcentration[7]. In a gradient chromatographic separation where the eluent strength (in terms of eluotropic strength) decreases from the column inlet to the column outlet, the analyte residing in front of its zone will experience a relatively weaker eluent and will be eluted forward at a slower pace and will eventually fall back into its zone. On the other hand, the analyte residing after its zone will experience a relatively stronger eluent and will be eluted forward at a fast pace and will eventually catch up with its zone. This effect is termed gradient focusing. On-column focusing often exists in a gradient elution process because analytes are highly retained in the relatively weak initial solvent composition as described by Snyder[13]. Was on-column focusing the primary contributor to the sharp peaks obtained in this experiment? In this work, we intended to answer all the above questions. After measuring the diffusion coefficients of analytes confined inside the NOTLC columns, we did not see any noticeable diffusivity increases. Therefore, the sharp peaks were not resulted from reduced diffusions of analytes in such columns. We designed an experiment and revealed a "re-focusing effect". Investigation of this re-focusing effect eventually led us to understand the occurrence of a gradient focusing effect caused by the composition difference between the eluent and the sample matrix. This gradient focusing effect turned to be the primary contributor to the sharp peaks, while on-column focusing participated in the peak sharpening as well. Nanoflow liquid chromatography is getting popularly utilized because it consumes very small amount of sample and generates minimal waste, but nanoflow gradient generation is not completely satisfactory. Cappiello *et al.*[14] employed a switching valve having a

set of injection loops prefilled with a series of eluents with increasing eluting power and programmed the valve so that the weakest eluent was delivered first, and then the next stronger eluent, and so on to the column for a multi-step gradient elution. The limited number of injection loops constrained the number of gradient profiles that could be produced. Deguchi *et al*.[15] used a ten-port switching valve with two injection loops, in conjunction with a conventional gradient delivery system, to mitigate this issue. The gradient eluent from the conventional gradient system had an increasing eluotropic power and it was delivered to the ten-port switching valve, loading the two loops alternatively. While an earlier loaded (weaker) eluent in one loop was discharged (for elution), a stronger eluent filled the other loop. Since these operations could be repeated, a large number of gradient segments could be combined to form a desired gradient profile. Brennen *et al*.[16] tested a microchip gradient generator with a purpose to particularly reduce the dead volume between the gradient front and the column and hence the delay time. In our group, we have developed a binary electroosmotic pump (EOP) gradient generator and used it for peptide separation[17]. However, robust and economic nanoflow gradient generators are still to be developed. Based on the understanding of the focusing effects involved in the NOTLC, we further constituted a simple and economic approach to perform pico-gradient OTLC. The working principle and detailed operation procedure were described as well.

2.3. Materials and methods

2.3.1. Reagents and materials

Fluorescein, amino acids, sodium hydroxide, ammonia bicarbonate, acetonitrile, toluene and trimethoxy(octadecyl) silane (C18) were obtained from Sigma-Aldrich (St. Louis, MO). ATTO-TAG™ FQ Amine-Derivatization Kit was obtained from Thermo Fisher Scientific (Waltham,

MA). All solutions were prepared using ultrapure water (Nanopure ultrapure water system, Barnstead, Dubuque, IA) and filtered through a 0.22-μm filter (VWR, TX), degassed before use. Fused-silica capillaries used for making NOTLC columns [2-μm inner diameter (i.d.), 150-μm outer diameter (o.d.)] were purchased from Polymicro Technologies, a subsidiary of Molex (Phoenix, AZ).

2.3.2. Narrow open tubular column preparation

Two pressure chambers (one reagent chamber and one waste chamber) were used for preparing NOTLC columns. A detailed configuration of the apparatus was presented in Fig. 2-2. The chambers were made of transparent acrylic. A septum was placed between the chamber base and the cap to make the chamber air-tight, and syringe(s) or a nitrogen line were connected to pressure chambers via the septum.

To prepare a NOTLC column, a 2-μm-i.d. capillary with a given length was cut and 1 cm polyimide coating at one end was removed. Referring to Fig. 2-2, two syringes were used to add/ remove solutions in/from the vials inside the pressure chambers. The N_2 lines and vents were used to control the flow of solution through the capillary. Briefly, a 25 G X 7/800 hypodermic needle was used as a guide to facilitate the insertion of this capillary through the septum into the reagent chamber holding a vial containing 50-ml 1 M NaOH solution. The other end (with polyimide coating) of the capillary was inserted into the waste chamber holding a vial containing DDI water. While nitrogen at the pressure of 500 psi was supplied to the reagent chamber to pressurize NaOH through the capillary, both pressure chambers along with the capillary were moved inside an oven at 100 °C for 2 h. The NaOH solution was then replaced with DDI water to rinse the capillary for another hour. After the entire setup was moved out of the oven, the

capillary was rinsed with acetonitrile for about 30 min at ambient temperature and dried with nitrogen overnight.

The setup was moved inside a dry glove box. A coating reagent of 50-ml trimethoxy(octadecyl) silane and 50-ml toluene was prepared in the dry glove box and placed inside the reagent chamber, and the polyimide-removed end of the capillary was dipped into the reagent. The other end of the capillary was dipped into a 0.5-ml vial containing toluene in the waste chamber. This setup was then moved into an oven set at 50 °C, a pressure of 500 psi was applied to the reagent chamber, and the coating reagent was flushed through the capillary for 16 h to coat the capillary inner wall. The coating reagent was then replaced with toluene to rinse the capillary for 1 h. The setup was then taken out of the oven. The column was ready for use after it was dried with nitrogen and the 1-cm capillary without polyimide coating was trimmed off.

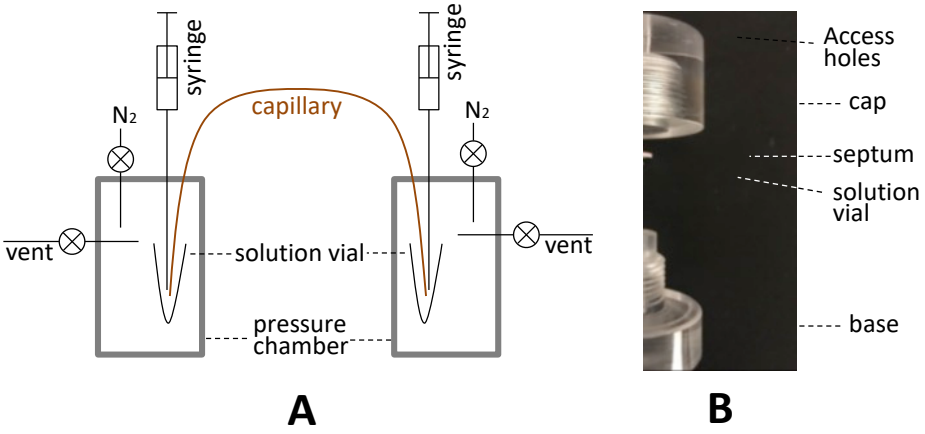

Figure 2-2. Apparatus for NOTLC column preparation.

A. Overall schematic of the apparatus. B. Exploded view of a pressure chamber. Figure with permission from Elsevier.

2.3.3. Amino acid labelling

Following the instruction provided with the ATTO-TAG™ FQ Amine-Derivatization Kit, a 10 mM ATTO-TAG™ FQ stock solution was prepared by dissolving 5.0 mg of ATTO-TAG™ FQ in 2.0 mL of methanol and stored in -20 °C before use. A 10 mM working KCN solution was prepared by diluting a 0.2 M KCN stock solution with 10 mM borax solution (pH 9.2). Amino acid stock solutions (each containing 1 mM of one amino acid) were prepared by dissolving individual amino acids in DDI water and filtered with 0.22-μm filter. A volume of 1.0 mL of the amino acid stock solution was mixed with 10 mL of the 10 mM KCN working solution, and 5 mL of the 10 mM FQ solution in a 0.25-mL vial. This mixture was maintained at room temperature for 1 h in dark environment before they were ready to test. The resulting FQ-labeled-amino acid was diluted with 10 mM NH_4HCO_3 or other indicated solution prior to analysis.

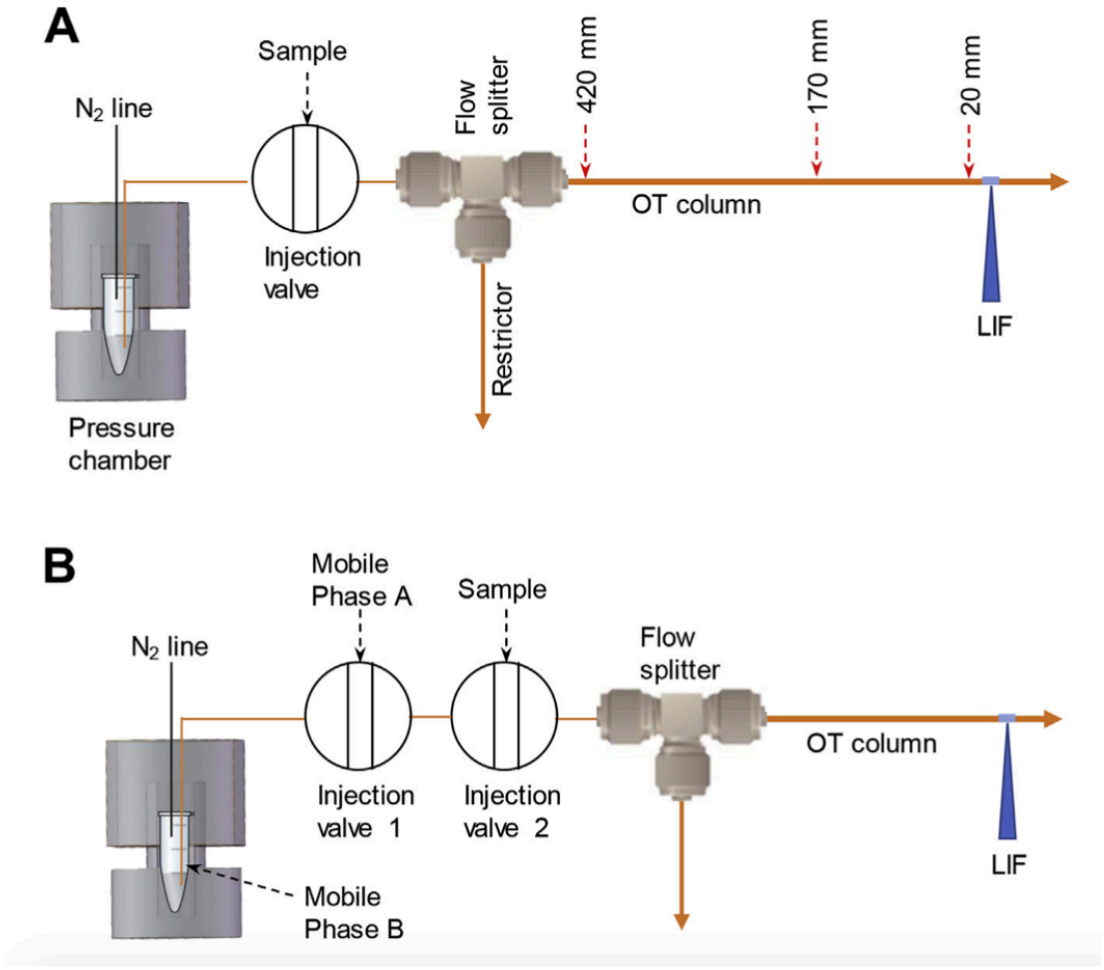

Figure 2-3. Apparatus for performing NOTLC separation.

(A) Design and construction of the pressure chamber were identical to that in Fig. 2-2. The NOTLC column had a 2-µm-i.d. and was trimethoxy(octadecyl) silane coated. Injection valves were VICI 6-port valves. The flow splitter was built using an Upchurch micro-T. A 10-cm-long and 20-µm-i.d capillary was used as a restrictor. A 200-µm-i.d. and 360-µm-o.d. capillary was used to connect the injection valve and the micro-T. Inside the flow splitter, a small portion (head) of the NOTLC column was inserted into the connection capillary to minimize the injection dead-volume. At the 5 cm from the effluent outlet of NOTLC column, a detection window was made by removing the polyimide coating. A laser-induced fluorescence detector[18] underneath the NOTLC column was used to monitor the resolved analytes. (A) Apparatus for performing isocratic NOTLC separation. Eluent was preloaded in the vial inside the pressure chamber. The dashed arrow indicates the distance between the indicated positions to the LIF detector. (B) Apparatus for performing picoflow gradient NOTLC separation. Figure with permission from Elsevier.

2.3.4. NOTLC apparatus

Fig. 2-3 presents the experimental apparatus used in this work. A pressure chamber was used for driving a mobile phase through a 6-port valve (VICI Valco, Houston, TX), via a flow splitter with a 20 mm i.d. and 20-cm-long restriction capillary, to an NOTLC column. The detection end of the column was affixed to a capillary holder on an x-y-z translation stage so that the detection window could be aligned for the maximum fluorescent output. The apparatus in Fig. 2-3A was used to perform isocratic NOTLC. An additional injection valve was included in Fig. 2-3B to facilitate gradient generations, and the apparatus in Fig. 2-3 B was utilized to perform pico-gradient NOTLC. The confocal laser-induced fluorescence (LIF) detector was described previously [1,2]. Briefly, an argon ion laser (LaserPhysics, Salt Lake City, UT) generated a 488-nm laser beam. Then the laser beam was directed by a dichroic mirror (Q505LP, Chroma Technology, Rockingham VT) and focused onto the detection window of the narrow capillary via an objective lens (20× and 0.5 NA, Rolyn Optics, Covina, CA). The emission of fluorescence was collimated by the same lens, and passed through the same dichroic mirror, an interference band-pass filter (532 nm, Carlsbad, CA) and a 1-mm pinhole, and finally were collected by a photosensor module (H5784-04, Hamamatsu). A data acquisition card USB-1208FS (Measurement Computing, Norton, MA) was used to measure the response from the photosensor module as voltage signal. The data were collected and analyzed by a home-made LabView program (National Instruments, Austin, TX).

2.3.5. NOTLC separation

Aligning the NOTLC column on the LIF detector was described previously[18]. Briefly, a 10 mM fluorescein solution was constantly flushed through the column while the fluorescence signal was monitored. By tuning the column position via the x-y-z translation stage until the maximum

fluorescence output was obtained, the x, y and z positions of the stage were then locked. The capillary needed to be rinsed thoroughly with an eluent (e.g., 50% acetonitrile with 10 mM NH_4HCO_3) before running NOTLC separations.

To initiate an NOTLC separation, the LIF detector was turned on and an isocratic eluent consisting of 80% mobile phase A (10 mM NH_4HCO_3 solution) and 20% mobile phase B (acetonitrile) preloaded in the vial inside the pressure chamber was delivered via the injection valve through the NOTLC column under a preset (usually 500 psi) pressure; most (>95%) of this pressure was dropped across the NOTLC column. Data acquisition (at a sampling rate of 40 Hz) was started upon injection and stopped after all analytes were eluted out. While the chromatogram was real-timely displayed on a computer monitor, the data was stored after the data acquisition was terminated.

2.4. Results and Discussion

2.4.1. High efficiency NOTLC separation

Fig. 2-4 presents a chromatogram of a typical high-efficiency NOTLC separation obtained using an isocratic eluent. More such high-efficiency separation results are provided in Fig. 2-5. The measured peak widths (full widths at half maximum or FWHM) were 0.28 s, 0.45 s and 0.45 s respectively for glycine, isoleucine and leucine. The number of the theoretical plates was calculated using the following equation,

$$N = 5.54 \times (t_R/w_{1/2})^2, \quad (1)$$

where t_R is the retention and $w_{1/2}$ is the peak width of an analyte, resulting in 1.1×10^7, 4.5×10^6 and 4.6×10^6 respectively. These efficiencies were several folds higher than the theoretically

predicted values[19]. Considering only diffusion-caused band broadening, neglecting all other band-broadening effects, the minimum peak variance was calculated using

$$\sigma^2 = 2 \times D \times t_R, \quad (2)$$

where D is the analyte diffusion coefficient. With the D values obtained from literature (6.71×10^{10} m^2 s^{-1} for Ile[20], 6.36×10^{10} m^2 s^{-1} for Gly[20] and 6.22×10^{10} m^2 s^{-1} for Leu[21]), band σ values of 0.73 mm, 0.72 mm and 0.71 mm, respectively for glycine, isoleucine and leucine were computed. Peak σ values were calculated by dividing the band s values by analyte velocity yielding 0.38 s, 0.39 s and 0.39 s, corresponding to FWHM values ($w_{1/2} = 4 \times \sigma/1.7$) of 0.90 s, 0.91 s and 0.91 s. These are the narrowest peak widths theoretically possible, yet empirical measurements obtained from Fig. 2-4 were showing narrower peak widths.

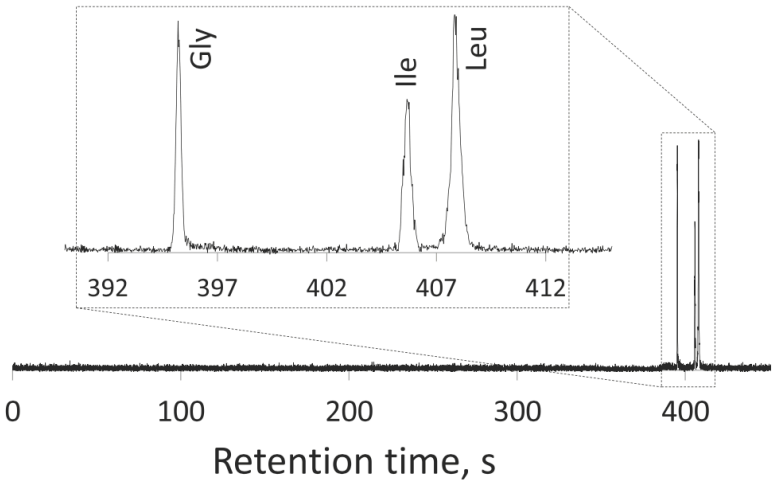

Figure 2-4. Chromatogram of a typical high-efficiency NOTLC separation.

(A) The separation column had a total length of 80 cm (75 cm effective), an o.d. of 150 mm and an i.d. of 2 mm. Isocratic eluent composition was 20% (v/v) acetonitrile and 80% 10 mM NH_4HCO_3 solution. The chamber pressure was ~1000 psi. The eluent linear velocity was measured as ~1.9 mm/s, resulting in the flowrate of 6 pL/s or 360 pL/min. The flowrate from the

restriction capillary was measured as ~18 mL/min. A splitting ratio of 1:5 × 10^4 was computed from the two flow rates. The external loop of the injection valve had a volume of ~6 mL. Based on the splitting ratio the actual injected volume was estimated to be ~120 pL. The sample was a mixture of glycine, isoleucine and leucine at concentrations of 0.4 mM, 0.8 mM and 0.8 mM, respectively. The inset expanded the peak portion of the chromatogram to show clearly the peak shapes. Figure with permission from Elsevier.

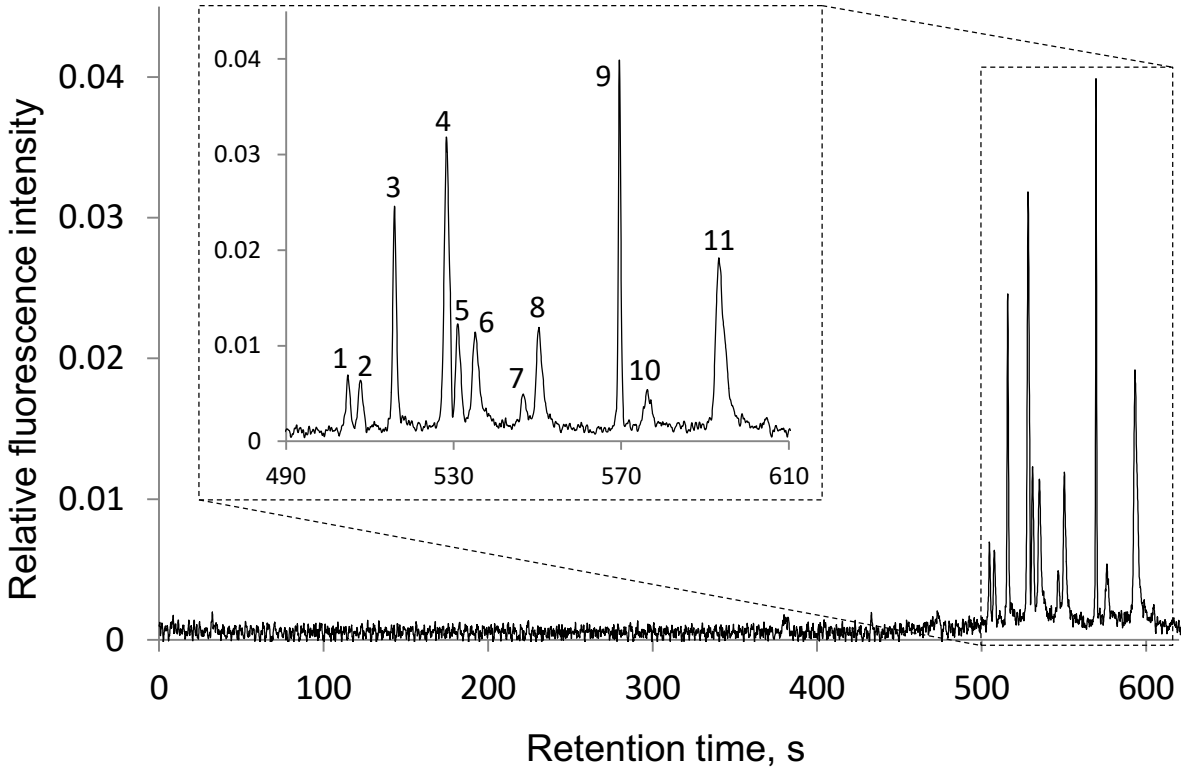

Figure 2-5. "Isocratic" separation of amino acid mixture.

The separation column had a total length of 48 cm (44 cm effective), an o.d. of 150 µm and an i.d. of 2 µm. Isocratic eluent composition was 20% (v/v) acetonitrile and 80% 10 mM NH_4HCO_3 solution. The sample was a mixture of histidine (1), asparagine (2), glycine (3), tyrosine (4), arginine (5), alanine (6), tryptophan (7), valine (8), isoleucine (9), phenylalanine (10) and leucine (11); each at 6.5 µM. Sample injection volume was ~19 pL. The chamber pressure was ~300 psi. The inset expanded the peak portion of the chromatogram to show clearly the peak shapes. Figure with permission from Elsevier.

2.4.2. Hypothesis of reduced diffusion

An instinct thought was that analyte diffusions inside the NOTLC column had been slowed down, because scientists had previously reported that diffusion coefficients of substances in confined spaces had decreased significantly[3-6]. To test this hypothesis, we used the apparatus as exhibited in Fig. 2-3 after the OTLC column was replaced with a 50 cm long and 2 mm i.d. uncoated capillary to measure the diffusion coefficient of fluorescein inside a 2 mm i.d. capillary. The working principle was described in appendix 2 (Measuring the diffusion coefficients of analytes confined in a NOTLC column). We injected a narrow band of fluorescein into the capillary, stopped the band at a location about 70 mm away from the detector, allowed fluorescein to diffuse for a preset period, and then drove the band out for chromatogram measurement. The results are presented in Fig. S2-1 and Fig. S2-2. Based on the measured peak widths, we estimated the diffusion coefficient of fluorescein to be 4.43×10^{10} m^2 s^{-1}, compared to 4.25×10^{10} m^2 s^{-1} from the literature [22]. This indicates that reduction diffusion was not the cause leading to the sharp peaks in Fig. 2-4, and therefore the reduced-diffusion hypothesis was disproved.

2.4.3. Confirmation of on-column focusing

To confirm the presence of on-column focusing, we carried out three isocratic separations by injecting a long plug (~300 s or ~230 pL) of sample and using a mobile phase containing 12% acetonitrile (ACN) and the three samples respectively dissolved in 0%, 6% and 12% ACN; all four above solutions were prepared in 10 mM NH_4HCO_3. Fig. 2-6 presents the results. When the sample was dissolved in 0% ACN, the sample matrix had the weakest eluting power, the greatest focusing occurred and the sharpest peak appeared (see Fig. 2-6A); the inset exhibited an expanded-view of the peak. For the sample dissolved in 6% ACN, a reduced focusing effect

occurred and the peak appeared broader (see the inset of Fig. 2-6B). This agrees well with the characteristics of on-column focusing [7]. When the sample was dissolved in 12% ACN, the on-column focusing effect disappeared and the analyte peak faded away (see Fig. 2-6C) because the eluting power of the sample matrix equaled that of the mobile phase. Fig. 2-6D presents the identical chromatogram of Fig. 2-6C after the scale of y-axis was magnified by 50-fold; a long (~300 s) flat band showed up representing the injected sample zone.

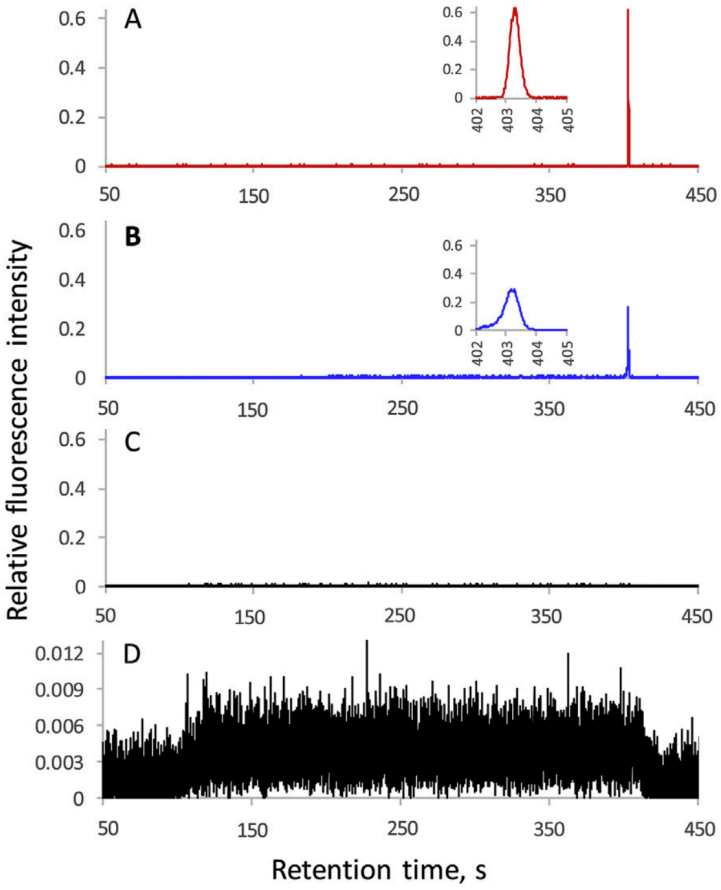

Figure 2-6. Peak profiles with or without on-column focusing.

The NOTLC column had an i.d. of 2-μm and a total length of 50 cm (45 cm effective). Three samples contained 0.625 nM fluorescein, 10 mM NH_4HCO_3 and different concentrations of acetonitrile (A) 0%, (B) 6% and (C) 12% respectively. The (D) is the same chromatogram as (C)

with 50-times of magnification. The elution pressure was ~600 psi. The mobile phase contained 10 mM NH_4HCO_3 and 12% acetonitrile. The flow rate through the restrictor was ~5.2 mL/ min. The volume of sample loop in the injection valve was ~52 mL. An injection time of 300 s was used to introduce sample into the NOTLC column. Figure with permission from Elsevier.

2.4.4. Observation of a re-focusing effect

In this research, we also performed the following experiments. Experiment #1: Utilizing the same setup as used in the above section, we injected ~19 pL of sample (0.010 mM fluorescein in 20% ACN and 80% 10 mM NH_4HCO_3) into the 2-μm-i.d. capillary, drove the sample forward with a mobile phase identical to the sample matrix and allowed it to stop (or park) at a position either 350 mm or 70 mm away from the LIF detector for 24 h, drove it across the detector, and recorded the chromatogram. The FWHM was 9.8 ± 0.1 s for fluorescein parked at 350 mm, while the FWHM was 9.9±0.1s for fluorescein parked at 70 mm away from the LIF detector.

Experiment #2: We replaced the above uncoated capillary column with a 48-cm-long C18-coated NOTLC column. After we injected ~19 pL of 0.010 mM fluorescein in mobile phase A (10 mM NH_4HCO_3) into the NOTLC column, we eluted the fluorescein forward and allowed it to park at a pre-selected position (420, 320 or 20 mm away from the LIF detector) for a preset period of time (0, 275, 550, 1100 and 1375 s) and then eluted it out. All elutions were carried out using an eluent containing 80% mobile phase A and 20% mobile phase B (acetonitrile). The 0s parking time indicated that the analyte elution was carried out continuously (without stopping). Fig. 2-7 presents the peaks after parking-time correction and peak height normalization.

Based on the results from Experiment #1, all analyte bands were broadened by diffusion, independent on the position the analyte parked. Based on the results from Experiment #2, a diffusion-broadened band could be re-focused back to its original width if adequate re-focusing

time was provided. For instance, when the fluorescein bands were parked 420 mm away from the detector (see the top group of the chromatograms), it took ~400 s for these diffusion-broadened bands to be re-eluted across the detector and all bands got completely re-focused. When the fluorescein bands were parked close to (320 mm or 20 mm away from) the detector, the broadened bands could not be fully re-focused because of the reduced re-focusing times.

Since on-column focusing occur only at the beginning of the column, it could not satisfactorily explain the above re-focusing results.

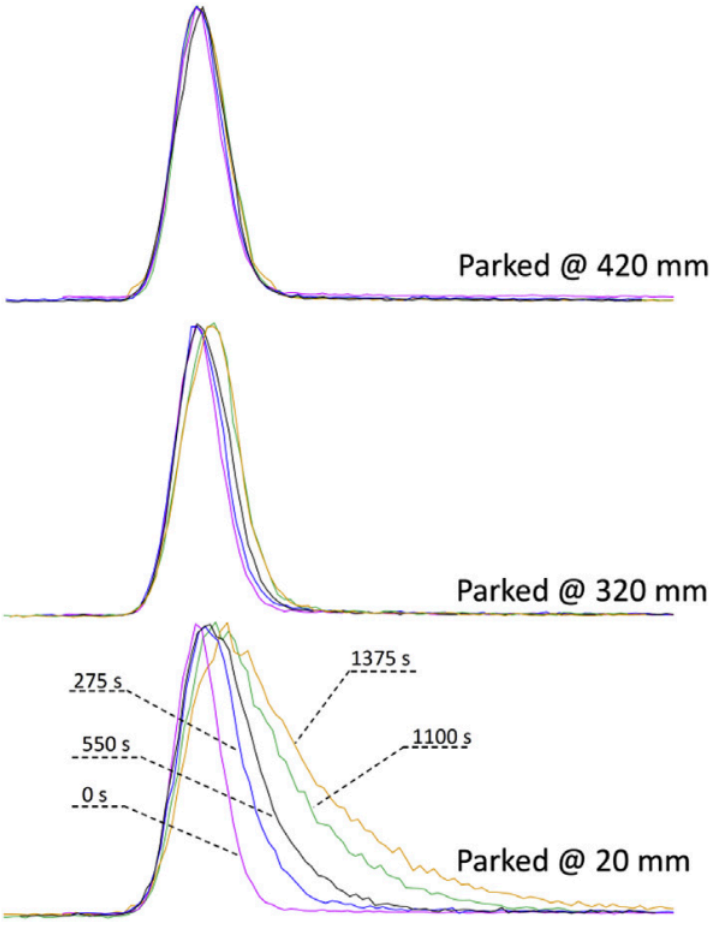

Figure 2-7. Observation of re-focusing.

The peaks were color-coded to indicate the fluorescein parking time. The distance on the right-hand side indicated the position the peaks were parked at. All peak heights were normalized for peak width comparisons. See text for experimental details. Figure with permission from Elsevier.

2.4.5. Gradient focusing

In the experiment presented in Fig. 2-4, the sample was dissolved in a matrix different from the eluent. The eluent contained 80% of mobile phase A (10 mM NH_4HCO_3) and 20% mobile phase B (100% ACN), while the analytes were dissolved in mobile phase A (Fig. 2-8A). This composition difference created two local interfaces (or gradients) before and after the analyte zone. If the analyte had no retention, it would get axially dispersed but would stay in between the two gradient zones (Fig. 2-8B) as it was driven forward. If the analyte was retained, analyte molecules residing in the front gradient would eventually merge back into the analyte's zone. Then, all analyte molecules would experience a normal gradient elution by the back gradient (Fig. 2-8C). A gradient focusing effect would occur for all these molecules, forming a gradient-focused peak. Therefore, this re-focusing or gradient focusing effect had contributed to the sharp peaks in Fig. 2-4.

The results in Fig. 2-7 could be well explained using this gradient focusing mechanism. Broadened fluorescein bands could always be re-focused as long as sufficient re-focusing time was provided.

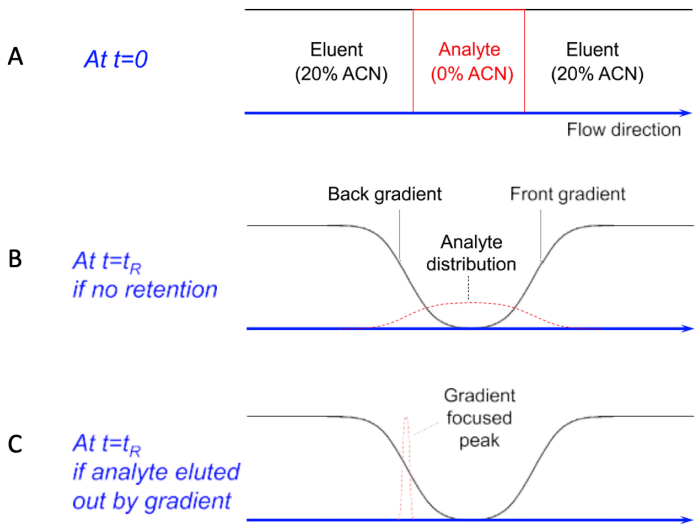

Figure 2-8. Schematic of gradient focusing mechanism.

(A) Right after the analyte was injected (at $t = 0$). (B) At $t = t_R$, two gradients before and after the analyte zone were formed, and non-retained analytes would stay in between the two gradients. (C) For a retained analyte, all analyte would be eluted out by the back gradient and get focused. Figure with permission from Elsevier.

2.4.6. Development of a simple and economic approach to run gradient NOTLC

The gradient focusing effect illustrated in Fig. 2-6 is interesting; we can perform a gradient elution using an isocratic system. To further develop this concept into a reliable method, we modified the isocratic NOTLC system (Fig. 2-3A) by adding an injection valve (for mobile phase A or MA injection) between the pressure chamber and the sample injection valve (Fig. 2-3B). Fig. 2-7A, 2-7C depict the working principle of using this system to perform gradient separations. After MA and a sample are loaded respectively in injection valves 1 and 2 (Fig. 2-7A), MA is first injected into the system and a portion of MA is allowed to pass through injection valve 2 bypassing the sample loop toward the NOTLC column (Fig. 2-7B). At a preset time (50 s in this work) after MA is injected, the sample is injected into MA (Fig. 2-7C). Fig. 6D

schematically presents the overall process. The NOTLC column is commonly washed/cleaned with mobile phase b (MB). The curve in Fig. 2-7D shows a representative MB concentration profile after the injection of a MA plug; the back-gradient profile is flatter than the front gradient profile because the second MA-MB interface experiences more mixing. Since the sample is injected after the front gradient has passed, only the back gradient is used for the elution. Fig. 6E presents an actual and typical chromatogram when NOTLC was performed in this fashion.

We essentially converted a simply isocratic system (Fig. 2-3A) to a gradient system (Fig. 2-3B) through an addition of an injection valve. Because a pressure chamber can be used as an isocratic pump, the gradient NOTLC system can be built economically.

Alternatively, one may use the pressure chamber (referring to Fig. 2-3B) to drive MA constantly and valve 1 to inject MB. A plug of MB can be injected after a sample injection to execute a gradient NOTLC separation and the front gradient is utilized for elution. We call this approach method #2, while the approach described in Fig. 2-9 is referred to as method #1. Fig. 2-10 presents a comparison between these two methods. In method #1, the NOTLC column is commonly washed with MB, and a relatively flat back gradient is applied for elution. In method #2, the NOTLC column is commonly equilibrated with MA, and a relatively steep front gradient is used for elution. While adequate MB needs to be injected in method #2 to ensure all analytes are eluted out and the column is cleaned, adequate MA needs to be injected in method #1 to ensure the column is equilibrated before the sample injection.

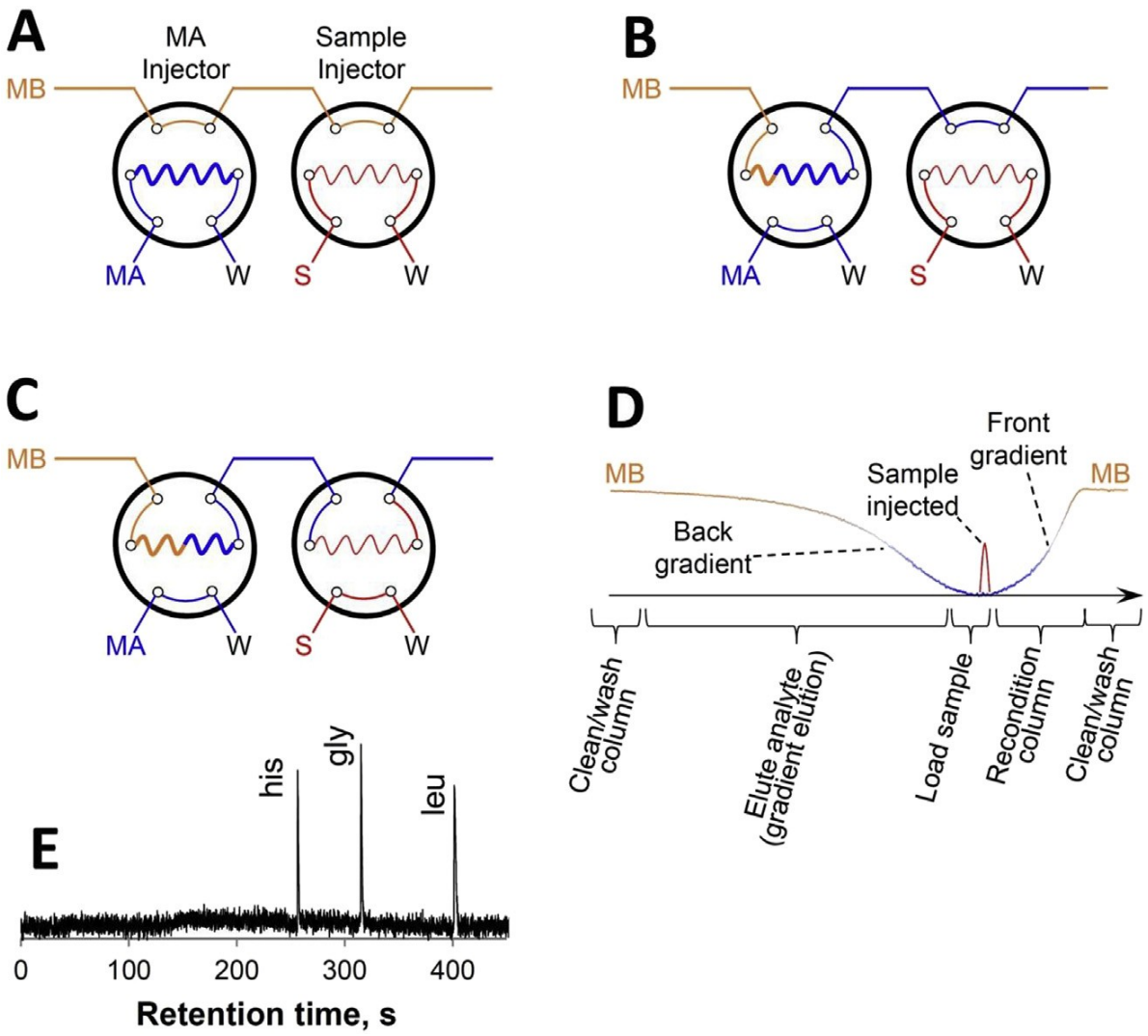

Figure 2-9. Simple and economic approach to run gradient NOTLC.

The orange line indicates MB, the blue line stands for MA, while the red line represents sample. (A) MA and sample are loaded respectively in valve 1 and valve 2. (B) MA is injected into the system and a portion of MA is allowed to pass through injection valve 2. (C) Sample is injected into the MA plug. (D) A schematic presentation of the gradient elution process. (E) A typical chromatogram obtained using this approach. NOTLC column: 45 cm (40 cm effective) x 2 mm i.d.; The splitting ratio of the flow splitter: 1:3.2 x 10^5; Sample: histidine, glycine and leucine (each at 0.1 mM) were dissolved in 10 mM NH_4HCO_3; MB: 20% (v/v) acetonitrile in 10 mM NH_4HCO_3; MA: 10 mM NH_4HCO_3; Injection loop volume of sample injector: 1.2 mL; Injection loop volume of MA injector: 29.4 mL; Elution pressure: 1200 psi; Eluent velocity: 1.6 mm/s. Sample was injected 50 s after MA injection and data acquisition started right after sample injection. Figure with permission from Elsevier.

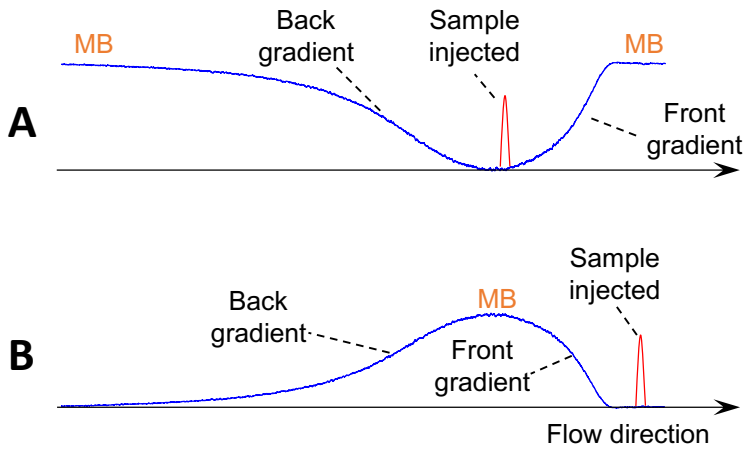

Figure 2-10. Comparison between method #1 and method #2.

Definitions of method #1 and method #2 are provided in the main text. In method #1, NOTLC column is commonly washed, while column is commonly equilibrated in method #2. Much steeper gradient is in in method #2 than in method #1. Adequate MB needs to be injected in method #2 to ensure all analytes and interferents are washed out of the column, while adequate MA needs to be injected in method #1 to ensure the column is completely equilibrated. Figure with permission from Elsevier.

2.5. Conclusion and perspectives

We have identified the focusing effects in NOTLC and used these effects to interpret the exceptionally sharp peaks obtained from "isocratic" NOTLC. Based on this focusing mechanism, we have developed a simple and economic approach to perform pico-gradient NOTLC; simple and economic HPLC systems are particularly desired in the developing countries. When using NOTLC columns, care must be taken to avoid column clogging, detector focal point shifting, etc. We have rarely encountered these problems in our lab. The pico-gradient NOTLC could be widely accepted, if it could be coupled with mass spectrometry (MS). There may be challenges for this coupling because NOTLC is executed under extremely low elution rates (several hundred pL/min or lower). We are optimistic that this issue can be addressed since pico-spray emitters

(>400 pL/min) have been reported [23,24]. With the advancement of MS instrumentation, we are confident that MS will be capable of handling flow rates at 100-200 pL/min level. Promising results have also obtained in our lab; these results will be published elsewhere. With NOTLC's high efficiency and MS's identification capability, we expect NOTLC-MS to become a powerful analytical technique for chemical separations.

The material in chapter 2 is adapted from Yang, Y., Xiang, P., Chen, H., Zhao, Z., Zhu, Z., & Liu, S. (2019). On-column and gradient focusing-induced high-resolution separation in narrow open tubular liquid chromatography and a simple and economic approach for pico-gradient separation. *Analytica chimica acta*, *1072*, 95-101. Copyright permission is obtained from Elsevier.

References

(1) Chen, H.; Yang, Y.; Qiao, Z.; Xiang, P.; Ren, J.; Meng, Y.; Zhang, K.; Lu, J. J.; Liu, S. *Analyst* **2018**, *143*, 2008-2011.
(2) Yang, Y.; Chen, H.; Beckner, M. A.; Xiang, P.; Lu, J. J.; Cao, C.; Liu, S. *Anal. Chem.* **2018**, *90*, 10676-10680.
(3) Xiao, B.; Wu, C.; Sun, Y.; Jin, Z. *Micro & Nano Letters* **2009**, *4*, 192-197.
(4) Ma, C.; Han, R.; Qi, S.; Yeung, E. S. *J. Chromatogr. A* **2012**, *1238*, 11-14.
(5) Ma, C.; Yeung, E. S. *Anal. Chem.* **2010**, *82*, 478-482.
(6) Schlipf, D. M.; Zhou, S.; Khan, M. A.; Rankin, S. E.; Knutson, B. L. *Advanced Materials Interfaces* **2017**, *4*, 1601103.
(7) Groskreutz, S. R.; Weber, S. G. *J. Chromatogr. A* **2015**, *1409*, 116-124.
(8) Vissers, J. P.; de Ru, A. H.; Ursem, M.; Chervet, J.-P. *J. Chromatogr. A* **1996**, *746*, 1-7.
(9) Foster, M. D.; Arnold, M. A.; Nichols, J. A.; Bakalyar, S. R. *J. Chromatogr. A* **2000**, *869*, 231-241.
(10) Héron, S.; Tchapla, A.; Chervet, J.-P. *Chromatographia* **2000**, *51*, 495-499.
(11) Claessens, H.; Kuyken, M. *Chromatographia* **1987**, *23*, 331-336.
(12) Bakalyar, S. R.; Phipps, C.; Spruce, B.; Olsen, K. *J. Chromatogr. A* **1997**, *762*, 167-185.
(13) Snyder, L. R. *J. Chromatogr. A* **1964**, *13*, 415-434.
(14) Cappiello, A.; Famiglini, G.; Fiorucci, C.; Mangani, F.; Palma, P.; Siviero, A. *Anal. Chem.* **2003**, *75*, 1173-1179.
(15) Deguchi, K.; Ito, S.; Yoshioka, S.; Ogata, I.; Takeda, A. *Anal. Chem.* **2004**, *76*, 1524-1528.
(16) Brennen, R. A.; Yin, H.; Killeen, K. P. *Anal. Chem.* **2007**, *79*, 9302-9309.
(17) Zhou, L.; Lu, J. J.; Gu, C.; Liu, S. *Anal. Chem.* **2014**, *86*, 12214-12219.
(18) Weaver, M. T.; Lynch, K. B.; Zhu, Z.; Chen, H.; Lu, J. J.; Pu, Q.; Liu, S. *Talanta* **2017**, *165*, 240-244.
(19) Golay,M.J.E. ; Desty, D.H. academic Press, New York, 1958, p. 36.
(20) Longsworth, L. *J. Am. Chem. Soc.* **1953**, *75*, 5705-5709.
(21) Ma, Y.; Zhu, C.; Ma, P.; Yu, K. *J. Chem. Eng. Data* **2005**, *50*, 1192-1196.
(22) Culbertson, C. T.; Jacobson, S. C.; Ramsey, J. M. *Talanta* **2002**, *56*, 365-373.
(23) Gibson, G. T.; Mugo, S. M.; Oleschuk, R. D. *Mass Spectrom. Rev.* **2009**, *28*, 918-936.

Chapter3. Experimentally Validating the Open Tubular Liquid Chromatography for a Peak Capacity of 2000 in 3 h

This project was a collaborative work that consists of the following authors: Piliang Xiang, Yu Yang (co-first author), Zhitao Zhao, Apeng Chen, Shaorong Liu

Piliang Xiang conducted the ultrafast-separation experiments including column coating and system adjustment.

Zhitao Zhao assisted the SEM images and figure analysis.

Apeng Chen contributed to the cell sample preparation.

All the other work was done by Yu Yang.

3.1. Abstract

The advancements in life science research mandate effective tools capable of analyzing large numbers of samples with low quantities and high complexities. As an essential analytical tool for this research, liquid chromatography (LC) encounters an ever-increasing demand for enhanced resolving power, accelerated analysis speed, and reduced limit of detection. Although theoretical studies have indicated that open tubular (OT) columns can produce superior resolving power under comparable elution pressures and analysis times, ultrahigh-resolution and ultrahigh-speed open tubular liquid chromatography (NOTLC) separations have never been reported. Here we present experimental results to demonstrate the predicted potential of this technique. We use a 2 μm i.d. × 75 cm long NOTLC column coated with trimethoxy(octadecyl)silane for separating pepsin/trypsin digested *E. coli* lysates and routinely produce exceptionally high peak capacities (e.g., 1900-2000 in 3-5 h). We reduce the column length to 2.7 cm and exhibit the capability of

NOTLC for ultrafast separations. Under an elution pressure of 227.5 bar, we complete the separation of six amino acids in ~800 ms and resolve these compounds within ~400 ms. In addition, we show that NOTLC has low attomole limits of detection (LOD) and each separation requires samples of only a few picoliters. Importantly, no ultrahigh elution pressures are required. With the ultrahigh resolution, ultrahigh speed, low LOD, and low sample volume requirement, NOTLC can potentially be a powerful tool for biotech research, especially single cell analysis.

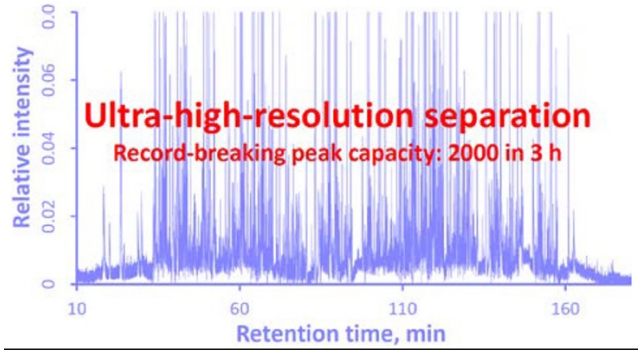

Figure 3-1. Graphic abstract

Figure with permission from the ACS.

3.2. Introduction

High-resolution and high-speed separation techniques have played pivotal roles in life science research such as human genome sequencing[1-5], and more recently in proteomics[6-9] and metabolomics[10-13] research. As life science research advances, the samples are getting more complex and more samples are being analyzed. The demand for improved resolving power and enhanced analysis speed is ever-increasing. Liquid chromatography (LC) is a relatively high-

resolution and high-speed analytical technique and has dominated chemical, biological, and especially pharmaceutical separations for decades, but approaches for increased resolution and accelerated speed are relentlessly explored. In fact, the evolution of LC is tied to the endeavor for continuously improving its resolution and speed.

A common approach to achieve enhanced resolution and speed is to pack a column with small and uniform particles. This has led to the transition from simple gravity-driven LC using columns packed with large and nonuniform particles to sophisticated high performance LC (HPLC) using columns packed with a-few-micrometers-diameter and uniform particles. Toward the end of the last century, the highest separation efficiencies were obtained using columns packed with 5 μm particles.[14] Investigation of packing columns with less-than-2-μm-diameter particles was reported first by Jorgenson's group in 1997.[15] Due to the reduced particle size, high elution pressures were required, and this effort eventually led to the state-of-the-art separation technique, ultrahigh performance LC (UPLC). The primary goals of reducing the particle size and making the particles uniform are (i) to decrease the pore sizes among particles and hence shorten the mass transfer times in the mobile phase and (ii) to reduce eddy dispersions. Fundamentally speaking, an effective and straightforward path to achieve these goals is to utilize a NOTLC column.

An OT column is referred to as a hollow tube with a layer of stationary phase on its interior wall. OT columns were first used by Golay[16] in gas chromatography (GC) more than a half century ago. Because OT columns achieved increased efficiencies under similar elution pressures and within comparable analysis times, these columns quickly replaced packed columns in GC. Under optimized conditions, OT columns had inner diameters (i.d.) of around several hundred micrometers. High efficiencies were predicted for OTLC[17-21] since chromatographic theory made

no distinction between gases and liquids as the mobile phase. However, because analyte diffusivities in liquid phases are generally 2-3 orders of magnitude smaller than those in gas phases, the column i.d. must be reduced by 100-1000 times compared to that used in GC to achieve the predicted high efficiencies.[22] The reduced column i.d. has caused challenges for preparing columns with adequate sample loadability and analyte retention; this has consequently impeded the OTLC advancement.

Increasing the surface area was experimented to mitigate the low-loadability and low-retention issue. For example, Jorgenson *et al*.[23] used hydrochloric acid to remove the non-silica components of a borosilicate glass capillary and created a thin layer of porous silica on the capillary inner wall. The authors claimed that they had increased the surface area by about thirty-fold compared to that of a geometrically smooth capillary. Ammonium hydrogen bifluoride was proved to be more effective toward creating porous silica having increased the surface areas by Pesek and Matyska,[24] and around 1000-fold surface-area enhancement was reported.[25] Etching the surfaces had indeed led to enhanced sample loadabilities, but ultrahigh-resolution results were not obtained. Alternatively, a porous polymer stationary phase was created on the capillary wall to improve the sample loadability, [26,27] and these columns are now called porous layer open tubular (PLOT) columns. High efficiency separations were obtained using PLOT columns.[28,29] For example, a poly(styrene-divinylbenzene) PLOT column was prepared by Yue *et al*.,[28] and a peak capacity of approximately 400 within a 3.5 h gradient was produced using this column for separating a tryptic digest mixture. Utilizing microfabrication technology, Desmet *et al*.[30] fabricated an array of radially elongated pillars in a microchannel and used all the surface to host a stationary phase. Because the pillars were accurately engineered and arranged so perfectly that the all gaps between the pillars had the same size and length, these channels

(gaps between the pillars) were virtually a parallel-OT-column. Using such a device, these researchers obtained efficiencies of 160 000 theoretical plates for unretained analytes and 70 000 theoretical plates for a retained coumarin derivative. It is worth mentioning that these high-efficiency results were obtained three decades after the first OTLC separation was demonstrated for separating 3-6 aromatic compounds using a 60 μm i.d. column by Tsuda *et al*.[31]

Ultrahigh efficiencies are possible for simple OTLC according to theoretical investigations,[16-18,23,32] but these four-decade-old predictions have never been experimentally validated. Here we present experimental results to demonstrate the predicted potential of narrow OTLC or NOTLC. We use a 2 μm i.d. × 80 cm long (75 cm effective) NOTLC column to separate pepsin/trypsin digested *E. coli* lysates and routinely produce exceptionally high peak capacities in the range of 1900-2000 in 3-5 h. Since the narrow bore is key to the high performances, we tentatively call the column "narrow open tubular column" and the technique "narrow open tubular liquid chromatography (NOTLC)". We also reduced the NOTLC column length to 6 cm (2.7 cm effective) to demonstrate NOTLC's capability of performing ultrafast (millisecond) separations. In addition, we show that a sample of only a few picoliters is required for each NOTLC separation and the technique has low attomole LOD.

3.3. Experimental section

3.3.1. Materials and Reagents

Fused-silica capillaries used for making the NOTLC columns (2 μm inner diameter, 150 μm outer diameter) were purchased from Polymicro Technologies, a subsidiary of Molex (Phoenix, AZ). Trypsin was purchased from Promega (Madison, WI). Pepsin was purchased from MP

Biomedicals (Santa Ana, CA). Amino acids, sodium hydroxide, ammonia bicarbonate, acetonitrile, toluene, and trimethoxy(octadecyl) silane were purchased from Sigma-Aldrich (St. Louis, MO). ATTO-TAG FQ Amine-Derivatization Kit was purchased from Thermo Fisher Scientific (Waltham, MA). All solutions were prepared with ultrapure water (Nanopure ultrapure water system, Barnstead, Dubuque, IA) and filtered through a 0.22 μm filter (VWR, TX), degassed before use.

3.3.2. Preparation of NOTLC Column

The columns were prepared as described previously.[33,34] Briefly, after the polyimide coating at one end of a 2 μm i.d. capillary was removed for about 1 cm in length, this end of the capillary was inserted into a vial containing 50 μL of 1 M NaOH solution inside a pressure chamber (made of transparent acrylic; see the appendix 3 for details). The other end (with polyimide coating) of the capillary was placed into a 0.5 mL sealed vial containing DDI water. Pressurized nitrogen at 35 bar was applied to wash the capillary with NaOH, DDI water, and then acetonitrile. Inside a dry glovebox, a trimethoxy(octadecyl) silane toluene solution was flushed through the capillary to coat the inner wall of the capillary.

3.3.3. Peptide Sample Preparation

One mL of *E. coli* lysate (~10 mg total protein/ml) was mixed with 5 μL of 1 M NaAc/HAc buffer (pH = 4) and 1 μL of pepsin (1 μg/mL), and the mixture was incubated at 37 °C for 1 h. A volume of 100 μL of the above solution was diluted with 900 μL of 25 mM NH_4HCO_3 and

mixed with 1 μL of 1 M DTT at room temperature for at least 1 h. Then, 10 μL of 0.2 mg/mL trypsin solution was added into above mixture, and the mixture was incubated at 37 °C for 24 h.

3.3.4. Fluorescent Dye Labeling

Amino acid and peptide labeling was proceeded following the instruction provided with the ATTO-TAG FQ Amine-Derivatization Kit by Thermo Fisher Scientific. Briefly, a 10 mM ATTO-TAG FQ stock solution was prepared by dissolving 5.0 mg of ATTO-TAG FQ in 2.0 mL of methanol and stored in -20 °C. A 10 mM working KCN solution was prepared by diluting a 0.2 M KCN stock solution with 10 mM borax solution (pH 9.2). Amino acid stock solutions (each containing 1 mM of one amino acid) were prepared by dissolving individual amino acids in DDI water and filtered with a 0.22 μm filter. A volume of 1.0 μL of the amino acid stock solution was mixed with 10 μL of the 10 mM KCN working solution and 5 μL of the 10 mM FQ solution in a 0.25 mL vial. This mixture was maintained at room temperature for 1 h in dark before use. The FQ-labeled-amino acid was diluted with 10 mM NH_4HCO_3 to an appropriate concentration prior to analysis.

To label the digested *E. coli* lysate, 10 μL of the peptide solution was mixed with 10 μL of 10 mM KCN and 10 μL of 10 mM FQ. After 1 h of reaction in the dark at ambient temperature, the peptides were ready for separation.

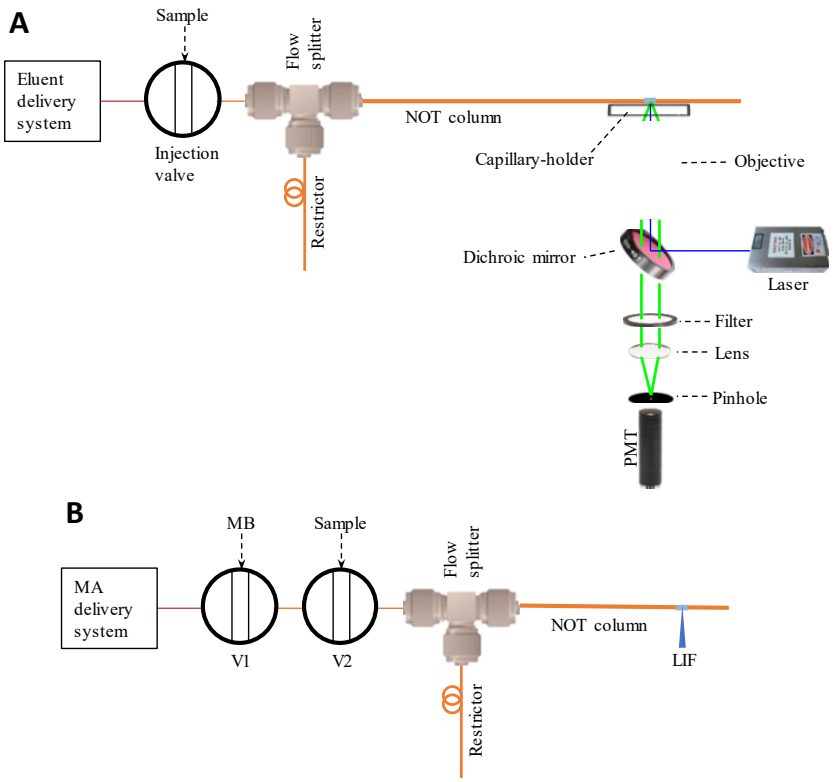

Figure 3-2. Schematic diagrams of experimental apparatus.

(A) Apparatus used to perform ultra-high-resolution separations and LOD determinations. The NOTLC column had a 2-μm i.d. and was trimethoxy(octadecyl) silane derivatized. The gradient pump was an Agilent 1200 capillary pump. The injection was a VICI 6-port valve. The flow splitter was built using an Upchurch micro-T. A 10-cm-long and 20-μm-i.d. capillary was used as a restrictor. A 200-μm i.d. and 360-μm o.d. capillary was used to connect the injection valve and the micro-T. Inside the flow splitter, a small portion (head) of the 2-μm i.d. and 150-μm o.d. NOTLC column was inserted into a 200-μm i.d. and 360-μm o.d. connection capillary to facilitate sample injection. At the 5 cm from the effluent outlet of NOTLC column, a detection window was made by removing the polyimide coating. A laser-induced fluorescence detector underneath the NOTLC column was used to monitor the resolved analytes. (B) Apparatus used to perform ultra-high-speed separations. An HPLC pump was used to supply mobile phase A (10 mM NH_4HCO_3) continuously. V1 had a 20-μL loop and was employed for injecting a plug of MB (50% acetonitrile in 10 mM NH_4HCO_3) into the MA conduit for gradient generation. V2 had a 2.6-μL loop and was utilized for sample injection. The identical LIF detector was used in both A and B. Figure with permission from the ACS.

3.3.5. Apparatus

Fig. 3-2A presents a schematic diagram of the experimental apparatus used in this work. For ultrahigh-resolution separations and LOD determinations, a gradient pump (Agilent 1200 quaternary pump, Santa Clara, CA) was used for driving a mobile phase through a six-port valve (VICI Valco, Houston, TX), via a flow splitter with a 20 μm i.d. and 20 cm long restriction capillary, to a NOTLC column. At 5 cm from the tip of the NOTLC column, polyimide coating was removed, forming a detection window. Fig. 3-2B presents a schematic diagram of the experimental apparatus used for ultrahigh-speed separations, a HPLC pump supplied mobile phase A (MA, 10 mM NH_4HCO_3) continuously. V1, along with a 20 μL loop, was employed for injecting a plug of MB (50% acetonitrile in 10 mM NH_4HCO_3) into the MA conduit for gradient (the so-called plug-gradient) generation. A plug of 900 pL of MB was injected into the NOTLC column. V2, along with a 2.6 μL loop, was utilized for sample injection. 120 pL of sample was injected into the NOTLC column. The detection end of the column was affixed to a capillary holder on an *x–y–z* translation stage so that the detection window could be aligned for the maximum fluorescent output. A confocal laser-induced fluorescence (LIF) detector, as described previously,[35] was employed to monitor the resolved analytes. More information about the apparatus and its operation is provided in the appendix 3.

3.4. Results and discussion

3.4.1. Ultrahigh-Resolution NOTLC Separation

Fig. 3-2 presents an ultrahigh-resolution chromatogram for a pepsin and trypsin digested *E. coli* lysate. Hundreds of compounds are nicely resolved as seen in Fig. 3-2, and many peaks are

sharp [had full widths at half-maxima (fwhm) of 3-5 s]. The chromatogram is presented in four separate panels to exhibit the extraordinarily high resolutions. The single-panel chromatogram is presented in Fig. 3-3. The peak widths of the 15 highest peaks across the chromatogram were measured, and the average fwhm value of these peaks was calculated to be 4.6 ± 0.5 s. Based on this value, the average full peak width ($4\sigma \approx 1.7 \times$ fwhm) was 7.9 s. The peak capacity of this separation was evaluated by dividing the time gap (245 min) between the first peak (the peak of an unretained analyte) and the last peak by the average full peak width, yielding a peak capacity of 1900. Although the 15 highest peaks were selected for peak capacity evaluation, there were many narrow low-intensity peaks. In fact, high-intensity peaks could have wider widths than low-intensity peaks because high-intensity peaks could be overloaded. Fig. S3-2 exhibits four zoomed-in regions. Again, the average fwhm of the highest peaks (with asteroids) in these groups was 4.72, leading to a peak capacity of 1830. Nevertheless, the estimated peak capacity of 1830-1900 within 245 min is very impressive and a record for one-dimension liquid chromatographic separations. Importantly, the separation was carried out under an elution pressure of only ~35 bar.

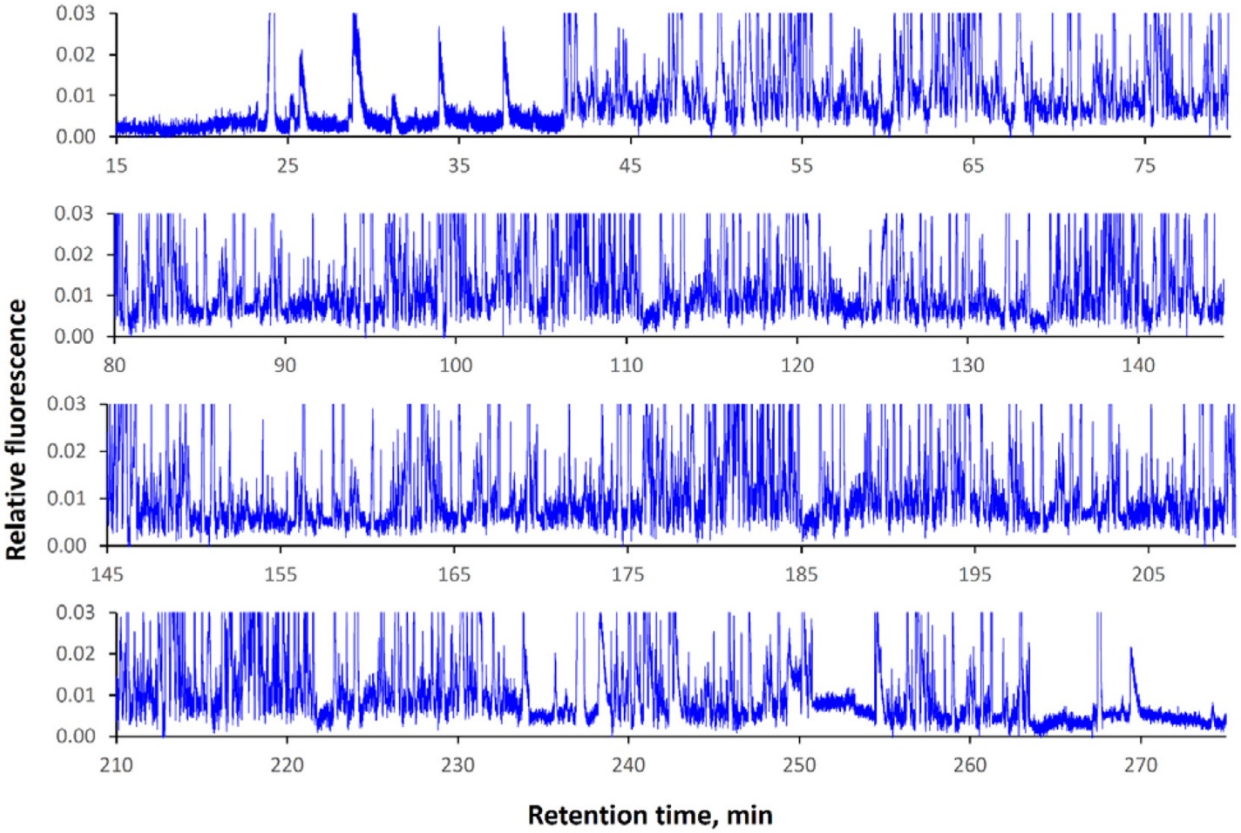

Figure 3-3. Ultrahigh-resolution NOTLC separation.

A NOTLC column: 2 μm i.d. × 80 cm (75 cm effective) capillary coated with C18; sample: *E. coli* lysates digested with pepsin/trypsin; mobile phase A: 10 mM NH_4HCO_3; mobile phase B: 80% acetonitrile in 10 mM NH_4HCO_3; injected volume: ~120 pL; elution pressure: ~35 bar; and gradient: mobile phase B increased from 5% to 100% in 300 min. Figure with permission from the ACS.

High peak capacities had been reported for one-dimension separations,[36–39] but they were usually obtained at high elution pressures and in long separation times. Han *et al*.[36] employed a meter-long packed nano-LC column and generated a peak capacity of 800 under an elution pressure of 400 bar in more than 10 h. Shen *et al*.[38] obtained peak capacities of 1000–1500 using a 1379 bar RPLC-MS in greater than 12 h. To the best of our knowledge, one-dimension separation peak capacities of higher than 1900 within 3-5 h were never reported.

The NOTLC column used in the above experiment was prepared first by activating an 80 cm long and 2 μm i.d. fused capillary with NaOH and then the surface was coated with trimethoxy(octadecyl) silane (C18) (see the appendix 3 for detailed protocols). Although 1 M NaOH was flushing through the capillary at 100 °C for 2 h to activate the surface in this work, we had no evidence that we had made the surface porous. We had tested flushing 1 M NaOH at 50 °C for 30 min and 75 °C for 1 h but did not observe any obvious column-performance differences. Fig. 3-4 presents SEM images of the capillary i.d. before any treatment, after NaOH activating, and after C18 coating. The capillary i.d. seemed to have increased slightly (by 190 nm) after NaOH activating, but this number was within the capillary i.d. variations (capillary i.d. = 2 ± 0.5 μm according to Molex, Lisle, IL).

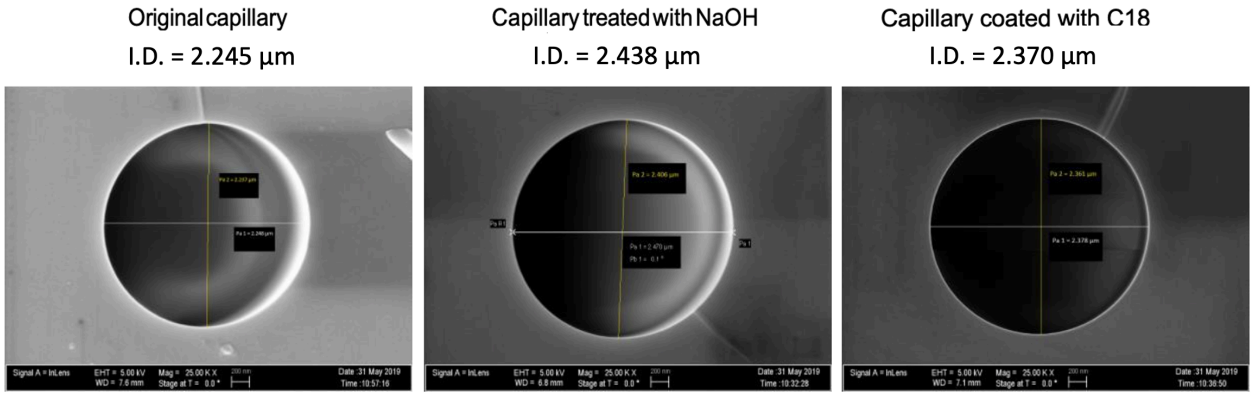

Figure 3-4. SEM images of 2-μm-i.d. capillary before treatment, after NaOH activation and after C18 coating

Figure with permission from the ACS.

It should be noted that analytes in Fig. 3-3 were labeled with ATTO-TAG FQ in order to use a laser-induced fluorescence detector. Although excessive labeling dye was added to label all binding sites on each peptide, there could be unlabeled sites, leading to multiple labeling and

hence multiple peaks for one peptide. Therefore, each peak in Fig. 3-3 represents only a specific fluorescent molecule (i.e., a peptide labeled with a specific number of fluorescent dye molecules at specific binding sites).

To further increase the peak capacity, we increased the NOTLC column length from 80 to 160 cm and separated similar samples under an elution pressure of ~35 bar and using a 3, 4, and 5 h gradient time (see results in Fig. 3-5). Using the same approach to evaluate the peak capacity for these separations, we obtained peak capacities of 2000, 1900, and 1900 respectively for the 3, 4, and 5 h separations. These results indicated that, under the experimental conditions, merely increasing the gradient time could no longer enhance the peak capacity. This could be explained by recognizing the fact that the initial (5% mobile phase B and 95% mobile phase A) and the final (100% mobile phase B) compositions of the gradient solutions were the same. The increased gradient time reduced the slope of the gradient profile (hence the gradient focusing) and consequently broadened the peaks. If we shortened the gradient time, the peak capacity did decrease with the gradient time (Fig. 3-6).

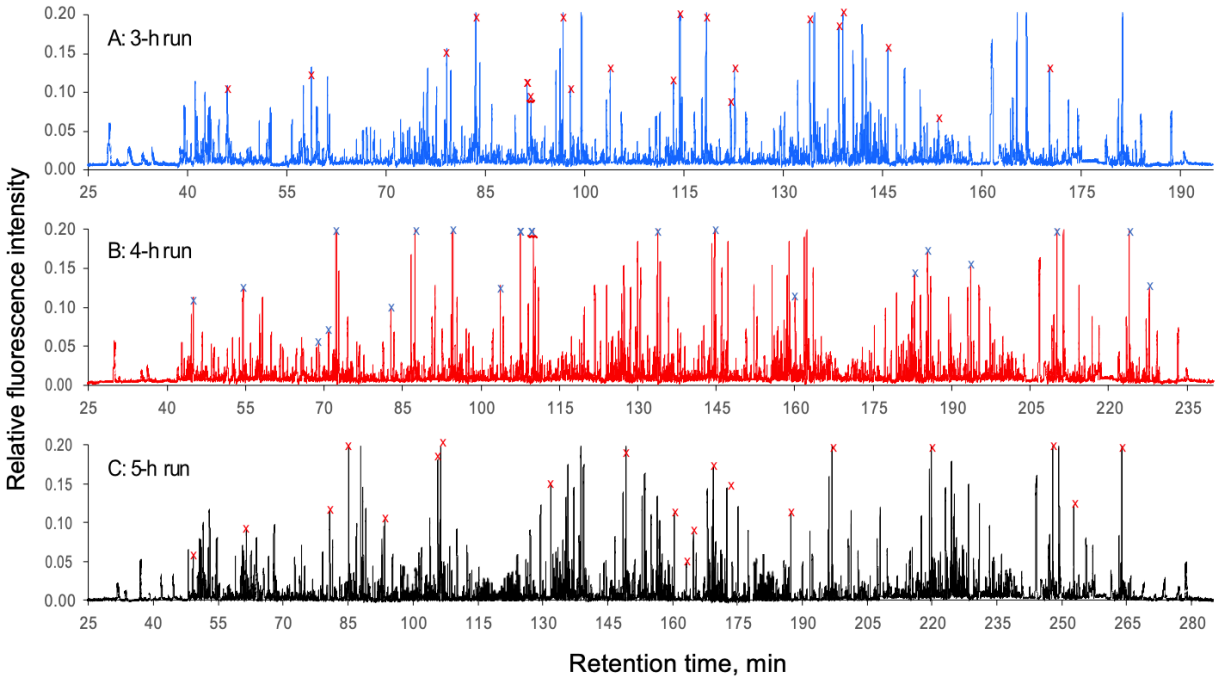

Figure 3-5. Typical ultra-high-resolution chromatograms

These chromatograms were obtained using a 160-cm-long (155 cm effective) and 2-µm-i.d. NOTLC column under an elution pressure of ~35 bar. Sample: *E. coli* lysates digested with pepsin/trypsin [Note: even the samples were prepared following the same protocols, there would always be some differences among samples.]; mobile phase A: 10 mM NH_4HCO_3; mobile phase B: 80% acetonitrile in 10 mM NH_4HCO_3; injected volume: ~120 pL; and gradient: mobile phase B increased from 5% to 100% in 180 min (top chromatogram), 240 min (middle chromatogram) or 300 min (bottom chromatogram). Figure with permission from the ACS.

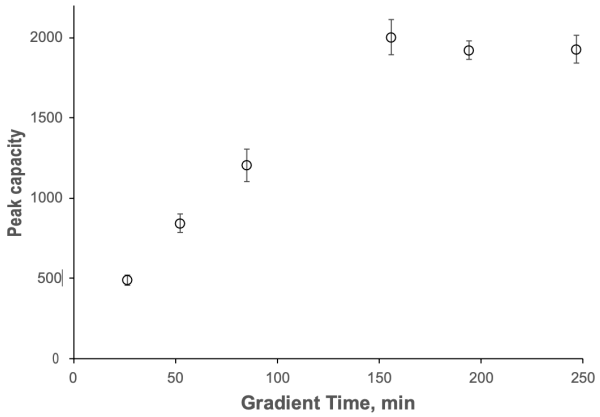

Figure 3-6. Relationship between peak capacity and gradient time

Figure with permission from the ACS.

In this work, all NOTLC separations were performed under a constant pressure source. A common concern associated with such a system was the separation reproducibility. In one of our earlier reports,[34] we had shown the good repeatability results for amino acid separations. Fig. 3-7A and B presents chromatograms for two repeated peptide separations. Insets I and III and insets II and IV in Fig. 3-7A and B present expanded views of the same retention time regions of the two chromatograms. Through peak pattern comparison, we can conclude that the separations were reproducible.

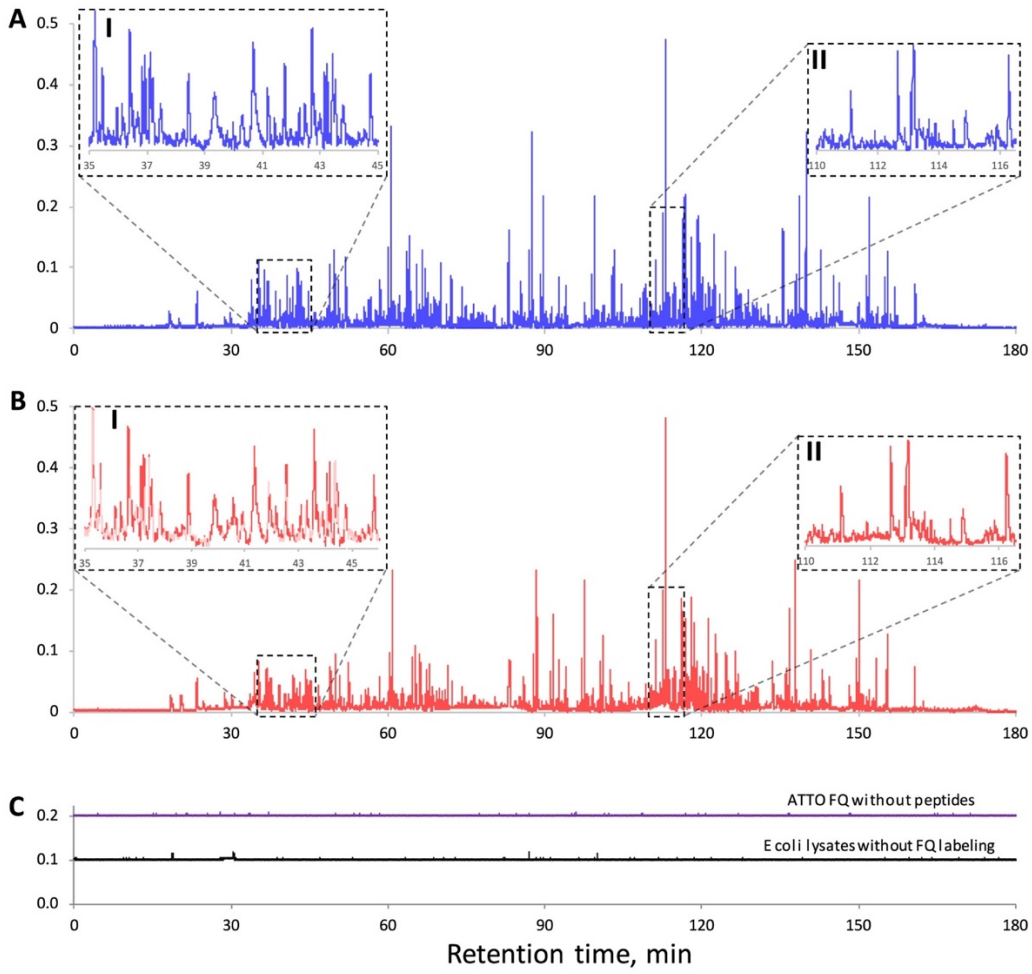

Figure 3-7. Chromatograms for repeated peptide separations.

NOTLC column: 2 μm i.d. × 160 cm (155 cm effective) length; mobile phase A: 10 mM NH_4HCO_3; mobile phase B: 80% acetonitrile in 10 mM NH_4HCO_3; injected sample volume:

~120 pL; elution pressure: 64.8 bar; gradient: mobile phase B increasing from 5 to 100% in 180 min. In (A)-(C), the *x*-axes and *y*-axes have the same scales. Insets I and III/insets II and IV in (A)/(B) show expanded views of the same retention-time regions of the two chromatograms Figure with permission from the ACS.

To check if any artifact peaks were present in the above chromatograms, we carried out two "control" separations: one for the fluorescent labeling dye without peptides and the other for the pepsin/trypsin digested *E. coli* lysate without fluorescent dye labeling. The chromatograms are exhibited in Fig.3-3C. The ATTO FQ chromatogram was raised by 0.2 and the *E. coli* lysate chromatogram was raised by 0.1 relative fluorescence intensity unit so that we could see the fluorescence signal variations. In general, the fluorescence signals were stable, and no high peaks were observed.

3.4.2. Ultrafast NOTLC Separation

It Fig. 3-8 presents an ultrafast separation using a 6 cm long (2.7 cm effective) NOTLC column. The sample contained six amino acids, and the separation was executed using a plug gradient (see Experimental Section for details) under an elution pressure of ~227.5 bar. The last analyte was eluted out in less than 800 ms, and all six amino acids were resolved within ~400 ms.

In Fig. 3-8, we might have set a speed record for that high resolution in liquid chromatography. Setting the speed record was not our intention, because we could have increased the speed simply by shortening the column length and/or boosting the elution pressure after reducing the number of anlytes. Fig. S3-3 presents a comparison between our results and the fastest LC separation reported[40] using a short packed-column. Both separations were completed in less than 1 s, but our results exhibited much sharper peaks and higher resolutions.

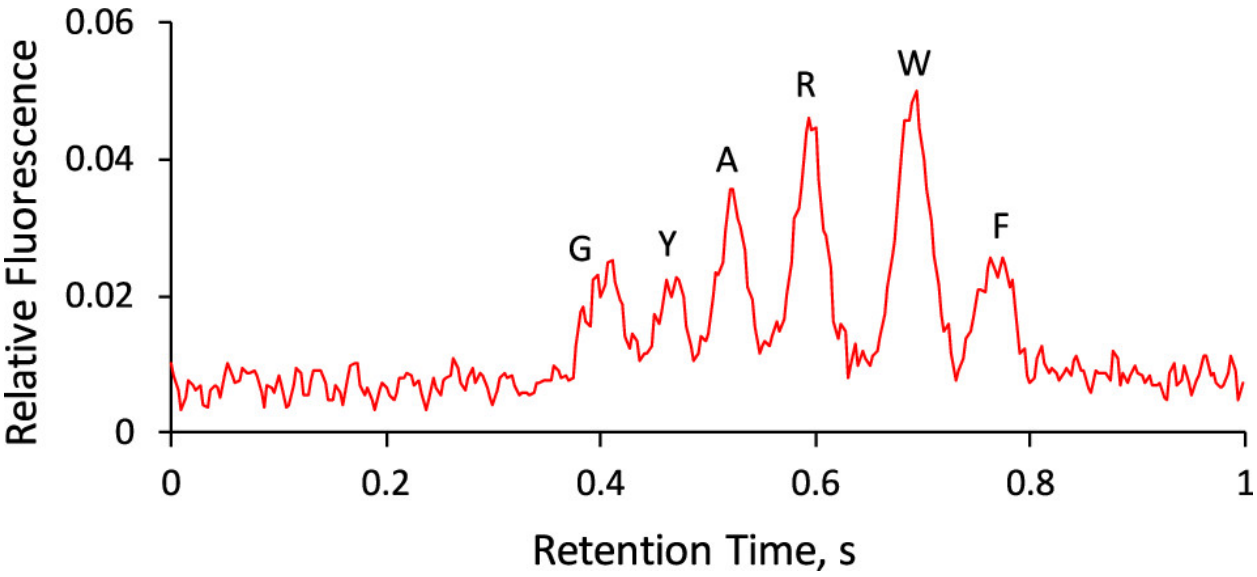

Figure 3-8. Typical chromatograms for fast NOTLC separations.

NOTLC column: 2 μm i.d. × 60 mm (27 mm effective) length capillary coated with C18; sample: mixture of glycine (1 μM), tyrosine (3 μM), alanine (3 μM), arginine (3 μM), tryptophan (10 μM), and phenylalanine (2.5 μM); sample volume injected: 120 pL; gradient: created by injecting into the NOTLC column a plug (900 pL) of 50% acetonitrile in 10 mM NH_4HCO_3; and elution pressure: 227.5 bar. Gradient delay time was subtracted from the retention time. Figure with permission from the ACS.

3.4.3. NOTLC Limit of Detection

Fig. 3-9 presents a chromatogram for three amino acids to evaluate the NOTLC's detection limits. The sample contained 0.04 μM Gly, 0.08 μM Ile, and 0.08 μM Leu in 10 mM NH_4HCO_3. After 157 pL of the sample was injected, the separation was carried out using a 2 μm i.d. × 80 cm long (75 cm effective) NOTLC column under an elution pressure of ~65.5 bar. From Fig. 3-5, a noise of 0.0006_9 was measured for the background signal, and net signals of 0.019_5, 0.016_1, and 0.026_5 were measured, respectively, for 0.04 μM Gly, 0.08 μM Ile, and 0.08 μM Leu. Using a criterion of S/N = 3, the LODs for Gly, Ile, and Leu were 0.73, 1.8, and 1.1 μM, respectively.

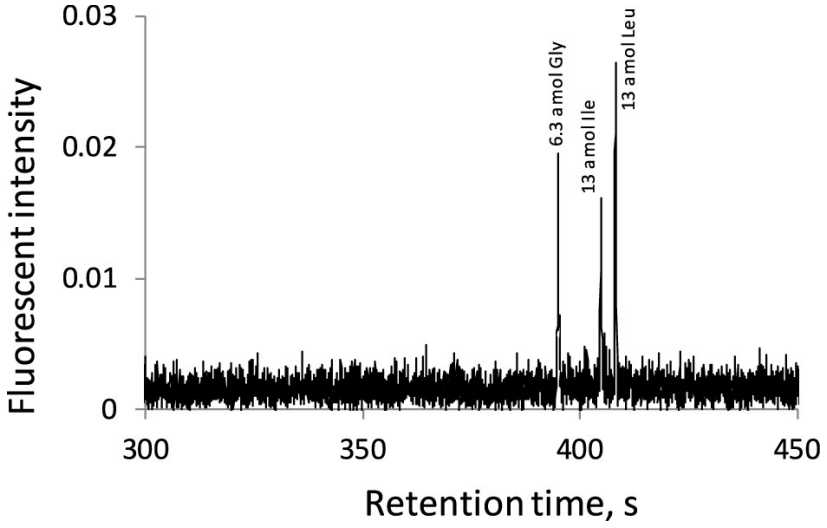

Figure 3-9. LOD determination of NOTLC column

2 μm i.d. × 80 cm length (75 cm effective) coated with C18; sample: 0.04 μM Gly, 0.08 μM Ile, and 0.08 μM Leu in 10 mM NH_4HCO_3; injection volume: ca. 157 pL; mobile phase: mixture of 4 parts of 10 mM NH_4HCO_3 and 1 part of acetonitrile; and elution pressure: 65.5 bar. Figure with permission from the ACS.

With the ultrahigh resolving power and ultrafast separation speed, combined with the low sample volume (pL) and low limit of detection (attomole), NOTLC has the potential to become a powerful tool for biotech research, especially for single cell analysis.

The material in chapter 3 is adapted from Xiang, P., **Yang, Y.**, Zhao, Z., Chen, A., & Liu, S. (2019). Experimentally Validating Open Tubular Liquid Chromatography for a Peak Capacity of 2000 in 3 h. *Analytical chemistry*, *91*(16), 10518-1052. The copyright permission is obtained from ACS.

References

(1) Zubritsky, E. *How Analytical Chemists Saved the Human Genome Project... or at least gave it a helping hand*; ACS Publications, **2002**.
(2)Mathies, R. A.; Huang, X. C. *Nature* **1992**, 359, 167.
(3)Dovichi, N. J.; Zhang, J. *Angew. Chem.*, Int. Ed. **2000**, 39, 4463− 4468.
(4)Ruiz-Martinez, M. C.; Berka, J.; Belenkii, A.; Foret, F.; Miller, A. W.; Karger, B. L. *Anal. Chem.* **1993**, 65, 2851−2858.
(5)Kambara, H. *Nature* **1993**, 361, 565−566.
(6)Washburn, M. P.; Wolters, D.; Yates, J. R., III *Nat. Biotechnol.***2001**, 19, 242.
(7)Plumb, R. S.; Johnson, K. A.; Rainville, P.; Smith, B. W.; Wilson, I. D.; Castro-Perez, J. M.; Nicholson, J. K. Rapid *Commun. Mass Spectrom.* **2006**, 20, 1989−1994.
(8) Chait, B. T. *Science* **2006**, 314, 65−66.
(9)Aebersold, R.; Mann, M. *Nature* **2003**, 422, 198.
(10)Nassar, A. F.; Wu, T.; Nassar, S. F.; Wisnewski, A. V. *Drug Discovery Today* **2017**, 22, 463−470.
(11)De Vos, R. C.; Moco, S.; Lommen, A.; Keurentjes, J. J.; Bino, R. J.; Hall, R. D. *Nat. Protoc.* **2007**, 2, 778.
(12)Wilson, I. D.; Plumb, R.; Granger, J.; Major, H.; Williams, R.; Lenz, E. M. *J. Chromatogr. B: Anal. Technol. Biomed. Life Sci.* **2005**, 817, 67−76.
(13)Jones, D. R.; Wu, Z.; Chauhan, D.; Anderson, K. C.; Peng, J. *Anal. Chem.* **2014**, 86, 3667−3675.
(14)Jorgenson, J. W. *Annu. Rev. Anal. Chem.* **2010**, 3, 129−150.
(15)MacNair, J. E.; Lewis, K. C.; Jorgenson, J. W. *Anal. Chem.* **1997**,69, 983−989.
(16)Golay, M. Gas Chromatography (Lansing Symposium, 1957), Coates, V. J., Noebels, H. J., Fagerson, I S., Eds.; *Academic Press*: New York, **1958**; pp 1−13.
(17)Knox, J. H. *J. Chromatogr. Sci.* **1980**, 18, 453−461.
(18)Jorgenson, J. W.; Guthrie, E. J. *J. Chromatogr. A* **1983**, 255, 335−348.
(19)Tock, P.; Stegeman, G.; Peerboom, R.; Poppe, H.; Kraak, J.; Unger, K. *Chromatographia* **1987**, 24, 617−624.
(20)Guo, Y.; Colon, L. A. *Anal. Chem.* **1995**, 67, 2511−2516.
(21)Crego, A. L.; Diez-Masa, J. C.; Dabrio, M. V. *Anal. Chem.* **1993**, 65, 1615−1621.
(22)Collins, D. A.; Nesterenko, E. P.; Paull, B. *Analyst* **2014**, 139, 1292−1302.
(23)Jorgenson, J.; Kennedy, R.; St. Claire, R.; White, J.; Dluzneski, P.; Dewit, J. *J. Res. Natl. Bur. Stand.* **1988**, 93, 403−406.
(24)Pesek, J. J.; Matyska, M. T. *J. Chromatogr. A* **1996**, 736, 255−264.
(25)Onuska, F.; Comba, M.; Bistricki, T.; Wilkinson, R. *J. Chromatogr. A* **1977**, 142, 117−125.
(26)Kennedy, R. T.; Oates, M. D.; Cooper, B. R.; Nickerson, B.; Jorgenson, J. W. *Science* **1989**, 246, 57−63.
(27)Hara, T.; Futagami, S.; Eeltink, S.; De Malsche, W.; Baron, G. V.; Desmet, G. *Anal. Chem.* **2016**, 88, 10158−10166.
(28)Yue, G.; Luo, Q.; Zhang, J.; Wu, S.-L.; Karger, B. L. *Anal. Chem.* **2007**, 79, 938−946.

(29)Rogeberg, M.; Wilson, S. R.; Greibrokk, T.; Lundanes, E. *J. Chromatogr. A* **2010**, 1217, 2782−2786.
(30)Desmet, G.; Callewaert, M.; Ottevaere, H.; De Malsche, W. *Anal. Chem.* **2015**, 87, 7382−7388.
(31)Tsuda, T.; Hibi, K.; Nakanishi, T.; Takeuchi, T.; Ishii, D. *J. Chromatogr. A* **1978**, 158, 227−232.
(32)Desmet, G.; Eeltink, S. Anal. Chem. **2013**, 85, 543−556.
(33)Chen, H.; Yang, Y.; Qiao, Z.; Xiang, P.; Ren, J.; Meng, Y.; Zhang, K.; Lu, J. J.; Liu, S. *Analyst* **2018**, 143, 2008−2011.
(34)Yang, Y.; Chen, H.; Beckner, M. A.; Xiang, P.; Lu, J. J.; Cao, C.; Liu, S. *Anal. Chem.* **2018**, 90, 10676−10680.
(35)Weaver, M. T.; Lynch, K. B.; Zhu, Z.; Chen, H.; Lu, J. J.; Pu, Q.; Liu, S. *Talanta* **2017**, 165, 240−244.
(36)Han, J.; Ye, L.; Xu, L.; Zhou, Z.; Gao, F.; Xiao, Z.; Wang, Q.; Zhang, B. *Anal. Chim. Acta* **2014**, 852, 267−273.
(37)Luo, Q.; Shen, Y.; Hixson, K. K.; Zhao, R.; Yang, F.; Moore, R. J.; Mottaz, H. M.; Smith, R. D. *Anal. Chem*. **2005**, 77, 5028−5035.
(38)Shen, Y.; Zhang, R.; Moore, R. J.; Kim, J.; Metz, T. O.; Hixson, K. K.; Zhao, R.; Livesay, E. A.; Udseth, H. R.; Smith, R. D. *Anal. Chem.* **2005**, 77, 3090−3100.
(39)Zhou, F.; Lu, Y.; Ficarro, S. B.; Webber, J. T.; Marto, J. A. *Anal. Chem.* **2012**, 84, 5133−5139.
(40)Wahab, M. F.; Wimalasinghe, R. M.; Wang, Y.; Barhate, C. L.; Patel, D. C.; Armstrong, D. W. *Anal. Chem.* **2016**, 88, 8821−8826.77.

Chapter4. Coating 2-μm-Bore Capillaries for Ultrahigh-Resolution Open Tubular Liquid Chromatography

This project was a collaborative work that consists of the following authors: Yu Yang, Piliang Xiang, Zhitao Zhao, Mingli Chen, Jianhua Wang, Apeng Chen, Shaorong Liu

Piliang Xiang and Zhitao Zhao assisted the column reproducibility tests.

Mingli Chen and Jianhua Wang helped analyzing the model for diffusion experiment.

Apeng Chen helped the cell sample preparation.

All the other work was finished by Yu Yang.

4.1. Abstract

Extraordinarily high peak capacities have been obtained using 2-μm-bore open tubular columns. A key to these results is to prepare columns with good coatings. In this technical note, we disclose the procedure of how to coat these narrow columns. We optimized various coating parameters (reagent concentration, coating temperature, reagent flushing pressure and time). For all optimizations, we separated mixtures of amino acids and targeted for the highest resolutions. We examined coating reproducibility by selecting 8 columns from 4 different batches and using them to separate an amino acid mixture. A relative standard deviation of <0.2% for retention times and a relative standard deviation of <11% for peak areas were obtained. We utilized columns prepared under the optimized conditions to separate a pepsin and trypsin digested *E.*

coli lysate and obtained a peak capacity of 770 within 47 min (using a 45-cm-long column) and a peak capacity of 1900 within 158 min (using a 155-cm-long column).

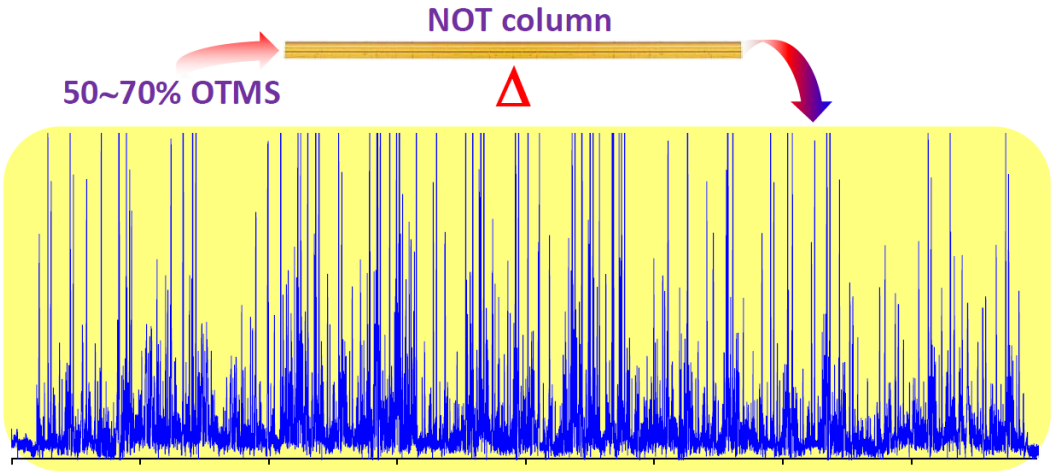

Figure 4-1. Graphic abstract.

4.2. Introduction

Open tubular (OT) columns were first introduced for gas chromatography (GC) by Golay[1] in 1957. OT columns had since quickly replaced packed columns in GC for most analytical applications because of the improved efficiencies. Theoretical studies [2-5] predicted that OT columns would achieve increased efficiencies for liquid chromatography (LC), but to obtain the high efficiencies the inner diameters (i.d.) of the OT column must be small (e.g., 1~2 μm).[5] Because of this requirement, open tubular liquid chromatography (OTLC) was never popular and no commercial products were ever yielded.[6]

One of the major obstacles for using narrow OT columns was the low mass loadability due to insufficient stationary phase. [7] To increase the mass loadability, Jorgenson *et al*. [8] first roughened a borosilicate glass capillary with hydrochloric acid leaching, rendering a porous silica layer by selectively removing the non-silica components of the glass. This process increased the internal surface area of the capillary roughly thirtyfold over a geometrically smooth capillary. These authors then coated this surface with a layer of siloxane polymer stationary phase and used these columns for single neuron analysis. However, limited success was achieved toward ultrahigh efficiencies. Much improved efficiencies were obtained through coating a thick layer of porous polymer on the capillary wall [7,9-14] as the stationary phase; this column is now called a porous layered open tubular (PLOT) column. Preparing PLOT columns is tedious, and often it is challenging to prepare PLOT columns reproducibly.

In our lab we have recently demonstrated ultrahigh performance of NOTLC using a 2-μm-i.d. NOTLC column coated with octadecyltrimethoxysilane (C18) for reversed-phase separations. When we used this column to separate pepsin/trypsin digested *E. coli* lysates, we obtained peak capacities of ~2000 within 3 h,[15,16] a record number for 1-dimensional liquid chromatographic separations. When we coupled this column with mass spectrometry (MS) and utilized it for proteomic analysis of *Shewanella oneidensis* MR-1, we identified ~1000 proteins reliably using only 30 pg of tryptic peptides, representing a 10-100-fold sensitivity improvement compared with the state-of-the-art LC-MS or capillary electrophoresis (CE)-MS methods. Because the narrowness of the OTLC columns was key to achieving these ultrahigh performance results, we termed these columns - narrow open tubular liquid chromatography (NOTLC) columns. Since NOTLC columns are not commercially available yet, it would be valuable if we can disclose how we make these columns so that other researchers can further explore the potential and

applications of NOTLC. In this technical note, we describe an optimized protocol for preparing 2-µm-i.d. NOTLC columns and how we optimize the various parameters of the procedure. We also examine the column preparation reproducibility and demonstrate the performance of these columns for ultra-high peak capacity separations.

4.3. Experimental section

4.3.1. Chemicals and materials

Fluorescein, amino acids, sodium hydroxide, ammonia bicarbonate, acetonitrile, toluene and octadecyltrimethoxysilane (OTMS) [also named trimethoxy(octadecyl) silane] were obtained from Sigma-Aldrich (St. Louis, MO). ATTO-TAG™ FQ Amine-Derivatization Kit was obtained from Thermo Fisher Scientific (Waltham, MA). Fluorescently labelled amino acids and peptides were prepared in our laboratory, and their preparation protocols were provided in appendix 3. All solutions were prepared using ultrapure water (Nanopure ultrapure water system, Barnstead, Dubuque, IA) and filtered through a 0.22-µm filter (VWR, TX), degassed before use. Fused-silica capillaries used for making NOTLC columns [2-µm inner diameter (i.d.), 150-µm outer diameter (o.d.)] were purchased from Polymicron Technologies, a subsidiary of Molex (Phoenix, AZ).

4.3.2. NOTLC column preparation

The Fig. 4-2A schematically presents the apparatus for activating the surface of a NOTLC column. A 50-cm-long and 2-µm-i.d. fused silica capillary was cut, and about 1 cm of the polyimide coating was removed from one end of the capillary. A 25 G × 7/8" hypodermic needle was used to guide the polyimide-coating-removed end of the capillary through the septum to the reagent reservoir loaded with 50 µL 1.0 M NaOH. The other end of the capillary was inserted

into a waste reservoir containing ~50 μL DDI water. The apparatus was then moved inside an oven at 100 °C, and pressurized N_2 was introduced to the pressure chamber to drive the NaOH solution through the capillary for 2 hours. The NaOH reservoir was then replaced with another vial containing ~50 μL DDI water to rinse the capillary for 1 hour. After the apparatus was moved out of the oven, the water reservoir was replaced with a vial containing ~50 μL acetonitrile, and the capillary was rinsed with acetonitrile at ambient temperature for 30 min. The acetonitrile reservoir was then replaced with an empty vial, and the capillary was dried with N_2 overnight.

Normally the same apparatus was used to coat the NOTLC column with OTMS, as we have described previously. [17] Inside a dry box, 100-μL OTMS reagents at various concentrations were prepared inside a dry box by mixing appropriate volumes of OTMS and toluene. After a reagent reservoir holding an OTMS reagent was placed in the pressure chamber, the polyimide-coating-removed end of the surface-activated capillary was inserted into the OTMS solution. The other end of the capillary was dipped into a vial containing 50 μL toluene. The apparatus was then moved inside an oven at a pre-set temperature, and pressurized N_2 was introduced into the pressure chamber to drive the OTMS reagent through the capillary for 6, 12, 18, 24 or 36 hours. The OTMS reservoir was replaced with a vial containing 50 μL toluene to rinse the capillary for 1 hour. The toluene reservoir was then replaced with an empty vial, and the capillary was dried with N_2 for 2 hours.

Fig. 4-2B presents the apparatus used to optimize pressure of flushing OTMS reagent through a NOTLC column. There were two loops on the valve. The top loop (in red) has a volume of 150 μL, and it was used to hold OTMS reagent. The bottom loop (in green) had a volume of 60 μL, and it was used to hold toluene. After the OTMS reagent was loaded in the 150-μL-loop, the

valve was switched to the position as shown in Fig. 4-2B. The setup was moved inside an oven at a pre-set temperature, and pressurized N_2 was applied to the valve to drive the OTMS reagent through the NOTLC column. Toward the end of this coating process, toluene was loaded in the 60-µL-loop. After the coating step was complete, the valve was switched to the other position to drive toluene through the capillary for 1 hour. The capillary was taken out, installed back to Fig. 4-2A device and dried with N_2.

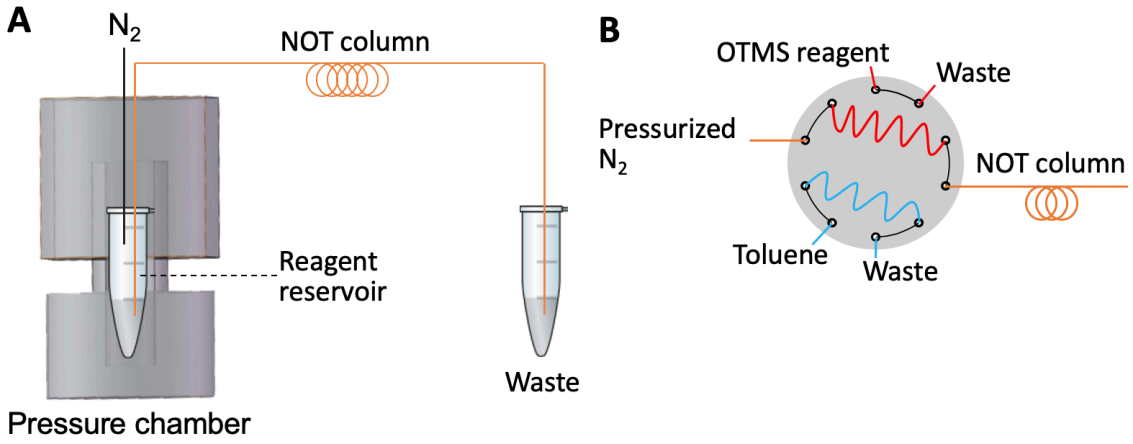

Figure 4-2. Apparatus for coating NOTLC column.

(A) apparatus for activating the surface of NOTLC column and coating NOTLC columns with OTMS. (B) alternative apparatus for coating NOTLC column with OTMS.

4.3.3. Apparatus for running NOTLC separations

This apparatus has been described previously, [18] and its configuration is also provided in appendix 4.

4.4. Results and discussion

Concerning the low mass loadability, most researchers coated OT columns with relatively thick polymer layers (including porous polymer layers), and limited research was conducted on thin coatings.[19] Because we used 2-μm-i.d. NOTLC columns, we deliberately tried not to produce thick coatings. Through this research, we noticed that thick coatings were not necessary for achieving high performance separations; in fact, a thin-layer coating may be critical toward achieving ultrahigh efficiency separations. While we are testing different coatings, we report the optimization and characterizations of only OTMS (or C18) coatings in this work.

4.4.1. Effect of OTMS concentration on amino acid retention and resolution

Although we did not intend to synthesize a thick layer coating, we did want a dense coating layer to obtain adequate mass loadability. We used relatively high concentrations (30-90%, v/v) of OTMS solution to coat our NOTLC columns. In the literature, [20,21] the OTMS concentrations used were usually <1% (v/v). We believed that using high concentrations of OTMS to coat our NOTLC columns was a key to achieving dense coatings.

Fig. 4-3 presents the effect of OTMS concentration on amino acid retention and resolution. As can be seen in Fig. 4-3A, poor results were obtained when OTMS concentration was lower than 30% under our experimental conditions. In general, amino acid retention and resolution increased with OTMS concentration. In this work, we selected 70% as the optimum condition, because resolutions started to plateau (see Fig. 4-3B) and because column clogging started to occur often at higher concentrations.

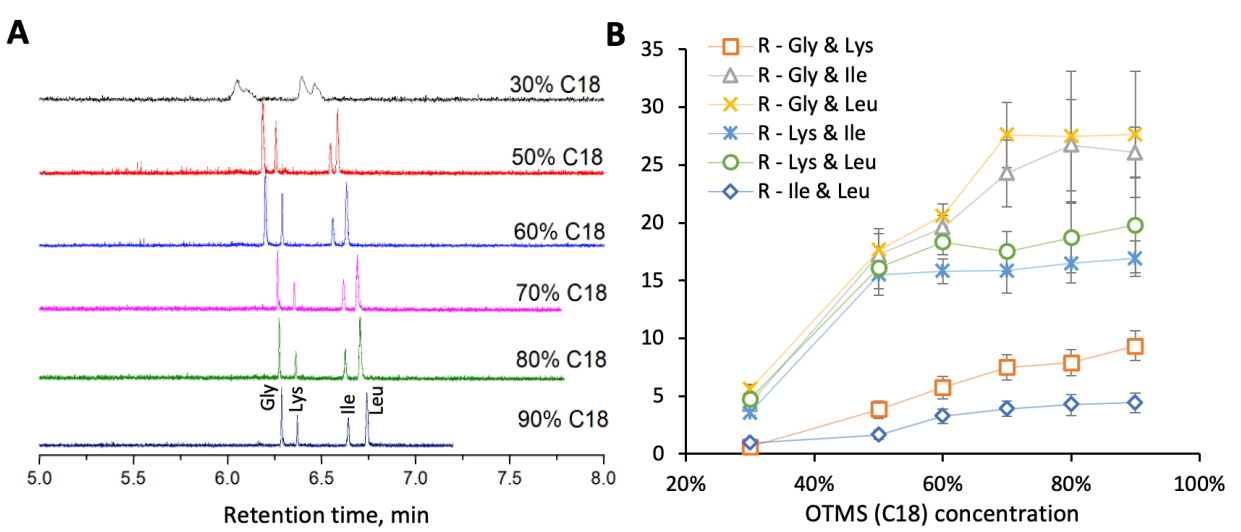

Figure 4-3. Influence of reagent concentration on NOTLC column.

4.4.2. Optimization of temperature, pressure and duration for flushing OTMS through NOTLC column

Fig. 4-4 presents effects of temperature, pressure and duration for flushing OTMS on resolution; the associated chromatograms are exhibited in Fig. S4-2, S4-3 and S4-4. Referring to Fig. 4-4A, resolution increased with coating temperature and plateaued after 50~60 °C. We had also test coating at ambient temperature, no good separation results were achieved. Since column clogging frequency also increased with the temperature, we selected 60 °C for coating in this work. From the results presented in Fig. 4-4B, we selected 1000 psi as the optimized pressure for flushing OTMS reagent through the NOTLC column. Resolutions increased with coating time initially and plateaued after about 18 hours (see Fig. 4-4C). We selected a coating time of 18 hours in this experiment.

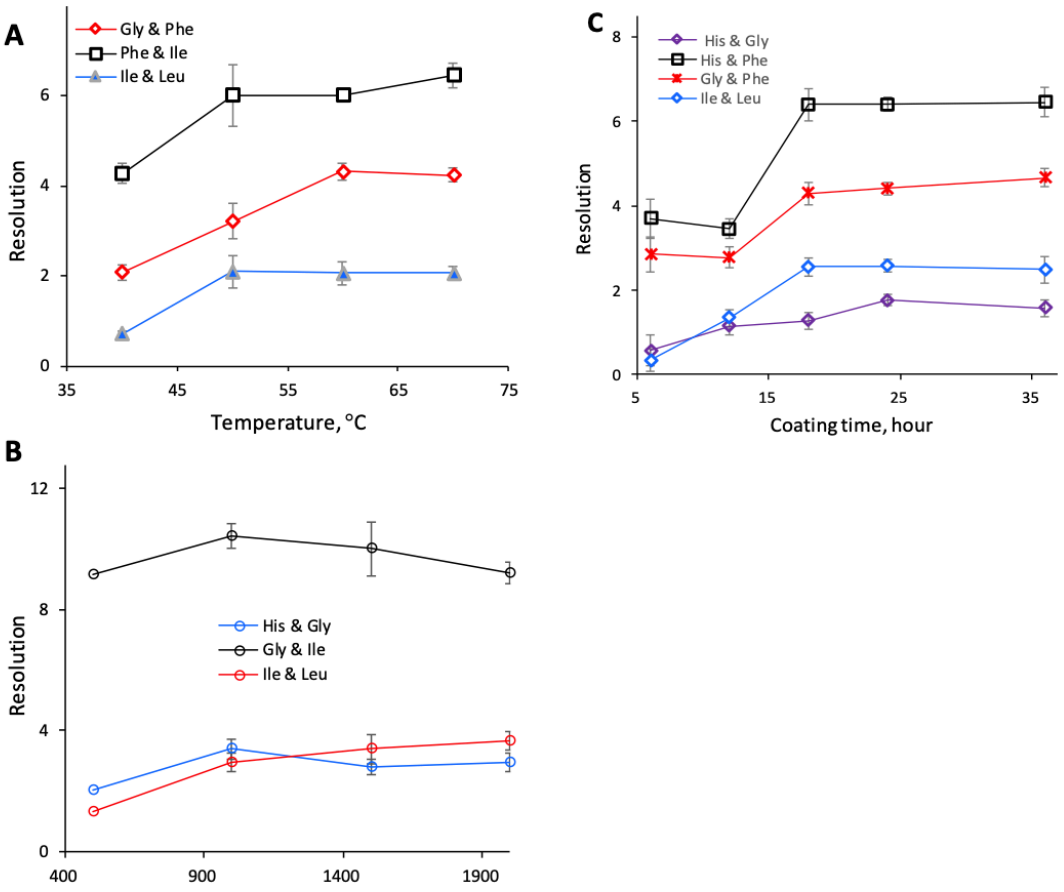

Figure 4-4. Effects of temperature, pressure and duration for flushing OTMS on resolution.

OTMS concentration: 70% (v/v) in toluene. The testing parameters were indicated by the number on the X-axes. All other conditions were the same as in Fig. 4-2.

4.4.3. Column coating reproducibility

Eight NOTLC columns of 2-µm-i.d. were prepared in four batches (2 columns per batch). These columns were used for amino acid separations, and the results were exhibited in Fig. S4-5. The relative standard deviations of the retention times of the four amino acids were between 0.15-0.18%, and that of the peak areas were between 7.3-11%. If we used retention time and the peak

area of glycine as an internal standard, the relative standard deviations of the retention times of the other three amino acids were between 0.13-0.17%, and that of the peak areas were between 2.9-8.0%.

4.4.4. Performance of NOTLC column.

Once the NOTLC column was coated, it was used to separate a peptide sample from pepsin and trypsin digested *E. coli* lysate, and the results are presented in Fig. S4-6. The column had an effective length of 45 cm, and all other experimental parameters were included in the figure legend. Using the same method as described previously,[16] the average peak width was estimated to be 3.4 s, the first peak appeared at 6.7 min, and the last peak showed up at 54.1 min. The peak capacity was computed to be 770 (= the gradient time between the first peak and the last peak divided by the average peak width).

To show the ultrahigh peak capacity of NOTLC separation, we increased the effective length of the column from 45 cm to 155 cm and used this column to separate the same sample. [Note: the pressure of flushing OTMS through this column was increased to ~3000 psi.] Fig. 4-5 presents the chromatogram. We displayed the chromatogram in four separate panels in order to resolve the individual sharp peaks in the presentation. The single-panel chromatogram was presented in Fig. S4-7. Similarly, we determined the average peak width to be 5.2 s, the retention time of the first peak to be 33.7 min and the retention time of the last peak to be 191.5 min. The peak capacity was calculated to be 1900 within 158 min.

4.5. Conclusion

We have described a protocol for coating NOTLC (2-μm-i.d.) columns. Optimization of various coating parameters and performances of the coated NOTLC columns have been presented. Columns coated in different batches have similar performances, indicating that the columns can be reproducibly prepared, and that the column preparation procedure is reliable. Column clogging didn't appear to be an issue, but care (e.g., column ends need to be put in solutions to prevent solvent evaporation and salt precipitation) must be taken to prevent it from happening. The primary goal of this technical note is to inform the journal readers how we prepare our NOTLC columns, and we hope that some of these readers can prepare their own columns so that they can exploit the use of NOTLC for practical applications.

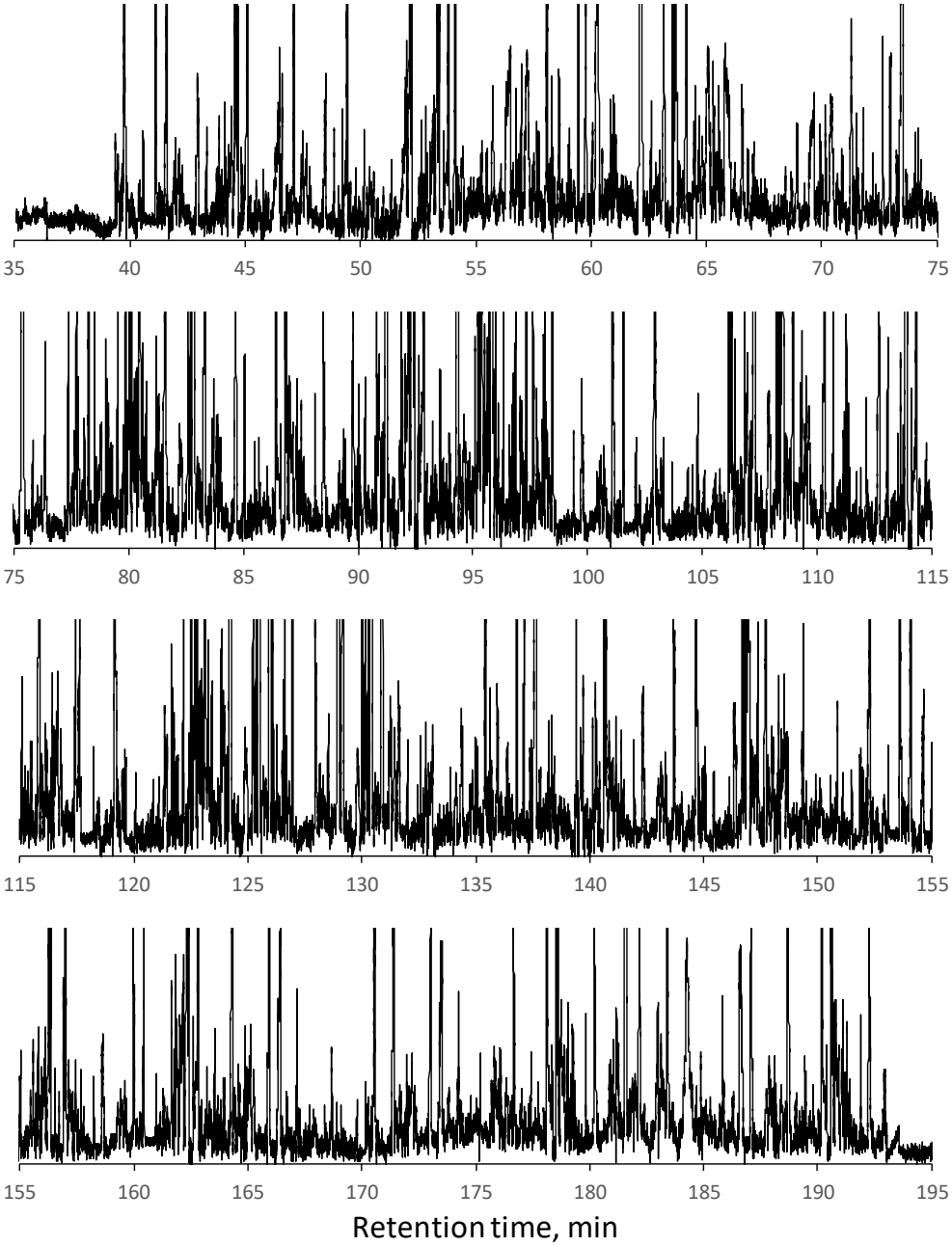

Figure 4-5. Ultrahigh performance of NOTLC column.

NOTLC column: 2 μm i.d. × 160 cm length (155 cm effective) coated with OTMS. Sample: pepsin and trypsin digested *E. coli* lysate (1 mg total protein/mL). Injected volume: ~120 pL. Elution pressure: 500 psi (corresponding to a flow velocity 0.6 mm/s). MA: 10 mM NH_4HCO_3 in DDI water. MB: 80% acetonitrile in 10 mM NH_4HCO_3. Gradient profile: starting with 100% MA, increasing MB from 0 to 100% linearly from 0 to 180 min, and staying at 100% MB for 20 min.

References

(1) Golay, M. J. E. *Gas Chromatography*; Academic Press Inc., 1957.
(2) Knox, J. H.; Gilbert, M. T. *J. Chromatogr. A* **1979**, 186, 405-418.
(3) Knox, J. H. *J. Chromatogr. Sci.* **1980**, 18, 453-461.
(4) Guiochon, G. *Anal. Chem.* **1981**, 53, 1318-1325.
(5) Jorgenson, J. W.; Guthrie, E. J. *J. Chromatogr. A* **1983**, 255, 335-348.
(6) Hara, T.; Izumi, Y.; Nakao, M.; Hata, K.; Baron, G. V.; Bamba, T.; Desmet, G. *J. Chromatogr. A* **2018**, 1580, 63-71.
(7) Tock, P.; Boshoven, C.; Poppe, H.; Kraak, J.; Unger, K. *J. Chromatogr. A* **1989**, 477, 95-106.
(8) Jorgenson, J.; Kennedy, R.; Stclaire, R.; White, J.; Dluzneski, P.; Dewit, J. *J. Res. Nat. Bureau Standards,* **1988**, 93, 403-406.
(9) Tock, P.; Duijsters, P.; Kraak, J.; Poppe, H. *J. Chromatogr. A* **1990**, 506, 185-200.
(10) Swart, R.; Kraak, J.; Poppe, H. *Chromatographia* **1995**, 40, 587-593.
(11) Yue, G.; Luo, Q.; Zhang, J.; Wu, S.-L.; Karger, B. L. *Anal. Chem.* **2007**, 79, 938-946.
(12) Rogeberg, M.; Wilson, S. R.; Greibrokk, T.; Lundanes, E. *J. Chromatogr. A* **2010**, 1217, 2782-2786.
(13) Causon, T. J.; Shellie, R. A.; Hilder, E. F.; Desmet, G.; Eeltink, S. *J. Chromatogr. A* **2011**, 1218, 8388-8393.
(14) Forster, S.; Kolmar, H.; Altmaier, S. *J. Chromatogr. A* **2012**, 1265, 88-94.
(15) Yang, Y.; Chen, H.; Beckner, M. A.; Xiang, P.; Lu, J. J.; Cao, C.; Liu, S. *Anal. Chem.* **2018**, 90, 10676-10680.
(16) Xiang, P.; Yang, Y.; Zhao, Z.; Chen, A.; Liu, S. *Anal. Chem.* **2019**, 91, 10518-10523.
(17) Chen, H.; Yang, Y.; Qiao, Z.; Xiang, P.; Ren, J.; Meng, Y.; Zhang, K.; Lu, J. J.; Liu, S. *Analyst* **2018**, 143, 2008-2011.
(18) Xiang, P.; Yang, Y.; Zhao, Z.; Chen, M.; Liu, S. *Anal. Chem.* **2019**, 91, 10738-10743.
(19) Lam, S. C.; Rodriguez, E. S.; Haddad, P. R.; Paull, B. *Analyst* **2019**, 144, 3464-3482.
(20) Tsuda, T.; Tsuboi, K.; Nakagawa, G. *J. Chromatogr. A* **1981**, 214, 283-290.
(21) Sander, L. C.; Wise, S. A. *Anal. Chem.* **1984**, 56, 504-510.

Chapter5. Overall Summary and Future Perspective

This dissertation was devoted to exploring the potential of narrow open tubular liquid chromatography. The focusing effect in NOTLC was identified and used to interpret the exceptionally narrow peaks obtained from "isocratic" separation. Based on this focusing mechanism, a simple and economic device to perform picogradient NOTLC was invented by adding a injection valve to the original "isocratic" system. This approach has demonstrated that NOTLC separations are extraordinarily highly efficient. Another great advancement of NOTLC separation is that it does not require high elution pressures due to its high permeability, which achieves the ultra-fast separation at a lower cost of equipment. The sample loadability, the column-coating durability, and the column-preparation reproducibility were initially concerned. These concerns have been solved nicely with the approaches for carefully preparing the columns and running the separations. The optimization of various coating parameters and performances of the coated NOTLC columns have been presented in the protocol for coating NOTLC (2-μm-i.d.) columns. The experimental result that columns coated in different batches have similar performances, indicated that the columns can be reproducibly prepared, and the column preparation procedure is reliable. This dissertation has fulfilled one of the main goals, that is to provide readers with a more practical method to prepare the NOTLC columns and inspire them to explore the wider applications of NOTLC.

The LIF detector is currently used as the main detection method to monitor the separations. Even though the sensitivity and cost of the detection is relatively good for concept proofing, the requirement of labeling the analytes with a fluorescent dye cause problems for future application. For example, there might be multiple labeling positions for one amino acid or peptide, resulting in "fake" peaks in NOTLC separations, especially those complex digested peptides. Also, the

fluorescent signal cannot tell what exactly the analyte is when there are no standards to refer. So NOTLC-MS is a very promising direction for utilizing NOTLC in more applications. It is possible that the pico-gradient NOTLC could be coupled with mass spectrometry (MS), one of the most powerful detectors for comprehensively recognizing the complicated bio-molecules. There are some challenges caused from the extremely low flowrates in NOTLC (less than one hundred picoliter per minute). Fortunately, this problem can be solved with the recent invention of picospray emitters.[1,2] and our lab is continuing the approach to make this happen. The flowrate might be optimized at a level of ~100-200 pL/min for the separation and the ionization efficiency will be tuned stable. A powerful analytical technique for separations will soon come true with the aid of NOTLC with high efficiency and the MS with resolving power.

References

(1) Gibson, G. T.; Mugo, S. M.; Oleschuk, R. D. *Mass spectrometry reviews* **2009**, *28*, 918-936.
(2) Marginean, I.; Tang, K.; Smith, R. D.; Kelly, R. T. *Journal of the American Society for Mass Spectrometry* **2013**, *25*, 30-36.

Appendix 2: Chapter 2 Supplemental

1. Measuring the diffusion coefficients of analytes confined in a NOTLC column

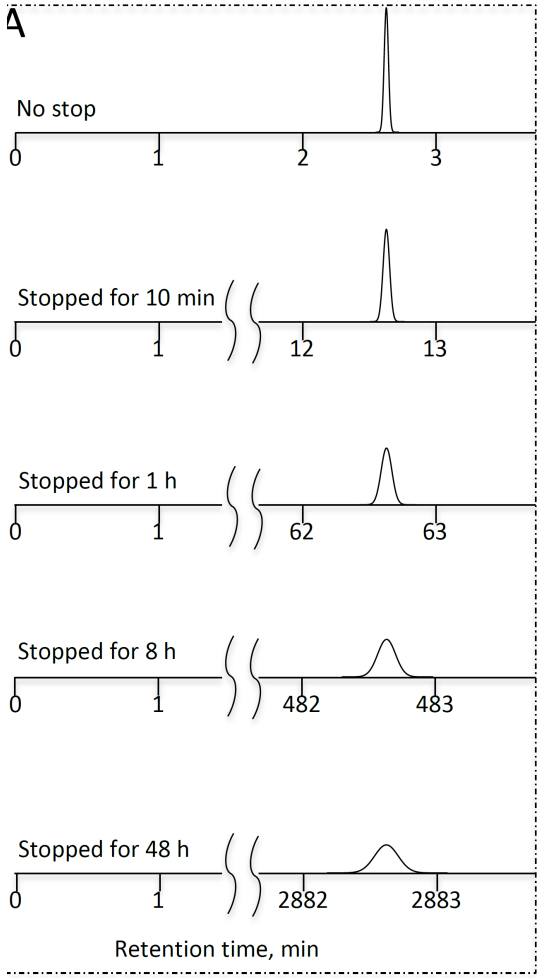

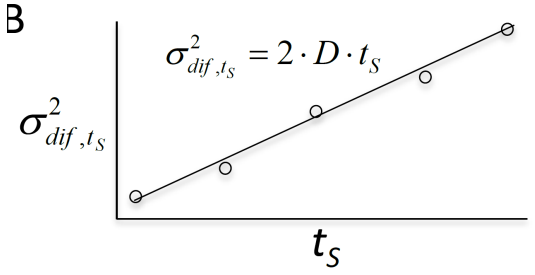

Figure S2-1. Schematic illustration of diffusion coefficient measurement

Figure with permission from Elsevier.

Here we use only one peak (one analyte) to illustrate the working principle. We run a NOTLC separation under a set of conditions as we did in Figure 2 and measure the FWHM ($w_{1/2}$) on the obtained chromatogram (see Figure S3A). We assume the peak profile follows the Gaussian distribution and calculate the overall variance using

$$\sigma^2 = \left(w_{1/2}/2.354\right)^2;\ \sigma^2 = \sigma^2_{dif,t_R} + \sigma^2_{other}, \quad \text{(S1)}$$

where σ^2_{dif,t_R} is the diffusion-caused variance, and σ^2_{other} is the sum of all other variance including that for sample injection (σ^2_{inj}), analyte detection (σ^2_{det}), flow dispersion (σ^2_{dis}), etc.

We run another NOTLC separation for the same sample, but we stop eluting before the analyte reaches the detector (e.g., at $t=t'<t_R$) and park the peak for a period, t_S. Then, we elute the analyte and obtain a chromatogram. We measure the FWHM, $w'_{1/2}$, and calculate the overall variance using equation S1. We change the parking time and obtain a series of σ^2_{dif,t_S} at different t_S. We plot σ^2_{dif,t_S} against t_S (see Figure S3B) and the slope of the line will be $2 \cdot D$ (Einstein diffusion equation, $\sigma^2_{dif,t_S} = 2 \cdot D \cdot t_S$).

2. Measured diffusion coefficient result

The chromatograms on the left were obtained after fluorescein was parked inside a NOTLC column for various times (0–28 h), and the plot on the right presents a relationship between variance and parked time. Dividing the slope by 2 yields the diffusion coefficient value.

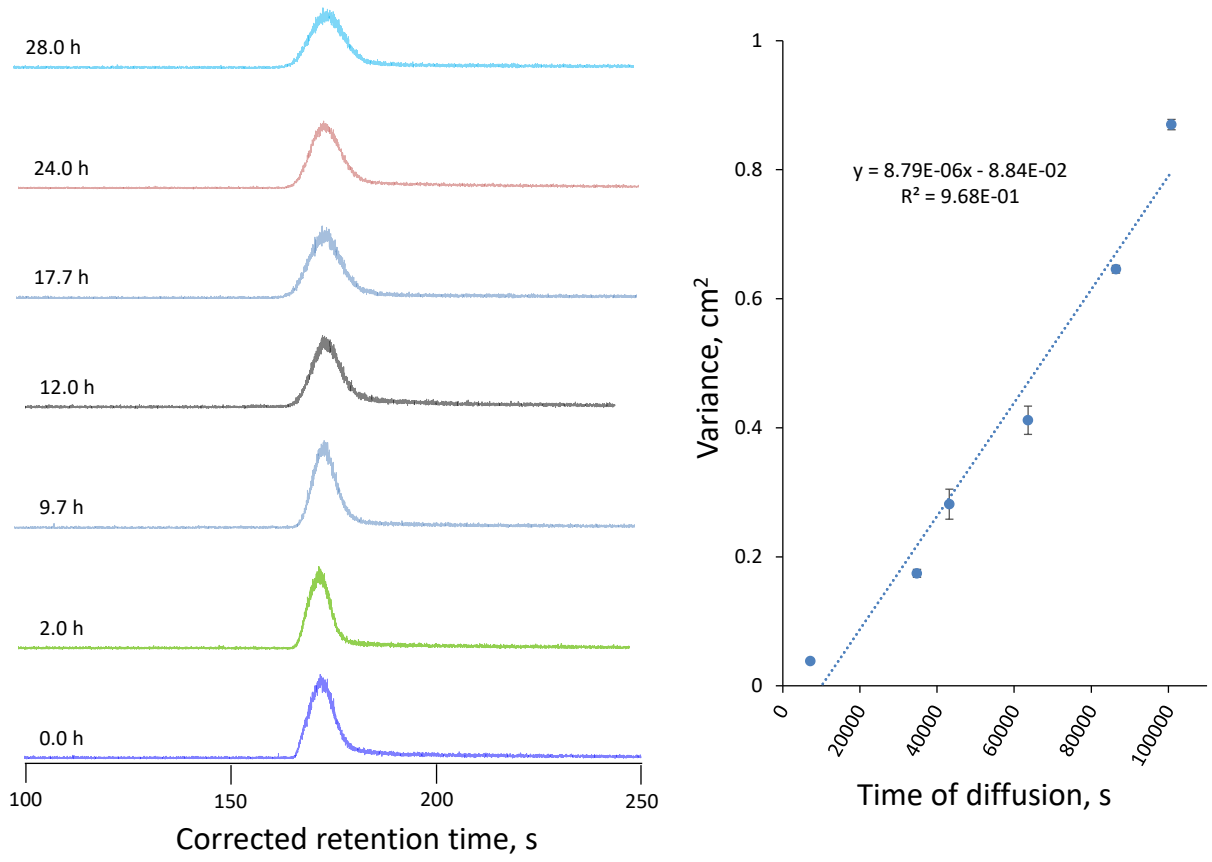

Figure S2-2. Measurement of diffusion coefficient of fluorescein residing in NOTLC column.
Left: chromatogram peaks after fluorescein was parked different times (0–28 h) for diffusion. A bare capillary of 2-μm-i.d., a total length of 50 cm (45 cm effective) and an o.d. of 150 μm was used for these tests. The analyte was parked at a position about 50 mm away from the detector. The mobile phase is 40% (v / v) acetonitrile with 10 mM NH_4HCO_3 solution. Sample contained 0.5 μM fluorescein dissolved in mobile phase. The injected volume is ~16 pL. The elution pressure was ~85 bar and flow velocity was ~2.5 mm/s. Figure with permission from Elsevier.

Appendix 3: Chapter 3 Supplemental

1. Apparatus.

NOTLC separation. To align the NOTLC column on the LIF detector, 10 μM fluorescein solution was pressurized through the column and the column was roughly aligned with the detector as shown in Figure S4. The fluorescein solution was constantly flushed through the column until the alignment was done. Then, the LIF detector was turned on and fluorescence signal was monitored. By tuning the column position via the x-y-z translation stage until the maximum fluorescence output was obtained, the x, y and z positions of the stage were locked. The capillary was thoroughly rinsed with an eluent (e.g., 50% acetonitrile with 10 mM NH_4HCO_3) before conducting a NOTLC separation.

In this work, we used 10 mM NH_4HCO_3 as the pH buffer for our mobile phase because that buffer was recommended for labelling amino acid or peptide with ATTO TAG FQ at a pH between 8.5 and 9.5. The pH of 10 mM NH_4HCO_3 was measured to baseline resolved. If the acetonitrile concentration was high (e.g., 80%), the amino acids could not be baseline-resolved, while the elution of the amino acids was slow if acetonitrile concentration was low (e.g., 20%). Under the conditions in the Figure caption, the linear velocity of the mobile phase was 79 mm/s. This velocity was much higher than the optimum velocity for high resolution. In this experiment, we were pursuing high separation speed.

The sample injection volume was estimated to be 120 pL. We used a couple of approaches to determine this volume. For the more common approach, we replaced the NOTLC column with an uncoated capillary having identical dimensions. Several windows at fixed locations on that capillary were made for LIF detection. An unretained analyte (e.g., 1 μM fluorescein) was injected into the column, and fluorescent signals were measured at different windows. The different arrival time of the dye revealed the velocity of the mobile phase. The flow rate through the restriction capillary was measured directly by collecting. The splitting ratio of the splitter was then calculated by ratio of the flow rate inside of restriction capillary and

that inside the uncoated narrow capillary. The sample injection volume was computed by dividing the loop volume on the injection valve by the splitting ratio.

For ultra-high-resolution separations and LOD determinations, data acquisitions started immediately after sample injection. Flor ultra-high-speed separations, MB was injected a couple of seconds after the sample injection, and data acquisitions started immediately after MB injection.

2. Single-panel exhibition of an ultra-high-resolution chromatogram

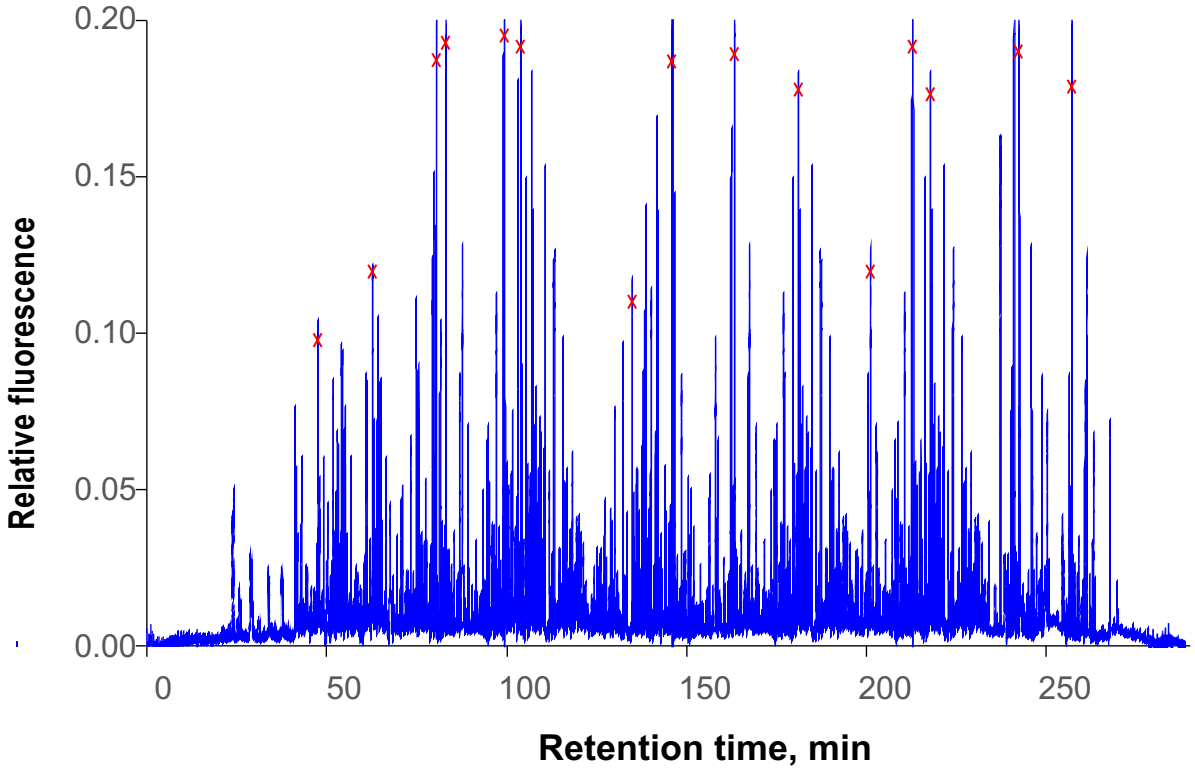

Figure S3-1. Single-panel exhibition of an ultra-high-resolution chromatogram.
The chromatogram is identical to the chromatogram presented in Fig.3-3 but exhibited in a single panel. The peaks marked with red crosses were used for peak capacity calculations. Figure with permission from the ACS.

2. Peak widths in four zoomed-in regions

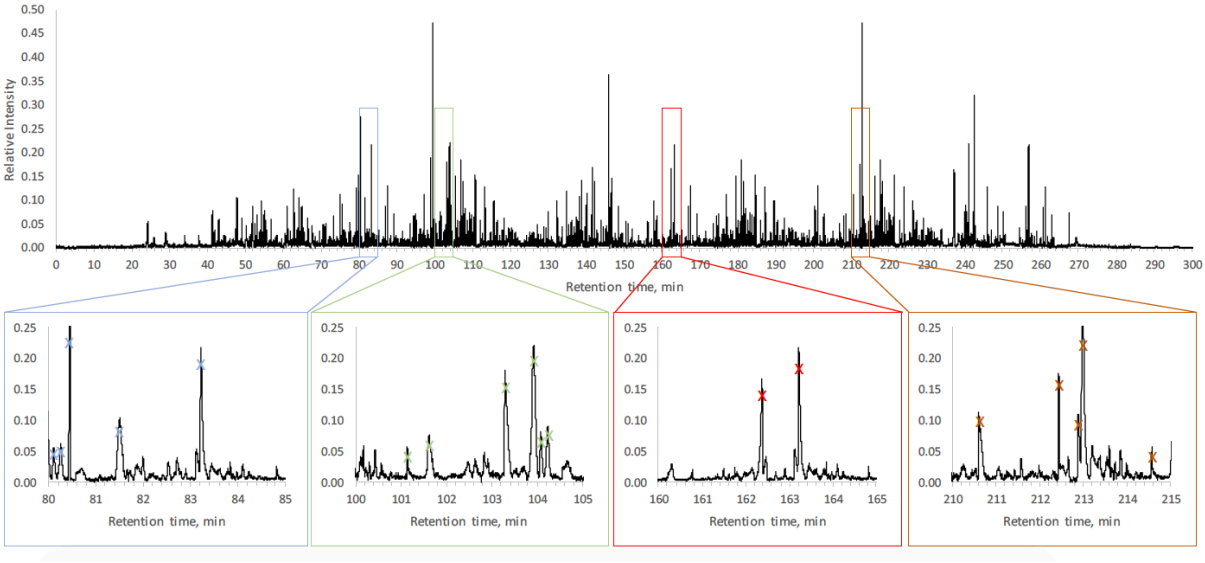

Figure S3-2. Single-panel exhibition of an ultra-high-resolution chromatogram showing four zoomed-in regions.

The chromatogram is identical to the chromatogram presented in Figure 1 but exhibited in a single panel. The peaks marked with asteroids were used for peak capacity calculations. Figure with permission from the ACS.

3. Chromatogram comparison between ultra-high-speed separations

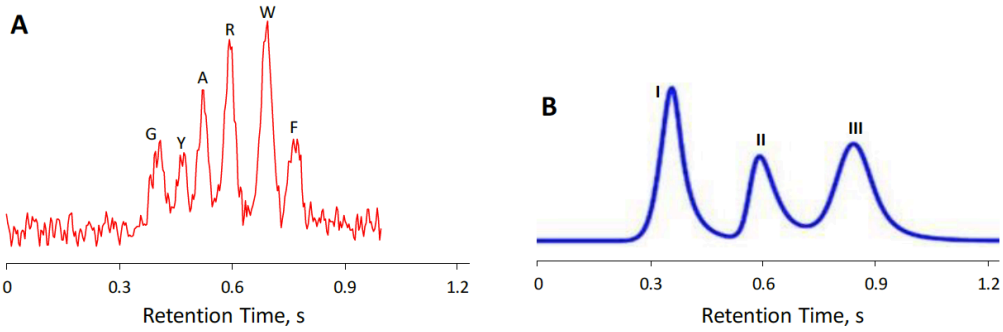

Figure S3-3. Chromatogram comparison between ultra-high-speed separations
(A) Chromatogram of an ultra-fast NOTLC separation. NOTLC column: 2-µm-i.d. × 60 mm (27 mm effective) length fused-silica capillary coated with c18. Sample: mixture of glycine (1 µM), tyrosine (3 µM), alanine (3 µM), arginine (3 µM), tryptophan (10 µM) and phenylalanine (2.5 µM); all labeled with ATTO-TAG™ FQ. Separation: gradient produced by injecting a plug of 50% acetonitrile in 10 mM NH_4HCO_3. Elution pressure was 3300. Gradient delay time was subtracted from the retention time. (B) Chromatogram of an ultra-fast HPLC separation[S2].Separation was performed on an Agilent 1290 UHPLC with a diode array detector. The in-line filter was removed for high flow rate. The pump outlet was directly connected to a presaturator column (5 × 0.46 cm i.d.) filled with silica (M.S. Gel, D-50-120A, AGC SciTech Co., Ltd.). The column had a length of 0.5 cm and an i.d. of 0.46 cm. Rheodyne 7520 manual injector with an internal loop size of 1 µL was connected to the presaturator outlet and then the analytical column. The mobile phase (70:30 ACN: water) flow rate was 5 mL/min. I: 4-Formyl-benzene-1,3-disulfonic acid, II: N-Acetyl-D-alanine, III: Methyl benzenesulfonate. The three peaks in B were sharpened by raising Gaussian functions to power 3 to fit all these peaks. Figure with permission from the ACS.

Appendix 4: Chapter 4 Supplemental

1. Amino acid labelling

Following the instruction provided with the ATTO-TAG^{TM} FQ Amine-Derivatization Kit by Thermo Fisher Scientific, a 10 mM ATTO-TAG^{TM} FQ stock solution was prepared by dissolving 5.0 mg of ATTO-TAG^{TM} FQ in 2.0 mL of methanol and stored in -20 °C before use. A 10 mM working KCN solution was prepared by diluting a 0.2 M KCN stock solution with 10 mM borax solution (pH 9.2). Amino acid stock solutions (each containing 1 mM of one amino acid) were prepared by dissolving individual amino acids in DDI water and filtered with 0.22-μm filter. A volume of 1.0 μL of the amino acid stock solution was mixed with 10 μL of the 10 mM KCN working solution, and 5 μL of the 10 mM FQ solution in a 0.25-mL vial. This mixture was maintained at room temperature for 1 hour in dark environment before they were ready to test. The resulting FQ-labeled-amino acid solution was stored in dark box and diluted with 10 mM NH_4HCO_3 just before analysis.

2. Peptide sample preparation

To prepare tryptic digests of E.coli lysates, 1 mL of the *E. coli* lysate (the solution was estimated to contain ~10 mg total protein/ml) was mixed with 5 μL of 1M NaAc/HAc buffer (pH=4) and 1 μL of pepsin (1 μg/ml) and incubated at 37 °C for 1 h. 100 μL of the above solution was diluted with 900 μL of 25 mM NH_4HCO_3 and mixed with 1 μL of 1 M DTT at room temperature for at least 1 hour. Then 10 μL of 0.2 mg/mL trypsin solution was added into above mixture, and the mixture was incubated at 37 °C for 24 h.

3. Peptide sample labeling

To label the digested *E. coli* lysate, 10 μL of the peptide solution prepared above was mixed with 10 μL of 10 mM KCN working solution and 10 μL of the 10 mM FQ solution. After 1-hour reaction in dark at

room temperature, the peptides were ready for separation. The peptide solution was stored in dark box at the temperature of 5°C and was diluted with 10mM NH_4HCO_3 prior to use.

4. Apparatus for NOTLC separation

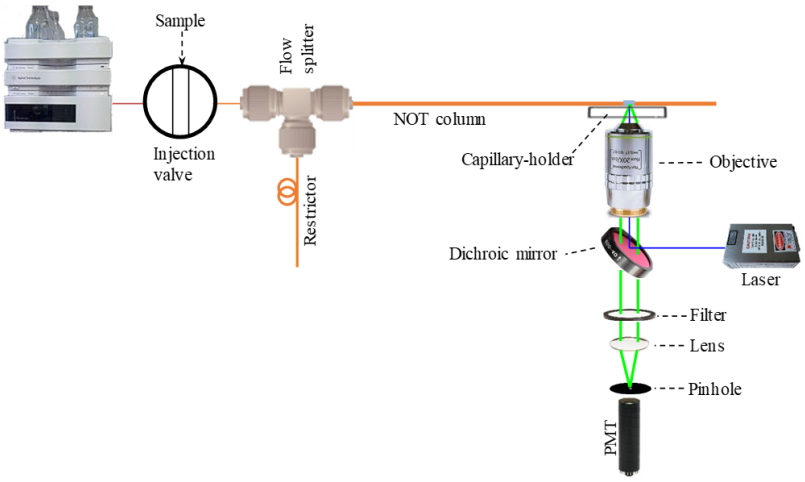

Figure S4-1. Schematic diagrams of experimental apparatus.
Figure presents a schematic diagram of the testing apparatus used in this work. The setup was used for testing the column, described elsewhere [S1]. A gradient pump (Agilent 1200 quaternary pump, Santa Clara, CA) was used for driving a mobile phase through a 6-port valve (VICI Valco, Houston, TX), via a flow splitter with a 20-µm-i.d. and 20-cm-long restriction capillary, to a NOTLC column. The NOTLC column had a 2-µm i.d. and was OTMS derivatized. At the 5 cm from the effluent outlet of NOTLC column, a detection window was made by removing the polyimide coating. A laser-induced fluorescence detector underneath the NOTLC column was used to monitor the resolved analytes. The confocal laser-induced fluorescence (LIF) detector was described previously.

5. Effect of OTMS coating temperature on amino acid retention and resolution

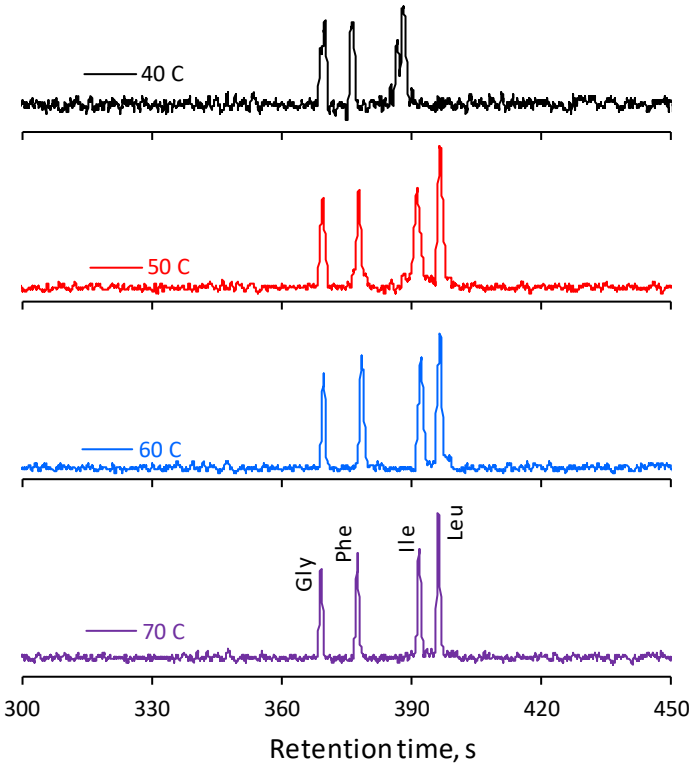

Figure S4-2. Influence of reaction temperature on NOTLC column.

The 2-µm-i.d. x 50 cm capillary columns were coated with 70% OTMS at the temperature of 40°C, 50°C, 60°C and 70°C for 18 hours. Higher than 70°C (e.g. 80°C) the column was blocked and cannot be fixed. The separation of amino acids mixture via different part of the column. Each column had a total length of 50 cm (45 cm effective), and an o.d. of 150-µm. The mobile phase is 20% (v / v) acetonitrile with 10 mM NH_4HCO_3 solution. Sample contained 0.05 µM gly, 0.1 µM phe,0.1 µM ile and 0.05 µM leu; The volume of sample injected was ~120 pL. The pump flowrate was set as 0.2 ml/min, pressure shows as 500 psi.

6. Effect of OTMS coating time on amino acid retention and resolution

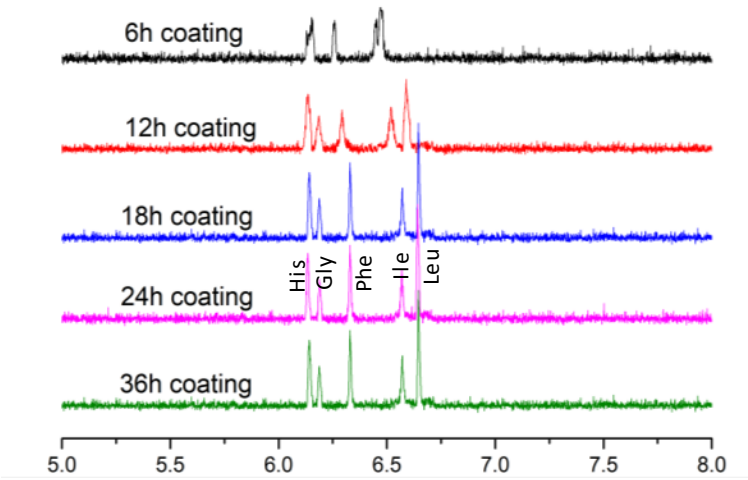

Figure S4-3. Influence of reaction time on NOTLC column.

The 2-μm-i.d. x 50 cm capillary columns were coated with 70% OTMS reagent for 6 h, 12 h, 18 h 24 h and 36 h. Longer than 36 h (e.g. 48 h) column was blocked and cannot be fixed. The separation of amino acids mixture via different part of the column. Each column had a total length of 50 cm (45 cm effective), and an o.d. of 150-μm. The mobile phase is 20% (v / v) acetonitrile with 10mM NH_4HCO_3 solution. Sample contained his, gly, phe, ile and leu, each at 0.1μM; The volume of sample injected was ~120 pL. The pump flowrate was set as 0.2ml/min, pressure shows as 500 psi.

7. Effect of OTMS flushing pressure on amino acid retention and resolution

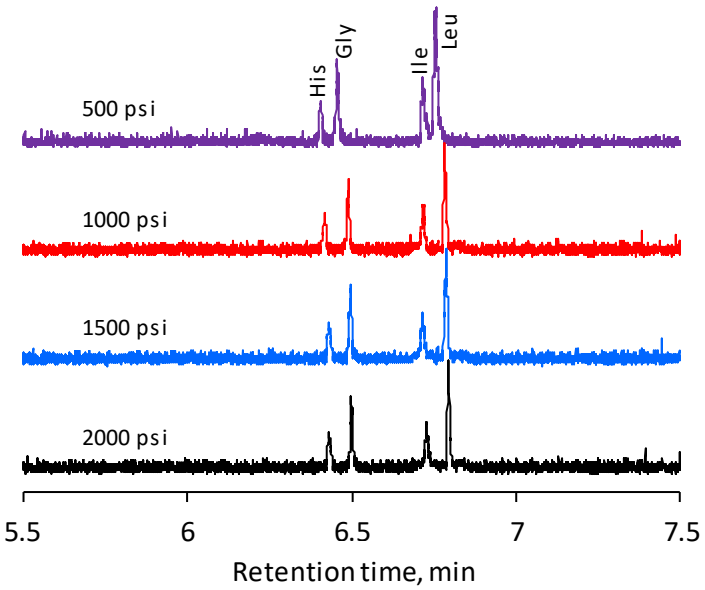

Figure S4-4. Influence of reaction pressure on NOTLC column.

The coating setup is shown as figure 1B due to the high pressure applied. Four columns with same size, 2-µm-i.d. x 50 cm (45 cm effective length) were treated under same condition except the pressure of nitrogen gas in the coating steps. The pump pressure was adjusted and stabilized at 500 psi, 1000 psi, 1500 psi and 2000 psi when the OTMS reagent was injected in the NOTLC column. When the NOTLC columns were coated, a volume of 120 pL sample was injected. Four labeled amino acids, his (1), gly (2), ile (3) and leu (4) each at 0.1 µM were separated with mobile phase of 20% acetonitrile with 10 mM ammonium bicarbonate at the pump pressure of 500 psi.

8. Column preparation reproducibility

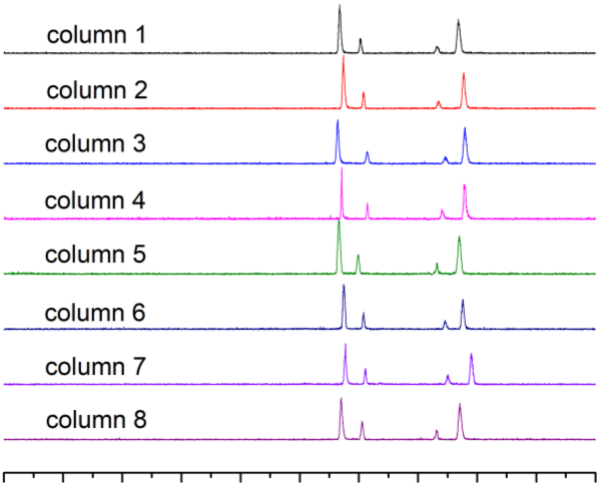

Figure S4-5. NOTLC column reproducibility tests.

Eight NOTLC 2-μm-i.d., 150-μm-o.d. and 45-cm-length columns were prepared in four batches (two columns are in one batch). All columns were prepared under the same condition (1000-psi N_2 for driving the reagent through the capillary, 70% OTMS in toluene (v/v), 18-hour reaction time and 60°C reaction temperature). The chromatograms from top to bottom represents the separation of amino acids mixture via multiple columns. The separation column had an effective length of 42 cm. The mobile phase is 20% (v / v) acetonitrile with 10mM NH_4HCO_3 solution. Sample contained 0.12 μM gly (1), 0.04 μM lys (2), 0.02 μM ile (3) and 0.12 μM leu (4); The volume of sample injected was ~120 pL. The pump flowrate was set as 0.2 ml/min, pressure shows as 500 psi.

9. Chromatogram for ultrahigh peak capacity separation of pepsin/trypsin digested *E. coli* lysate using a 50-cm-long NOTLC column

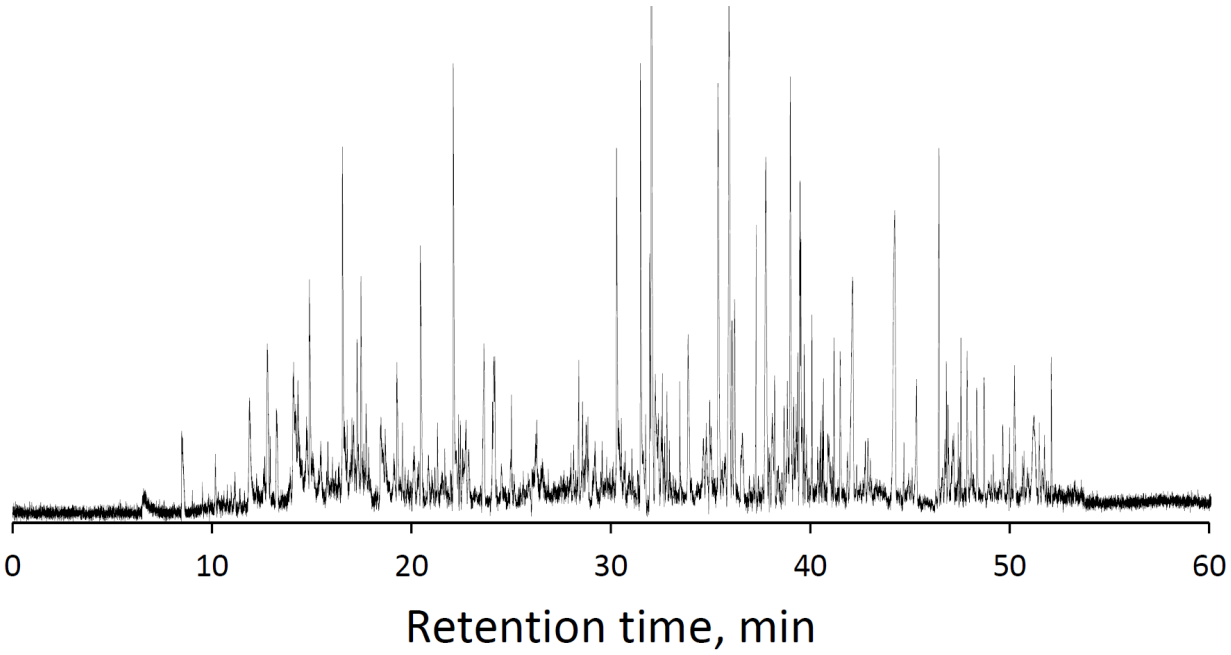

Figure S4-6. The separation of the enzyme digest of *E. coli* lysate.

The NOTLC column coated at the optimized condition (70% OTMS derivatized, 1000-psi N_2, 18-h reaction time and 60°C reaction temperature) was used to separate the sample. The NOTLC column had an i.d. of 2 μm, a length of 50 cm (45 cm effective). Mobile phase A was 10 mM NH_4HCO_3 in DDI water, and mobile phase B was 80% acetonitrile in 10 mM NH_4HCO_3. The volume of sample injected was ~120 pL. The elution pressure was 500 psi. The gradient was as set as mobile phase B increases from 5 to 100% within 60 min.

10. Chromatogram for ultrahigh peak capacity separation of pepsin/trypsin digested *E. coli* lysate using a 160-cm-long NOTLC column

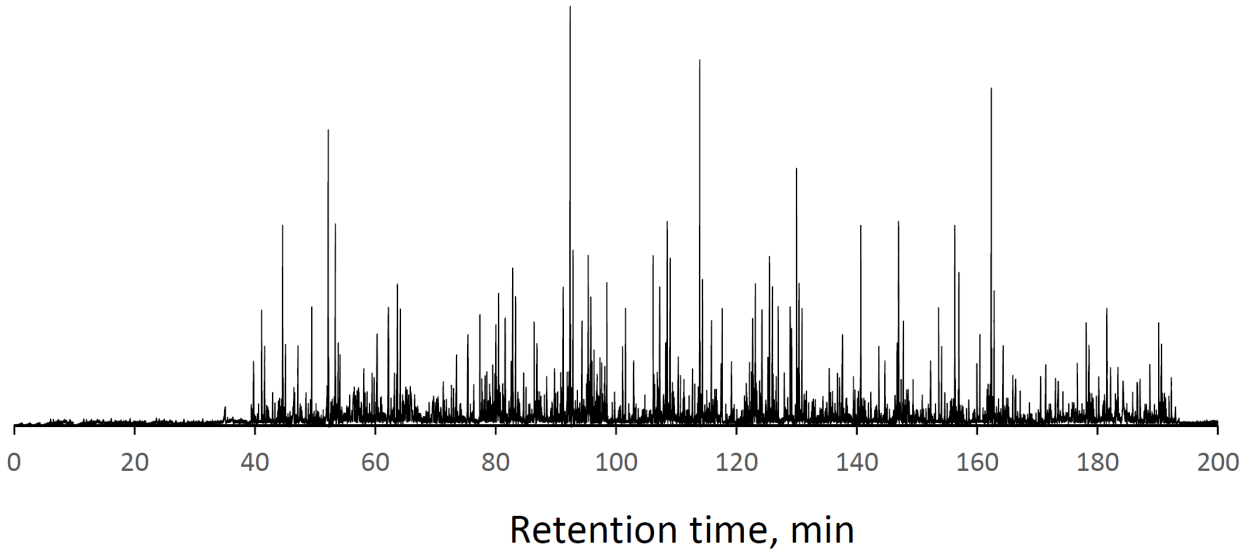

Figure S4-7. The chromatogram for separating enzyme-digested *E. coli* lysate.
The enzyme-digested *E. coli* lysate was separated using a 2 μm i.d., 160 cm long (155 cm effective) OTMS coated NOTLC column (coating condition: 75% OTMS, 18 hours reaction time, 1000 psi N_2 pressure, 60°C); 10 mM NH_4HCO_3 in DDI water was used as mobile phase A, and 80% acetonitrile in 10 mM NH_4HCO_3 was used as mobile phase B. The elution pressure was ~500 psi. The external loop of the injection valve had a volume of 6 μL. The flow rate in the restriction capillary was ~5.6 μL/min (measured), and it took ~64 s for the 6 μL sample to pass across the head of the NOTLC column. Under these conditions, an eluent linear flow velocity of 0.6 mm/s was measured inside the NOTLC column, and the injected volume was estimated to be ~120 pL. For separating pepsin/trypsin-digested *E. coli* lysates, the gradient started with 100% mobile phase A, whereas mobile phase B increased linearly from 0 to 100% within 180 min.

Appendix 5: Copyright Clarification

The Chapter 2 and chapter 3 are published works. The reuse permissions of the full ariticle were obtained as the figure S5-1 shows. All the other cited figures were permitted.

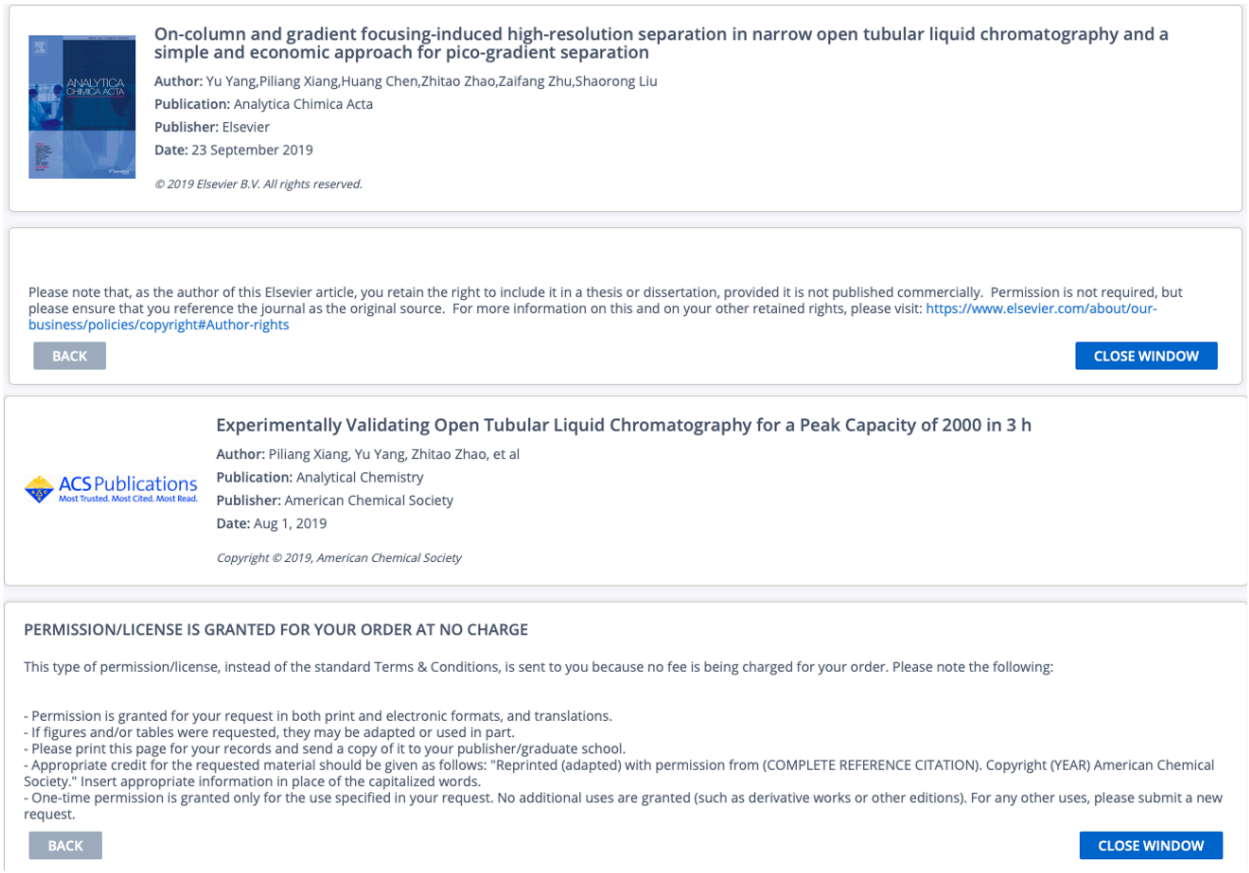

Figure S5-1 the reuse permissions of the full paper for chapter 2 and chapter 3.

Chapter 4 is submitted by the time when the dissertation was finished. The author of this dissertation contributed to all the writings for those chapters. In terms of the experimental part, all the NOTLC columns were prepared by the author. Data analyzing and sample preparation were also done by the same author. Most of the separations were run by the author. The data analysis was conducted by the author, including the peak capacity calculation, column efficiency, etc.